

City University of New York (CUNY)

CUNY Academic Works

Dissertations, Theses, and Capstone Projects

CUNY Graduate Center

2-2017

Removal of Organic Micro-Pollutants from Water Using Sewage Sludge Based Composite Adsorbents

Rui Ding

The Graduate Center, City University of New York

[How does access to this work benefit you? Let us know!](#)

More information about this work at: https://academicworks.cuny.edu/gc_etds/1903

Discover additional works at: <https://academicworks.cuny.edu>

This work is made publicly available by the City University of New York (CUNY).

Contact: AcademicWorks@cuny.edu

REMOVAL OF ORGANIC MICRO-POLLUTANTS FROM WATER
USING SEWAGE SLUDGE BASED COMPOSITE ADSORBENTS

by

RUI DING

A dissertation submitted to the Graduate Faculty in Earth and Environmental Sciences in partial fulfillment of the requirements for the degree of Doctor of Philosophy, The City University of

New York

2017

© 2017

Rui Ding

All Rights Reserved

Removal of Organic Micro-pollutants from Water Using Sewage Sludge Based Composite

Adsorbents

by

Rui Ding

This manuscript has been read and accepted for the Graduate Faculty in Earth and Environmental Sciences in satisfaction of the dissertation requirement for the degree of Doctor of Philosophy.

Date

Pengfei Zhang

Chair of Examining Committee

Date

James Biles

Executive Officer

Supervisory Committee:

Pengfei Zhang

Teresa J. Bandosz

Karin A. Block

Zhongqi Cheng

Dibyendu Sarkar

THE CITY UNIVERSITY OF NEW YORK

ABSTRACT

Removal of Organic Micro-pollutants from Water Using Sewage Sludge Based Composite Adsorbents

by

Rui Ding

Advisor: Pengfei Zhang

Millions of tons of sewage sludge, waste oil sludge and fish waste are produced annually, and improper treatment/disposal of these wastes have resulted in numerous environmental issues. On the other hand, these wastes are rich in organic materials, metals, and inorganic minerals and could be sustainable resources if utilized properly. The main purpose of this dissertation study was, therefore, to convert these wastes into composite adsorbents, and then use these adsorbents to remove various types of organic pollutants, emerging organic contaminants in particular, from wastewater and drinking water sources.

It is hypothesized that a hydrophobic carbon phase in the composite material would promote the physical adsorption of non-polar organic compounds, and an increase in the pores similar to the sizes of the non-polar adsorbates would further enhance physical adsorption on the carbon phase. It is further hypothesized that a polar mineral phase in the composite material would promote the chemical adsorption of polar organic compounds via specific interactions between the polar surface and functional groups of the adsorbates, and further diversifying the surface chemistry (e.g., introducing more elements especially catalytic metals to the mineral phase) would further enhance chemical adsorption of the polar compounds.

To increase carbon content and diversify surface chemistry of the sewage sludge derived composite materials, two types of wastes were added to sewage sludge: 1) waste oil from a shipyard that is rich in organic carbon and metals, and 2) fish waste from a local food market that is rich in organic content as well as P and other elements. Different pyrolysis temperatures and acid wash procedures were employed in an effort to increase material surface area and porosity. The performances of these different composite materials for the adsorption of various types of organic contaminants were then evaluated, under batch, column, and in some cases field conditions. The metal leaching behavior of the sewage sludge/fish waste derived composite materials was thoroughly investigated to assure that these adsorbents would not yield secondary contamination when applied in water treatment. The impact of natural organic matter (NOM) on the analysis of selected organic contaminants (pharmaceutical compounds) via liquid chromatography-tandem mass spectrometry (LC/MS/MS) was also examined to make sure that such impact would not significantly alter the quality of the data collected.

Adding waste oil or fish waste not only increased the C content by a few percent by weight in the hydrophobic carbon phase of the composite materials but also increased the content of some other elements such as Mg and P in the mineral phase. Increasing the pyrolysis temperature from 650 °C to 950 °C increased the surface area and total pore volume by as much as 100%, due to the decomposition of thermally unstable contents at high temperatures. Wash the sludge/fish waste derived composite materials with dilute acetic acid almost doubled the pore volume and surface area, due to the dissolution of some basic oxides such as CaO and also the removal of some tarry residues which may block the accesses to pores.

When the performance of the sewage sludge/waste oil sludge derived composite materials was evaluated for antibiotic removal, it was found that these materials have maximum adsorption capacities ranging from 80 to 300 mg/g, comparable to activated carbons. A large volume of pores similar in size to the adsorbate molecules within the hydrophobic carbon phase was indicated as an important factor promoting the separation process. Moreover, the polar surface of an inorganic phase in the adsorbents attracted the functional groups of target molecules. The presence of reactive alkali metals promoted reaction with acidic groups, formation of salts and their precipitation in the pore system.

When the adsorptive removal of 8 pharmaceuticals and endocrine disrupting compounds (EDCs) with the sewage sludge/fish waste based adsorbents was evaluated, it was found that the materials have the maximum adsorption capacities ranging from 16.9 to 38.6 mg/g, again comparable to activated carbons. Adsorption capacities obtained from rapid small scale column tests were about 50% of those obtained from batch equilibrium tests, demonstrating that the maximum adsorption capacities obtained from batch tests would be very relevant to the design of

column experiments or the prediction of performance under rapid flow through conditions. During the field experiment, 14 pharmaceutical compounds were detected in the source water of the Little Falls Water Treatment Plant. The large size columns were able to consistently remove 85-90% of the input pharmaceutical compounds and did not show any degradation of performance after a month of operation (~3500 bed volumes).

The sewage sludge/fish waste based adsorbents were also able to remove 6 nitrosamines from water under batch equilibrium and dynamic flow through conditions. The adsorption capacities determined from batch experiments ranged from 4.3 to 17 mg/g, comparable to those of many other materials such as modified zeolite, mesoporous silica, and metal impregnated activated carbons. The strong correlation between the adsorbed amounts and $\log K_{ow}$ values of the compounds suggests that hydrophobic interaction play a significant role on adsorption on the composite materials.

When the metal leaching behavior of the raw and acid washed adsorbents (sewage sludge/fish waste based) was examined, it was found that dilute acetic acid wash significantly reduced metal leaching with only 5 metals exceeded their maximum contaminant levels (MCLs, or drinking water standards). When column leaching tests were conducted, the concentrations of all the 5 metals dropped to below their respective MCLs within 10 bed volumes. Acid wash also neutralized the materials and significantly increased their surface area and pore volumes, resulting in an enhancement on the adsorption of three organic compounds by 2-5 times. This result suggests that the acetic acid washed composite materials could be potentially used in packed filters to treat wastewater or even drinking water without the concern of metal leaching.

As to the impact of NOM on the quantitative analysis of pharmaceutical by LC/MS/MS, it was found that NOM interacted with pharmaceuticals differently depending on the physicochemical properties of the analytes. The two anticonvulsants did not experience significant signal changes when mixed with NOM, whereas all 11 antibiotics experienced some signal suppression when mixed with one or more of the NOM. Possible mechanisms leading to the signal suppression include hydrogen bonds and electrostatic interaction between positively charged antibiotic species and negatively charged acidic groups of NOM, and π -interaction between the electron-withdrawing groups bonded to aromatic rings of the analytes and NOM. Overall the signal suppression was moderate (up to 24%), and the impact on quantitation by LC-ESI-MS could be mitigated by using a standard mixed with a typical NOM, at a concentration similar to that in the sample matrix.

Acknowledgments

This work is supported by U.S. Environmental Protection Agency (Grant # RD835178) and a fellowship from Dean of Science, CCNY.

I am very grateful to my advisor Dr. Pengfei Zhang, for his generous help and guidance in both of my research work and life.

I would also like to thank my committee members, Dr. Teresa J. Bandosz, Dr. Karin A. Block, Dr. Zhongqi (Joshua) Cheng and Dr. Dibyendu Sarkar, for their support throughout my dissertation research.

I would like to extend my gratitude to Sadie Barnes, Stephanie DeVries and many other friends and colleagues for their help and advice.

Last but not least, I would like to thank my family, my grandmother, my parents, my wife and my lovely daughter, for building up my life, for their support and encouragement as always, and for everything they gave to me.

Table of Contents

Chapter 1 Introduction	1
1.1 Sludge based composite materials.....	1
1.2 Organic micro-pollutants.....	3
1.3 Hypotheses and scope of the dissertation research	4
1.4 Significance of Study	5
Chapter 2 Impact of Natural Organic Matter on Quantitative Detection of 11 Antibiotics in Water by Liquid Chromatography-ESI-Tandem Mass Spectrometry	7
2.1 Introduction	8
2.2 Materials and Methods	10
2.2.1 Chemicals	10
2.2.2 Methods	10
2.2.3 Statistical Analysis	12
2.3 Results	13
2.3.1 Solution pH and ionic species of analytes	13
2.3.2 Instrument signal change by addition of organic matter	16

2.4 Discussion	19
2.4.1 General mechanisms for LC-ESI_MS signal suppression	19
2.4.2 Signal changes related to physicochemical properties of analytes.....	21
2.4.3 Signal changes related to NOM characteristics.....	24
2.5 Conclusions	25
Chapter 3 Removal of antibiotics from water on sewage sludge and waste oil sludge derived adsorbents	27
3.1 Introduction.....	28
3.2 Materials and methods	31
3.2.1 Adsorbents.....	31
3.2.2 Characterization of adsorbents	31
3.2.3 Adsorption of pharmaceuticals.....	32
3.2.4 LC/MS/MS method	33
3.3 Results and discussion.....	34
3.3.1 Adsorption isotherms and capacities	34
3.3.2 Material characteristics and adsorption performance.....	40

3.3.3 FTIR result.....	45
3.3.4 Thermal analysis result.....	47
3.3.5 Environmental Implications	49
3.4 Conclusions	50
Chapter 4 Leaching of heavy metals from sewage sludge/fish waste based composite adsorbents and the effects of post carbonization acid wash.....	
4.1 Introduction	52
4.2 Materials and Methods	54
4.2.1 Materials	54
4.2.2 Acid washing after carbonization	54
4.2.3 Characterization of SBAs	55
4.2.4 Leaching test.....	55
4.2.5 Column leaching with pure water.....	56
4.2.6 Metal analysis	56
4.2.7 Batch adsorption experiment.....	56
4.2.8 LC/MS/MS method	57

4.3 Results and Discussion.....	57
4.3.1 Metal leaching before acid wash	57
4.3.2 Metal leaching after acid wash.....	60
4.3.3 Characterization of SBAs before and after acetic acid wash.....	66
4.3.4 Batch absorption before and after acetic acid wash	68
4.4 Conclusions	73
Chapter 5 Adsorption of multiple pharmaceuticals and endocrine disrupting compounds (EDCs) from water by sewage sludge-fish waste based adsorbents	
5.1 Introduction.....	75
5.2 Materials and Methods	78
5.2.1 Adsorbents	78
5.2.2 Acid wash of sludge based adsorbents	78
5.2.3 Batch adsorption experiment	79
5.2.4 Column transport experiment	79
5.2.5 Field Experiment	80
5.2.6 LC/MS/MS method	81

5.3 Results and Discussion.....	81
5.3.1 Material properties.....	81
5.3.2 Batch adsorption experiment.....	83
5.3.3 Rapid Small Scale Column Test (RSSCT).....	90
5.3.4 Field Column Test.....	94
5.4 Conclusions.....	95
Chapter 6 Adsorption of aqueous nitrosamines by sewage sludge and fish waste based adsorbents	97
6.1 Introduction.....	98
6.2 Materials and Methods.....	100
6.2.1 Adsorbents.....	100
6.2.2 Acid wash.....	101
6.2.3 Batch adsorption experiment.....	101
6.2.4 Column transport experiment.....	102
6.2.5 LC/MS/MS analysis.....	102
6.3 Results and Discussion.....	103

6.3.1 Batch adsorption.....	103
6.3.2 Column transport experiments.....	110
6.4 Conclusions.....	114
Chapter 7 Future Research.....	115
Appendix.....	118
Appendix A.....	118
Appendix B.....	121
Appendix C.....	128
Appendix D.....	135
Appendix E.....	137
Bibliography.....	139

Lists of Tables

Table 2-1 Fraction of species (%) of the antibiotics and anticonvulsants at pH 6 and 7. The symbols \ominus \circ \oplus represent negative, neutral, and positive functional groups, respectively.	15
Table 2-2 Statistical results of the instrument signals with and without the presence of NOM. Statically significant m values are highlighted in red (95% confidence level).....	18
Table 3-1 Some physical properties of the antibiotics and anticonvulsants tested in this study. .	36
Table 4-1 Leaching of unwashed composite materials by DI water, tap water, and TCLP fluid. Concentrations are in $\mu\text{g/L}$. Values above the drinking water standards are highlighted in red. .	59
Table 4-2 Leaching of metals from acid washed composite materials (in $\mu\text{g/L}$). Be, Ru, Th, Tl, U were all below detection and therefore are not tabulated. Metals in the Milli-Q (DI) and tap water (TAP) leachate that exceeded MCLs are highlighted in red.....	62
Table 5-1 BET surface area and pore volume of unwashed and acid washed materials.	82
Table 6-1 Adsorption at the highest contaminant loading for unwashed materials.....	105
Table 6-2 Adsorption at the highest contaminant loading (acid washed materials).....	107
Table 6-3 Nitrosamines adsorbed in batch (at highest loading) and column transport experiment	111
Table A1 MRM transitions and Mass Spectrometry parameters.....	118

Table A2 R ² values of linear fitting of peak area vs. concentration for all of the compounds with or without NOM.....	119
Table B1 Formula, molecular weight (MW), pKa, solubility, and logK _{ow} of the antibiotics and anticonvulsants examined in this study.....	121
Table B2 Concentrations (mg/L) and corresponding loadings (mg/g) of pharmaceuticals used in the isotherm study. Each of the 12 solutions contains all 13 compounds. ENR, OFL, SZ, and CBZ have solubilities less than 200 mg/L and therefore lower concentrations were used.	123
Table B3 MRM transitions used to identify (both transitions) and quantify (primary transition) the antibiotics and anticonvulsants.	124
Table B4 Solution pH at adsorption equilibrium.....	124
Table B5 Fraction of species (%) of the analytes at pH of 6.8 and 8.7	125
Table C1 physicochemical properties of the adsorbates.....	128
Table C2 Leaching of unwashed composite materials by DI water, tap water, and TCLP fluid. Concentrations are in µg/L.....	129
Table C3 pH of leachate from composite materials.....	130
Table C4 Major mineral phases present in sludge composites.....	131
Table C5 Leaching of HCl washed composite materials by DI water. Concentrations are in µg/L	131

Table C6 Leaching of acetic acid washed composite materials by DI water, tap water, and TCLP fluid. Concentrations are in $\mu\text{g/L}$	132
Table D1 Properties of pharmaceuticals and EDCs.....	135
Table E1 Properties of nitrosamines	137

Lists of Figures

Figure 2-1 Calibration curves of ERY with and without NOM in constant ratio (A) and constant concentration (B) experiment.	17
Figure 3-1 Examples of the adsorption isotherms for OTC, ENR, and ERY on the sludge derived adsorbents SS950, WO 950 and SSWO950. The smooth lines represent best fit to the data with the L-F model.....	35
Figure 3-2 Maximum observed adsorption capacities (A) and percent removal of each species at the highest contaminant loading (B).....	38
Figure 3-3 Comparison of the total adsorption capacities for the compounds tested on the sludge derived adsorbents. “Measured” represents the amount adsorbed at the highest contaminant loading, whereas “Fitted” represents the values obtained from the L-F model.....	38
Figure 3-4 A) Surface area (S_{BET}) and average pore sizes (D_{BJH}); B) Total volume (V_t) and volume of the micropores (V_{micro}) of the adsorbents, and the volume occupied by the compounds derived from the amount adsorbed at the maximum contaminant loading ($V_{occup, m}$) and from the maximum capacity predicted from the L-F model ($V_{occup, p}$).....	39
Figure 3-5 FTIR spectra for the initial, water exposed, and exhausted (after adsorption under the highest loading of pharmaceuticals) sludge materials.	45
Figure 3-6 DTG curves for the initial, water exposed (-W), and exhausted (-E, after adsorption under the highest loading of pharmaceuticals) sludge materials.	48

Figure 4-1 Leaching of metals with DI water from acetic acid washed SBAs under dynamic flow through conditions.	65
Figure 4-2 Surface area and pore volume of SABs before (A) and after (B) acetic acid wash. “_W” indicates acid wash.	67
Figure 4-3 BJH Pore size distribution.....	68
Figure 4-4 Adsorption isotherms of ATN, CBZ and NMEA.	70
Figure 4-5 Observed and simulated adsorption capacity and removal efficiency.....	71
Figure 5-1 Examples of adsorption isotherms of unwashed materials.	84
Figure 5-2 Adsorption on unwashed materials at the highest contaminant loading. Triplicate tests were performed with each adsorbent.	84
Figure 5-3 Removal efficiency of unwashed adsorbents at the highest contaminant loading.....	85
Figure 5-4 Examples of adsorption isotherms of acid washed materials.....	86
Figure 5-5 Adsorption on acid washed materials and activated carbon (AC) at the highest contaminants loading, each represents the average of triplicate tests.....	87
Figure 5-6 Removal efficiency of acid washed adsorbents at the highest contaminants loading.	88
Figure 5-7 Total concentration of 8 contaminants in the effluent of column transport experiment of acid washed materials.	91

Figure 5-8 Comparison of maximum adsorption of individual compound by acid washed materials, tested in batch adsorption and column transport experiment.....	93
Figure 5-9 Comparison of total adsorption capacities of acid washed materials measured in batch adsorption and column transport experiment.....	93
Figure 5-10 Results from the field column test at the Little Falls Water Treatment Plant in New Jersey.....	95
Figure 6-1 Adsorption isotherms of the 6 nitrosamines by the unwashed materials	104
Figure 6-2 Adsorption isotherms of the 6 nitrosamines by the acid-washed materials.....	108
Figure 6-3 The correlation between hydrophobicity (logKow) of nitrosamines and adsorption.	109
Figure 6-4 Breakthrough curves of the 6 nitrosamines as well as the sum of the 6 compounds	111
Figure 6-5 Comparison of maximum adsorption of individual analyte by acid washed materials, tested in batch adsorption and column transport experiment.....	113
Figure 6-6 Comparison of total adsorption capacities of acid washed materials measured in batch adsorption and column transport experiment.....	113
Figure A1 Chemical structures of analytes in this study	120
Figure B1 Pore size distributions for the adsorbents studied.....	126

Figure B2 Proton binding curves for the adsorbents studied.....	127
Figure C1 XRD data for original and acetic acid washed materials.....	134

Chapter 1 Introduction

1.1 Sludge based composite materials

Municipal sewage sludge, also called biosolids, is a mixture of inorganic materials such as sand and metal oxides and exhausted biomass from aerobic and anaerobic digestion of the organic constituents of municipal sewage. Industrial sludges include wastes from industries such as shipyards, foundry, electroplating, tobacco, paper mills, etc. Sewage sludge typically contains high levels of nutrients, metals, persistent organic pollutants, pathogens, etc. [1-3], and requires proper treatment and disposal. It is estimated that the United States and the European Union each produce about 10 million tons of dry sewage sludge annually [4, 5]. China produces another 6 million tons of dry sludge per year [6], and this number is likely to grow in the near future as the extent of wastewater treatment increases.

Like sewage sludge, fish waste is also produced in large quantities annually and needs proper treatment/disposal. During industrial processing of various fish species, up to 50% of the raw fish were converted into waste [7, 8], resulting in over 100 million tons of waste annually [9]. Over the past years, commercial fish waste was usually landfilled or discharged as processing effluents into water bodies. The processing effluents contain high levels of BOD (biological oxygen demand), TSS (total suspended solid), nutrients, and hydrogen sulfide, and are highly likely to produce adverse effects on the receiving coastal and marine environments [10].

The reuse of fish waste is currently limited to digestion to produce biogases [8]. In contrast, various methods have been used to dispose of or utilize municipal sewage sludge [4], including incineration, landfilling, road surfacing, conversion to fertilizer, compression into building blocks,

and carbonization [5, 11-14]. Since 1976 several patents have been issued on carbonization of sewage sludge and various applications of the final materials [15-17]. Industrial sludges after dewatering processes/drying are either used in landfills or disposed of, mainly as hazardous wastes.

The processes of carbonization of sewage sludges and applications of the resultant adsorbents have been studied in detail previously and are described extensively in the literature [1, 5, 18]. Sludge derived composite materials typically have surface areas between 100 and 500 m²/g. Their performance as adsorbents to hydrogen sulfides [19-21], sulfur dioxide [22], basic or acidic dyes [23], phenol [24, 25], copper [26-30], or mercury [31] has been reported comparable to or better than that on activated carbons. In many processes the excellent sorption ability of these materials is linked to the catalytic action of metals present in various forms in the final products [32]. In contrast, typical activated carbon does not contain such catalytic metals.

Waste oil and metal sludge have been added to sewage sludge to produce composite materials with enhanced properties [33]. First, mixing sludges leads to the development of additional pores (mesopores in particular), resulting in an increased adsorption capacity. Second, surface chemistry is also altered during pyrolysis of the sludge mixture compared to the single components. A huge, reaching 100 % enhancement found in the performance of hydrogen sulfide adsorbents was linked to the changes in the composition and the surface distribution of an inorganic phase [33].

In order to further diversify the surface features of sludge based adsorbents and explore more options of waste reclamation, fish waste rich in carbonaceous material and elements such as P, Ca, and Mg that could form catalytic centers after pyrolysis, was added to sewage sludge as a

secondary component to produce a new type of composite materials. It has been proven that these adsorbents with fish waste as additives work effectively in removing pharmaceuticals such as carbamazepine, sulfamethoxazole and trimethoprim from water [34, 35].

1.2 Organic micro-pollutants

N-nitrosamines are a family of extremely potent carcinogens. Six nitrosamine disinfection byproducts are listed in USEPA's second Unregulated Contaminant Monitoring Rule [36] and cited in USEPA's new Drinking Water Strategy as a group of contaminants to be addressed in the near-term, following the carcinogenic VOCs [37]. These nitrosamines include N-nitrosodiethylamine (NDEA), N-nitrosodimethylamine (NDMA), N-nitrosodinbutylamine (NDBA), N-nitrosodinpropylamine (NDPA), N-nitrosomethylethylamine (NMEA), and N-nitrosopyrrolidine (NPYR). NDMA which is frequently detected in water resources in US and Canada is classified as a B2 carcinogen by the Integrated Risk Information System (IRIS) of USEPA [38] and 2A carcinogen by the World Health Organization's International Agency for Research on Cancer [39]. It is typically observed in the low ng/L range in drinking water. However, concentrations equal to or above 1000 ng/L have been recorded in chloraminated raw water and chlorinated or chloraminated wastewater effluent [40].

Pharmaceuticals and endocrine disrupting compounds (EDCs) are organic contaminants present ubiquitously in wastewater, surface water, and drinking water [41, 42]. These organic contaminants are introduced into the terrestrial environment via the application of animal waste as fertilizer and discharge of inefficiently treated hospital effluent [43] and wastewater [44, 45]. The toxicological implications of chronic exposure to suites of these contaminants are still unclear, but

it is suspected that the antibiotics in the environment can promote the natural selection of antibiotic resistant genes [46, 47]. Another effect is that antibiotics challenge microbial populations and will affect the composition of natural microorganism communities [48]. Thus, there is a great concern about these compounds from medical professionals, environmental scientists, drinking water municipalities, government agencies, and the general media. Studies on antibiotics removal from water have already been carried on by some researchers [49-51]. An extensive survey of the source water of 19 US water utilities for 51 pharmaceuticals and EDCs found that 11 compounds were frequently detected [42].

1.3 Hypotheses and scope of the dissertation research

It is hypothesized that a hydrophobic carbon phase in the composite material would promote the physical adsorption of non-polar organic compounds, and an increase in the pores similar to the sizes of the non-polar adsorbates would further enhance physical adsorption on the carbon phase. It is further hypothesized that a polar mineral phase in the composite material would promote the chemical adsorption of polar organic compounds via specific interactions between the polar surface and functional groups of the adsorbates, and further diversifying the surface chemistry (e.g., introducing more elements especially catalytic metals to the mineral phase) would further enhance chemical adsorption of the polar compounds.

To increase carbon content and diversify surface chemistry of the sewage sludge derived composite materials, two types of wastes were added to sewage sludge: 1) waste oil from a shipyard that is rich in organic carbon and metals, and 2) fish waste from a local food market that is rich in organic content as well as P and other elements. Different pyrolysis temperatures and

acid wash procedures were employed in an effort to increase material surface area and porosity. The performance of these different composite materials for the adsorption of various types of organic contaminants were then evaluated, under batch, column, and in some cases field conditions. The metal leaching behavior of the sewage sludge/fish waste derived composite materials was thoroughly investigated to assure that these adsorbents would not yield secondary contamination when applied in water treatment. The impact of natural organic matter (NOM) on the analysis of selected organic contaminants (pharmaceutical compounds) via liquid chromatography-tandem mass spectrometry (LC/MS/MS) was also examined to make sure that such impact would not significantly alter the quality of the data collected.

The dissertation consists of 7 chapters. Chapter 1 is the general introduction, and Chapters 2-6 are the results, where each chapter is intended to be a standalone article, with its own Introduction, Materials and Methods, Results and Discussion, and Conclusions. Chapter 7 proposes some future research directions related to my dissertation work.

1.4 Significance of Study

This research is aimed to develop new strategies of waste recycling technologies and to utilize sewage sludge and other wastes to produce composite adsorbents for water treatment. The organic micro-pollutants of concern (N-nitrosamines, pharmaceuticals and EDCs) are expected to be removed from aqueous phase. Currently materials of such characteristics are in high demand, especially in developing new filtration technologies.

Utilization of the sewage sludges will relieve the environmental stress caused by accumulation of these wastes. Materials obtained will create a new class of inexpensive adsorbents for the removal of contaminants from air and water, which would contribute to a more sustainable environment.

**Chapter 2 Impact of Natural Organic Matter on Quantitative
Detection of 11 Antibiotics in Water by Liquid Chromatography-
ESI-Tandem Mass Spectrometry**

2.1 Introduction

Antibiotics are widely used as human and veterinary medicine [52, 53], and 30-90% of administered antibiotics may be excreted in its original or conjugated form [54]. Many antibiotics can survive, to some degree, both conventional and advanced wastewater treatment processes [49, 55, 56]. Antibiotics are introduced into surface water, soils, and groundwater from wastewater treatment plant effluents and/or from manure- or sewage sludge-based fertilizers [53, 57]. Antibiotics have been shown to affect soil bacterial community structure and enzymatic activities [58], and may lead to the development and spreading of antibiotic resistance [53]. A few recent studies [59-61] also indicate that even trace amounts of residual antibiotics in soils may impact the soil nitrogen cycle and lead to an increased emission of N_2O , a potent greenhouse gas.

Many advanced treatment processes (e.g., ozonation, chlorination, ultraviolet irradiation, nanofiltration, reverse osmosis, and activated carbon adsorption) have been used to remove antibiotics from secondary effluent [56]. Among these, adsorption is one of the best available technologies to remove antibiotics and other undesirable synthetic organic compounds in water [62, 63]. However, this approach is often affected by the presence of natural organic matter (NOM) in water [64-67]. NOM includes both humic and non-humic fractions. The humic part includes humic acid and fulvic acid, together with tannic acid comprise the majority of dissolved organic matter (DOM) in water [68]. DOM may reduce the capacity of adsorbents such as activated carbon by competing with and/or blocking access of target compounds to some nanoscale pores of adsorbents [65, 69, 70].

NOM in water may also interfere the quantitative analysis of antibiotics and other trace

organic pollutants by liquid chromatography tandem mass spectrometry (LC/MS/MS), the most widely used analytical technique for antibiotics and pharmaceuticals in general in complex environmental samples nowadays [63, 71]. This interference stems from the intermolecular association of analytes and NOM, including hydrophobic, H-bonding, electrostatic, and van der Waals interactions [72, 73]. Most of the antibiotics have positive $\log K_{ow}$ values, indicating medium to high hydrophobicity. Moreover, humic and fulvic acids have negatively charged carboxylate groups, which may interact with positively charged moieties on some of the antibiotic molecules under environmentally relevant pH. It has been shown that aqueous NOM may directly adsorb a wide range of compounds by hydrophobic interactions and/or other mechanisms [64, 74-77].

The interactions of NOM and antibiotics/pharmaceuticals occurring in a gas phase environment such as the ion source of a mass spectrometer may be different from those in the aqueous environment. There are very few studies investigating the influences of NOM on the detection of pharmaceuticals during MS analysis and the mechanisms remain unclear [72, 78-80]. NOM appears to have no influence on the electrically neutral carbamazepine, bisphenol A and negatively charged ibuprofen [72, 80]. However, when tested for more compounds Wickramasekara et al. [79] observed signal suppression at high NOM concentrations (up to 50 mg/L). Rivera et al. [78] also observed a broad range of recoveries (from 13% to > 200%) for 11 pharmaceutical compounds. To our knowledge, there is no systematic study on the influence of NOM on antibiotic analysis by LC/ESI/MS. Thus, the objectives of this study are to investigate the impact of NOM on the quantitation of a wide range of antibiotics by LC-ESI-MS, and to relate the impact to the physicochemical properties of the compounds.

2.2 Materials and Methods

2.2.1 Chemicals

Eleven antibiotics from five major categories and two anticonvulsants (carbamazepine and primidone) were examined in this study. Amoxicillin (AMO), carbamazepine (CBZ), chloramphenicol (CHP), chlorotetracycline·HCl (CTC), enrofloxacin (ENR), ofloxacin (OFL), sulfadiazine (SDZ), sulfamethazine (SMZ) and sulfamethoxazole (SMX) were purchased from Sigma-Aldrich (St. Louis, USA). Erythromycin (ERY) and Penicillin-G Potassium (PEN-G) were purchased from Calbiochem (San Diego, USA). Oxytetracycline·HCl (OTC) and primidone (PRM) were obtained from MP Biomedicals (Santa Ana, USA). These compounds are selected because they have been frequently detected in either sewage or the effluent of wastewater treatment plants (WWTPs) [56, 81]. The chemical structures of these analytes are summarized in Figure A1 in Appendix A and their physicochemical properties such as pKa and logK_{ow} could be found in the supplementary material of previous work [63]. Three types of NOM were obtained from the International Humic Substances Society (IHSS, St. Paul, USA): Suwannee River NOM 1R101N (SRNOM), Nordic Reservoir NOM 1R108N (NRNOM) and Suwannee River Fulvic Acid Standard I 1S101F (SRFA).

2.2.2 Methods

A stock solution with a mixture of the 11 antibiotics and two anticonvulsants (~1000 µg/L each, with some variations due to solubility limitations) was freshly prepared in Milli-Q water (18mΩ) before experiments. The NOM stock solution was prepared at 20 mg/L and filtered

through a 0.45 μ m filter.

To examine the effects of NOM on antibiotic detection, three types of calibration curves (CC) were obtained: antibiotics only (CC I), constant ratio of NOM to antibiotics (CC II) and constant concentration of NOM (CC III). The stock antibiotic solution was first diluted with milli-Q water to yield six different concentrations: 5, 10, 50, 100, 200 and 500 μ g/L. For each concentration 8 sets of 10 mL aliquots were prepared for further use: CC II (3 sets) was made by adding a proper volume of one of the three NOM stock solutions to the 10 mL antibiotic solution to obtain NOM to antibiotics mass ratio of 1:1 (with the highest NOM concentration of 6.7 mg/L associated with 500 μ g/L analytes); CC III (3 sets) was produced by adding 1 mL of one of the three NOM stock solutions to the 10 mL antibiotic solution to yield a constant NOM concentration of 9.09 mg/L (within the typical range of WWTP effluents [82, 83]); CC I (2 sets) are controls with antibiotics only, but with the addition of proper volumes of water (as opposed to the NOM solution) to keep the antibiotic concentrations exactly the same as either CC II or CC III standards.

All samples were analyzed within 12 hours of preparation by HPLC/MS/MS with electron spray ionization (ESI) and multiple reaction monitoring (MRM). A Shimadzu HPLC, consisting of a DGU-20A3 degasser, LC-20AD binary pumps, a SIL-20AC HT autosampler, and a CTO-20AC oven, was used. An Agilent Eclipse Plus C18 (1.8 μ m \times 4.6mm \times 50mm) column was applied for separation. The temperature of the column oven was kept at 40°C. The mobile phase consisted of water (component A) and methanol (component B) buffered with 0.1% (v/v) formic acid. The flow rate was 0.4 mL/min, and the following gradient elution program was used: equilibrate for 2 mins before injection, 5% B for 1 min, 95% B from 2.5 to 5.5 min, and 5% B from 6 to 7 min. Ten μ L of each sample was injected through the autosampler, and the needle was

automatically rinsed with 200 μ L methanol between injections.

Mass spectrometry was performed with an ABI 4000 Q-trap mass spectrometer (Applied Biosystems) with an ESI ion source and N300DR nitrogen generator (Peak Scientific, Billerica, MA). Nitrogen was used as both the collision gas and nebulizing gas. The curtain gas, collision gas, and ion source gas 1 and gas 2 were set at 20, 6, 50, and 50 psi, respectively. The nebulizer current was set at 3 mA and the temperature of the interface heater was maintained at 400°C. Quantitation of all compounds was made by primary MRM transitions and the secondary transitions were used as confirmation (Table A1 in Appendix). All samples were injected three times and the peak areas were used for calibration curves (peak area vs. concentration) and statistical analysis, described below.

The pH of the mixed solutions at equilibrium was measured with Orion 290A+ pH meter (Thermo Electron Corporation, Waltham, USA).

2.2.3 Statistical Analysis

For each analyte, instrument signals (i.e., peak areas) of different analyte concentrations with NOM (y-axis) were plotted against corresponding peak areas without NOM (x-axis), and then the data were fitted with linear regression. The slope (m), intercept (b), standard deviation of slope (S_m), standard deviation of intercept (S_b) and square of correlation coefficient (R^2) were calculated by least squares method using Microsoft Excel.

To test whether the two series of instrument signals (i.e., peak areas with and without NOM) are statistically different, analysis of covariance (ANCOVA), a general linear model that

blends ANOVA (analysis of variance) and regression, was used. In ANOVA, the total variance includes between-group variance and within-group variance, so the F-test is computed by dividing the explained variance between groups by the unexplained variance within the groups. However, in ANCOVA the within-group variance is further divided into covariance (e.g., variance generated by different analyte concentrations) and systematic error, and the covariance could be separated when looking at the variance of instrument signals (peak areas). Comparing to ANOVA, ANCOVA can increase the ability to find statistical difference between groups with different treatment (e.g., with and without NOM) by reducing the within-group error variance (e.g., variance created by analyte concentration) [84]. To determine whether two series of instrument signals are statistically different, the assumption of “Homogeneity of Regression Slopes” in the ANCOVA model was tested. In our case the regression slopes refer to the slopes of the plots of instrument signals (peak areas) vs. analyte concentrations. SPSS (version 20, IBM Corporation) was used for the statistical analysis. Significance values higher than 0.05 indicate no differences between the instrument signals with and without NOM, while the values lower than 0.05 indicate differences, at the confidence interval of 95%.

2.3 Results

2.3.1 Solution pH and ionic species of analytes

All the analytes examined here have one or more functional groups, thus the fraction of different ion species may change as solution pH changes through protonation or deprotonation. After mixing analytes with NOM, the solutions have pH values from 6 to 7. Based on each compound's pKa values, the percentages of different ion species of each analyte at pH = 6 or 7

were calculated and tabulated in Table 2-1. At pH 6, ERY (99.9%) exists as cations; PEN-G (99.9%) and a majority of SMX (70%) exist as anions; CHP (100%), CBZ (100%), PRM (100%), and a majority of SMZ (97%) and SDZ (76%) are neutral; all the rest compounds are zwitterions in solutions. The distribution of different ionic species shifted a bit (towards more negative) at pH 7 for most compounds as a result of more deprotonation.

Table 2-1 Fraction of species (%) of the antibiotics and anticonvulsants at pH 6 and 7. The symbols $\ominus\circ\oplus$ represent negative, neutral, and positive functional groups, respectively.

Category	Compounds	pH	Fraction of species (%)					
Beta-lactam	AMO		$\circ\oplus\circ$	$\ominus\oplus\circ$	$\ominus\circ\circ$	$\ominus\circ\ominus$		
		pH 6	0.0	96.1	3.8	0.0		
		pH 7	0.0	71.5	28.5	0.1		
	PEN-G			\circ	\ominus			
		pH 6		0.1	99.9			
		pH 7		0.0	100.0			
Fluoroquinolones	ENR		$\circ\oplus\oplus\oplus$	$\ominus\oplus\oplus\oplus$	$\ominus\circ\oplus\oplus$	$\ominus\circ\circ\oplus$	$\ominus\circ\circ$	
		pH 6	0.4	59.9	38.7	1.0	0.0	
		pH 7	0.0	11.0	70.8	18.2	0.0	
	OFL			$\circ\oplus$	$\ominus\oplus$	$\ominus\circ$		
		pH 6	48.1	51.6	0.3			
		pH 7	8.1	87.3	4.6			
Sulfonamides	SDZ		$\circ\oplus$	$\circ\circ$	$\circ\ominus$			
		pH 6	0.0	76.0	24.0			
			pH 7	0.0	24.0	76.0		
	SMZ			$\circ\oplus$	$\circ\circ$	$\circ\ominus$		
		pH 6	0.0	96.9	3.1			
			pH 7	0.0	75.6	24.4		
SMX			$\circ\oplus$	$\circ\circ$	$\circ\ominus$			
	pH 6	0.0	28.5	71.5				
		pH 7	0.0	3.8	96.2			
Macrolides	ERY		\oplus	\circ				
		pH 6	99.9	0.1				
		pH 7	98.8	1.2				
Tetracyclines	OTC		$\circ\circ\oplus$	$\ominus\circ\oplus$	$\ominus\ominus\oplus$	$\ominus\ominus\circ$		
		pH 6	0.2	96.5	3.3	0.0		
			pH 7	0.0	74.0	25.7	0.3	
	CTC			$\circ\circ\oplus$	$\ominus\circ\oplus$	$\ominus\ominus\oplus$	$\ominus\ominus\circ$	
pH 6		0.2	97.1	2.7	0.0			
		pH 7	0.0	77.9	22.0	0.1		
Other	CHP			\circ	\ominus			
		pH 6		100.0	0.0			
		pH 7		100.0	0.0			
Anticonvulsants	CBZ		\oplus	\circ	\ominus			
		pH 6	0.0	100.0	0.0			
		pH 7	0.0	100.0	0.0			
	PRM			\circ	\ominus			
		pH 6		100.0	0.0			
		pH 7		100.0	0.0			

2.3.2 Instrument signal change by addition of organic matter

A few examples of peak area vs. concentration plots are presented in Figure 2-1. The square of correlation coefficients (R^2) of peak area vs. concentration for all of the compounds with different NOM are greater than 0.99 (Table A2 in Appendix A) except for ENR (~0.98), OFL (~0.97), and CBZ (~0.96), which are still quite robust for LC/MS/MS method. It is noted that the low R^2 value for CBZ is caused by the high instrument sensitivity for this compound and the saturation of the detector at the highest concentration point (the R^2 value would be greater than 0.99 if that point were excluded). The R^2 of all the area-with-NOM (y axis) vs. corresponding area-without-NOM (x axis) plots are higher than 0.99 except for ENR (0.95-0.98 in three cases) and OFL (0.97-0.98 in two cases) (Table 2-2), indicating strong correlations between the two series of corresponding instrument signals.

For the 11 antibiotics examined here, in 52 out of the 66 cases (79%) statistically significant signal suppression (i.e., m values < 1) was observed in LC-ESI-MS analysis after mixing with the NOM, and the decline ranges from 4 to 24% of the original signals (Table 2-2). In 13 out of the 66 cases there was no signal change, and only in 1 case (PEN-G with SRFA in CC III experiment) a 4% signal enhancement was observed (Table 2-2). The two anticonvulsants (CBZ and PRM) did not experience any statistically significant signal changes when mixed with any of the three NOM, under either constant ratio or constant concentration conditions (Table 2-2).

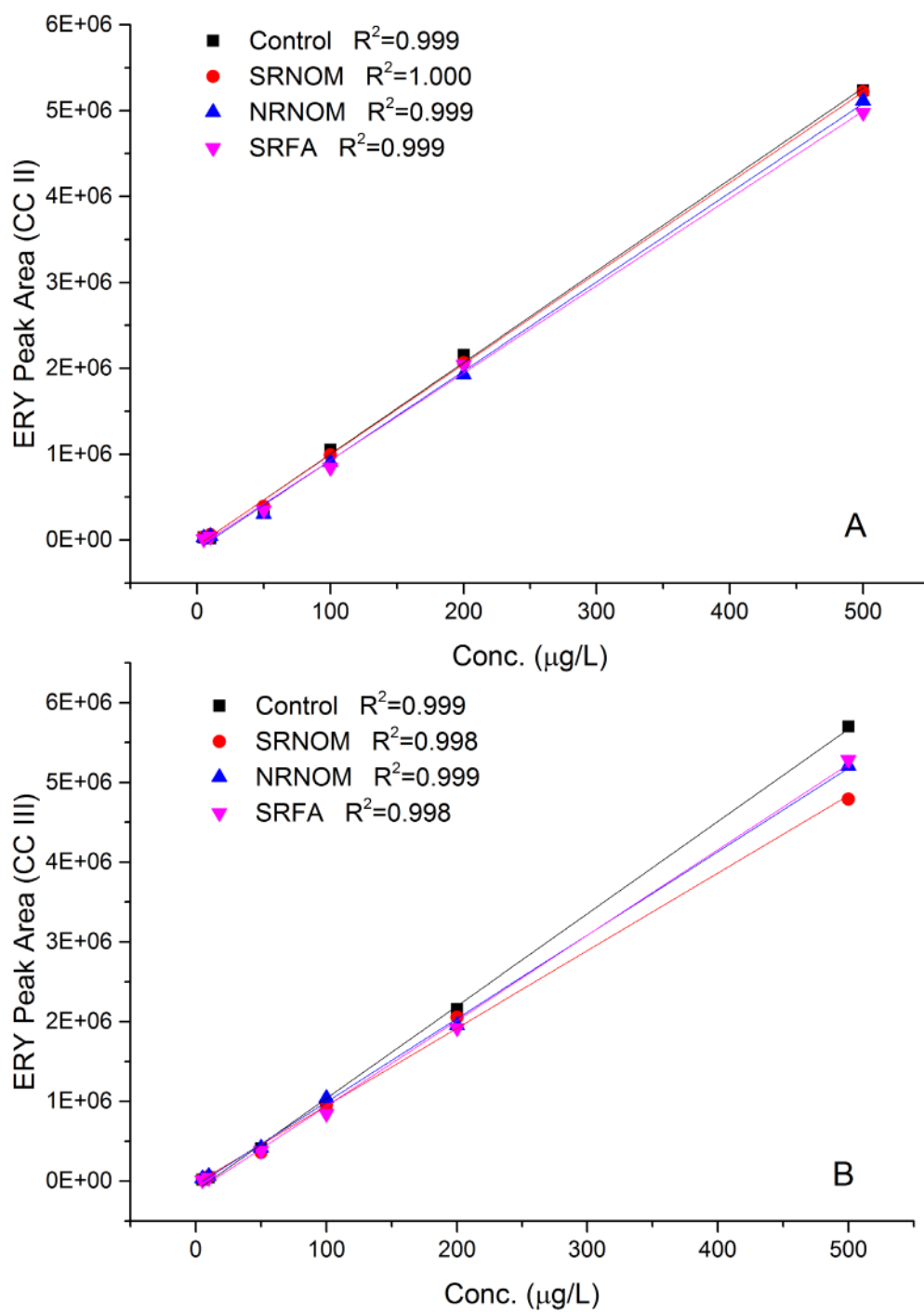


Figure 2-1 Calibration curves of ERY with and without NOM in constant ratio (A) and constant concentration (B) experiment.

Table 2-2 Statistical results of the instrument signals with and without the presence of NOM. Statically significant m values are highlighted in red (95% confidence level).

Antibiotics		Constant Ratio Experiments (CC II)								
		SRNOM			NRNOM			SRFA		
Category	Abbr.	m	Sig.	R ²	m	Sig.	R ²	m	Sig.	R ²
Beta-lactam	AMO	0.980	0.409	0.999	0.920	0.004	0.999	0.920	0.004	0.999
	PEN-G	0.910	0.001	1.000	0.860	0.000	1.000	0.850	0.000	1.000
Fluoroquinolones	ENR	0.840	0.000	0.996	0.920	0.063	0.999	0.840	0.000	0.984
	OFL	0.850	0.001	0.997	0.960	0.395	0.997	0.870	0.001	0.994
Sulfonamides	SDZ	0.990	0.860	1.000	0.950	0.138	1.000	0.950	0.142	1.000
	SMZ	0.960	0.038	1.000	0.940	0.000	1.000	0.930	0.000	1.000
	SMX	0.980	0.412	1.000	0.970	0.176	1.000	0.960	0.074	1.000
Macrolides	ERY	0.990	0.439	0.999	0.970	0.079	0.998	0.950	0.005	0.999
Tetracyclines	OTC	0.930	0.000	1.000	0.840	0.000	0.999	0.910	0.000	1.000
	CTC	0.850	0.000	1.000	0.790	0.000	0.988	0.830	0.000	0.994
Other	CHP	0.920	0.005	0.999	0.860	0.000	1.000	0.880	0.000	1.000
Anticonvulsants	CBZ	0.990	0.925	1.000	0.980	0.738	1.000	0.980	0.814	1.000
	PRM	0.970	0.277	1.000	0.970	0.191	1.000	0.960	0.139	1.000
Antibiotics		Constant Concentration Experiments (CC III)								
		SRNOM			NRNOM			SRFA		
Category	Abbr.	m	Sig.	R ²	m	Sig.	R ²	m	Sig.	R ²
Beta-lactam	AMO	0.930	0.004	1.000	0.960	0.035	0.999	0.950	0.000	0.999
	PEN-G	0.990	0.384	1.000	1.010	0.367	1.000	1.040	0.005	1.000
Fluoroquinolones	ENR	0.760	0.003	0.951	0.770	0.003	0.965	0.840	0.040	0.991
	OFL	0.760	0.000	0.970	0.800	0.000	0.976	0.830	0.005	0.994
Sulfonamides	SDZ	0.940	0.019	1.000	0.940	0.009	1.000	0.940	0.014	1.000
	SMZ	0.930	0.000	1.000	0.940	0.000	1.000	0.930	0.000	1.000
	SMX	0.920	0.000	1.000	0.910	0.000	1.000	0.930	0.000	1.000
Macrolides	ERY	0.840	0.000	0.997	0.900	0.000	0.999	0.930	0.000	1.000
Tetracyclines	OTC	0.970	0.109	1.000	0.860	0.000	0.999	1.010	0.820	0.999
	CTC	0.830	0.000	0.997	0.800	0.000	0.986	0.900	0.000	0.997
Other	CHP	0.920	0.000	1.000	0.930	0.000	1.000	0.930	0.001	1.000
Anticonvulsants	CBZ	1.010	0.922	1.000	1.010	0.882	1.000	1.030	0.662	1.000
	PRM	0.990	0.770	1.000	1.030	0.106	1.000	1.010	0.530	1.000

“m” is the slope of peak area-with-NOM (y axis) vs. peak area-without-NOM (x axis);

“Sig.” is the value of significance of difference between two series of instrument signals (with and without NOM);

“R²” is the square of correlation coefficients of the peak area-with-NOM (y axis) vs. peak area-without-NOM (x axis).

In the constant ratio (CC II) experiments, signals for SDZ and SMX (in addition to CBZ and PRM mentioned before) showed no statistical differences before and after the addition of either one of the three NOM (Table 2-2). AMO and ERY experienced either no effects or slight signal suppression (up to 8%) with the NOM (Table 2-2). Statistically significant signal suppression occurred to the remaining analytes to some degree, where fluoroquinolones (ENR and OFL) and tetracyclines (OTC and CTC) suffered the most (by as much as 17%).

In the constant concentration (CC III) experiments, the signal suppression is slightly higher than those in the CC II experiments in most cases. The fluoroquinolones (ENR and OFL) again appeared to have suffered the greatest suppression (by > 20%). Signals of ERY decreased by 16% while those of CTC dropped by 17% (Table 2-2). The signals of OTC (in the same group as CTC) however, did not show any statistical differences. The signals for PEN-G did not change when SRNOM or NRNOM was added but some minor enhancement was observed with the addition of SRFA (by 4%, the only one in all 78 cases). The remaining compounds all experienced suppression to a certain extent (within 10%).

2.4 Discussion

2.4.1 General mechanisms for LC-ESI_MS signal suppression

Sorptive interactions between organic compounds and NOM have been well observed and described [64, 67, 76, 85]. Possible interactions include van der Waals forces, hydrophobic

interaction, hydrogen bond, π interaction and electrostatic effects between opposite charges [72, 73]. These weak interactions have clear effects on solution phase spectroscopic analysis to a certain extent [72, 80].

However, noncovalent interactions in a gas phase such as in the ion source act quite differently than in a solution phase. Other than hydrophobic interaction which is a strong attraction in water but becomes partly or completely lost in a gas phase [86], interactions based on charges, dipoles, and polarizability could survive in a gas phase environment. Electrostatic bonding between opposite-charged organic species in solution decreases by the dielectric constant of water, however it is expected to become strengthened in a solventless gas phase environment in the ion source and produces a signal reduction in comparison to a control [72, 87].

Weak interactions imply that they can be broken down easily. For example, proteins and other biomolecules can interact weakly via hydrophobic interactions, van der Waals associations as well as hydrogen bonding in a solution phase, but they could be separated chromatographically to become labile in the gas phase during ionization [72]. Furthermore, although ESI is a very soft ionization technique and noncovalent complexes can be transferred intact from the solution phase into the gas phase [86, 88, 89], in general the noncovalent bonding is easily dissociated by the application of excess heat or high voltages in the atmospheric pressure ion source [87], as indicated by their relatively low bonding energies [90, 91]. In fact, temperature lower than 120 °C is often used as the capillary temperature to study noncovalent bonding energies in macromolecules such as drugs, peptides, proteins, and DNAs [86, 92-94].

Voltage or thermally induced dissociations of these weak interactions between

pharmaceuticals and NOM during ionization should be able to eliminate their effects on quantitative analysis [80]. For example, much broader recovery range (from 13% to over 200%) reported previously [78] may be partly due to relatively low ion source temperatures. However, noncovalent interactions may still persist at higher temperatures [89, 95]. For example, interactions (mostly hydrogen bonds) between cyclodextrin and peptide were still observed at a high ion source temperature of 400 °C, with a stable range of 180-260 °C [89]. π interactions were studied with ESI source at 120 °C [96], but there is a lack of direct support for the π interactions to tolerate higher temperature. However, considering their attractive energy (8-14 kcal/mol and 9-23 kcal/mol for selected $\pi^+-\pi$ and cations- π interactions, especially, which are higher than the typical hydrogen bond energy of ~5 kcal/mol [90, 91]), π interactions also have the potential to persist at temperatures above 120 °C. The declustering potentials used in this study are in a relatively low range except for PEN-G and ERY, and would not likely contribute significantly to the dissociation of weak interactions between pharmaceuticals and NOM [97, 98].

2.4.2 Signal changes related to physicochemical properties of analytes

Most of the m values in this study are less than 1 (Table 2-2), indicating that the MS instrument signals of most of our analytes have been suppressed by the presence of NOM.

AMO signal was affected by complexation with NOM which resulted in m values of 0.92-0.98 (all statistically significant except for the value of 0.98). AMO existed primarily as zwitterions under the experimental conditions (see Table 2-1), and the positive and negative charges in the AMO molecules are spatially separated and may act independently. Thus, positive moieties of AMO may interact with negatively charged functional groups in NOM, such as the carboxylic acid

group, leading to signal suppression. Similar influences could be found on other compounds with positively charged functional groups such as ERY (100% positive charge) and/or zwitterions such as ENR, OFL, CTC, and OTC (see Table 2-1 for distribution of ionic species).

The fluoroquinolones (ENR and OFL) suffered the largest signal suppression among all of our analytes (m values as low as 0.76). ENR has multiple positive charges and two aromatic rings in the structure (see Table 2-1 and A1), more than most of the other analytes. The fluorine and oxygen bonded to the aromatic rings would lower the π -electron density and hence promote the formation of π interaction with NOM. Moreover, they may also increase the bonding energy of π interaction [90] and make it difficult to disassociate at high temperatures. There are also multiple O and N atoms which could be involved in the formation of H-bonds. All of these would encourage noncovalent interactions between fluoroquinolones and NOM.

OTC and CTC are within the same compound classification (tetracyclines) and share similar molecular structures, but their signal suppression is somewhat different. CTC has a much larger suppression than OTC which may result from chlorine in the CTC structure. The chlorine bonded on the aromatic ring of CTC would significantly change the distribution of the electron cloud and hence reduce repulsion between aromatic rings and NOM, which would help to form π interaction. The chlorine may also generate a stronger dipole moment for CTC compared to OTC which would encourage other types of electrostatic interactions with NOM.

ERY experienced signal suppression with NOM in four out of six cases (Table 2-2), despite of the high declustering potential applied. Besides its positive charge (>98%, Table 2-1), ERY is the largest molecule in this study with a molecular weight of 733.9. The large molecule size would

positively contribute to London dispersion force. More importantly, there are many hydroxyl and carbonyl groups in the structure which are expected to form numerous hydrogen bonds with NOM, leading to signal suppression.

Sulfonamides (SMZ, SDZ and SMX) which show moderate suppressions are neutral/negative in solution under experimental conditions (Table 2-1). Electrically negative features may not contribute significantly to signal suppression because the NOM has been desalted and cation complexation would be limited. Nevertheless, like fluorine in NOR and OFL, the sulfonyl and amine groups bonded to the benzene ring would also reduce its electron density, therefore promote π -interaction. Hydrogen bonds are also possible on the H, N and O sites.

The electrically neutral CBZ and PRM were not significantly impacted by NOM because hydrophobic interaction in the gas phase is weakened in the absent of water. Even though CBZ and PRM also have aromatic rings, their structures are somewhat symmetric and thus the polarities are greatly reduced. As such, dispersion force would be limited. The electrostatic interactions like π stacking may not be as strong as other compounds and could be dissociated before entering the MS. Similar recoveries [78, 80] obtained in previous studies at a lower ion source temperature and cone voltage also suggest that the bond between CBZ and NOM is weak.

The situation is quite different for CHP which is also neutral but experienced some suppression. This discrepancy also could be explained by their structure differences. Besides more potential H-bonding sites, CHP contains two strongly electronegative chlorine atoms. The chlorines may also significantly change the polarity of the molecule, therefore increase the London dispersion force and dipole and quadrupole moments which are important factors in π stacking.

PEN-G was almost 100% anionic under the experimental conditions (Table 2-1) and, as previously mentioned, electrically negative features may not significantly contribute to signal suppression. Nonetheless, PEN-G contains one aromatic ring which could lead to π interaction, and H, N and O sites which could form H-bonds, resulting in signal suppression. The high declustering potential applied may partially dissociate weak interactions but moderate suppression was still apparent in the constant ratio experiments (CC II) (Table 2-2). In the constant concentration experiments (CC III) no suppression was evident in the presence of SRNOM and NRNOM, and a minor signal enhancement (statistically significant) was observed (Table 2-2). This result is counterintuitive because higher NOM concentrations were used in the CC III experiments, therefore, more suppression was expected (as was the case for most other antibiotics tested here). One possibility is that a higher background was registered in the PEN-G signals as the NOM content increased, masking the suppression resulted from the interactions between PEN-G and NOM, and even leading to a slight signal enhancement. Other studies have also observed signal enhancement for some compounds but there is no clear trend between enhancement and NOM concentrations [78, 99]. It was speculated that signal enhancement was due to the charge stabilization caused by NOM during the electrospray process [99].

2.4.3 Signal changes related to NOM characteristics

As reported by previous studies and reconfirmed in this study (data not shown), SRNOM masses were distributed around 400 m/z which can be the result of multiple charges [79]. The SRNOM and NRNOM contain not only the hydrophobic and hydrophilic acids but also other organic solutes that are present in natural water. They have been desalted and saturated with H⁺.

SRFA shows a similar mass spectrum [100] but contains only hydrophobic organic acids. The isolation of SRFA was performed using XAD-8 resin adsorption method which also involved a desalting step. The average molecular weight of SRNOM in filtrate is 12,800 [101] and it is speculated that NOM consists of supermolecular aggregates of small fragments held together by numerous noncovalent interactions [102]. The average molecular weight of SRFA is ~ 600 [103]. SRNOM consists of more aromatic but less aliphatic carbon than NRNOM. According to Thorn et al. [104], the aromatic carbon accounts for 23%, 19% and 24% of total carbon of SRNOM, NRNOM and SRFA, respectively, while carboxyl carbon accounts for 20%, 21% and 20%, respectively. While there are some differences among the three NOM, there is no clear correlation between the degree of signal suppression and types of NOM used. One possibility is that although there might be different associations between the analytes and different NOM in aqueous solution, such associations would be broken up to certain extent due to the relatively high temperature during ionization, thereby masking any differences caused by the differences in NOM properties.

2.5 Conclusions

The impact of three NOM on the quantitation of 11 antibiotics and 2 anticonvulsants using LC-ESI-MS was examined. The two anticonvulsants did not experience any signal changes when mixed with any of the three NOM, whereas all 11 antibiotics experienced some signal suppression when mixed with one or more of the NOM. The fluoroquinolones and tetracyclines experienced the most suppression (up to 24%) whereas the remain antibiotics experienced minor to moderate signal suppression (generally within 10%). Possible mechanisms leading to the signal suppression include hydrogen bonds and electrostatic interaction between positively charged

antibiotic species and negatively charged acidic groups of NOM, and π -interaction between the electron-withdrawing groups bonded aromatic rings of the analytes and NOM. The extent of signal suppression could be related to the physicochemical properties of the analytes, but a clear relationship with the types of NOM was lacking. Overall the signal suppression was moderate (up to 24%), and the impact on quantitation by LC-ESI-MS could be mitigated by using a standard mixed with a typical NOM (e.g., one of those used in this study), at a concentration similar to that in the sample matrix.

Chapter 3 Removal of antibiotics from water on sewage sludge and waste oil sludge derived adsorbents

Rui Ding, Pengfei Zhang, Mykola Seredych and Teresa J. Bandosz

Published on Water Research (46(13) p 4081-4090)

3.1 Introduction

One of the wastes produced by contemporary society in an abundant quantity is municipal sewage sludge, often referred to as biosolids. Biosolids are a mixture of exhausted biomass generated in the aerobic and anaerobic digestion of the organic constituents of municipal sewage and inorganic materials such as sand and metal oxides. Other sludges include wastes from such industries as shipyards, foundry, electroplating, tobacco, or paper mills. It is estimated that about 10 million dry tons of sewage sludge are produced in the US annually [105].

Various methods have been used to dispose of or utilize municipal sewage sludge [105], including incineration, landfilling, road surfacing, conversion to fertilizer, compression into building blocks, and carbonization [11]. Since 1976 several patents have been issued on carbonization of sewage sludge and various applications of the final materials [15-17]. Carbonization of sludge in the presence of chemical activating agents such as zinc chloride and sulfuric acid produces new sorbents, with applications in such processes as removal of organics in the final stages of water cleaning, and removal of chlorinated organics. Industrial sludges after dewatering processes/drying are either used in landfills or disposed mainly as hazardous wastes.

Materials resulted from carbonization of sludges have surface areas between 100 and 500 m²/g. Their performance as adsorbents of hydrogen sulfides [106], sulfur dioxide [107], basic or acidic dyes [108], phenol [24], copper [109], or mercury [110] has been reported as comparable or better than that on activated carbons. In many processes the excellent sorption ability of these materials is linked to the catalytic action of metals present in various forms in the final products. Their chemical states along with the location on the surface were reported as important factors

governing the pollutant removal capacities [111].

An estimated 100,000 to 200,000 tons of antibiotics are produced each year [112] as human and veterinary medicine [52, 53], and as much as 30% to 90% of administered antibiotics can be excreted without being metabolized [54]. The excreted antibiotics are often discharged into surface waters or leached into soils and groundwater from manure-based fertilizers or sewage sludge [53, 57], and have begun to accumulate in aquatic and terrestrial environments. In aquatic resources, measured antibiotic concentrations are typically $\mu\text{g/L}$ levels in hospital effluent, low $\mu\text{g/L}$ in wastewater, and low to high ng/L in various surface waters [54, 56, 57, 113]. Antibiotics have been shown to affect soil bacterial community structure and respiratory and enzymatic activities [58]. In addition, antibiotics in the environment may lead to the development and spreading of antibiotic resistance, a critical concern as it relates to the effectiveness of antibiotics in the treatment of human disease [53].

Advanced treatment processes including ozonation, chlorination, ultraviolet (UV) irradiation, nanofiltration (NF) and reverse osmosis (RO), and activated carbon adsorption have been applied to remove antibiotics from secondary effluent [56]. Ozonation is effective in removal of antibiotics from water and wastewater effluent but the potential transformation of antibiotics to products that remain biologically active and resistant to further ozonation is a concern [114]. Likewise, a major concern for treating pharmaceuticals by chlorination is the formation of chlorinated byproducts that may be more toxic than the parent compounds [115]. High UV radiation doses (20-100 times the typical disinfection dose) are often required to effectively degrade antibiotics in wastewater effluent due to the presence of dissolved organic carbon [116, 117]. In NF/RO filtration, fouling by the buildup of precipitated chemicals or microbial biomass

and membrane degradation due to exposure to residual chlorine can impact rejection of some antibiotics [118]. Adsorption capacity of 1-2 mmol/g of nitroimidazoles on activated carbon was reported [62]. In general, non-polar antibiotics can be effectively removed with activated carbon by hydrophobic interactions but the adsorption of more polar and charged compounds on these materials is much more difficult to predict [56]. Other methods of antibiotic removal reported in the literature include photodegradation with UV/catalysts or Fenton's reagent [119, 120], adsorption by carbon nanotubes [121] or clays [122], and ion exchange [123], and each has its limitations.

Since adsorption is one of the most promising methods for separation of various water pollutants, the objective of this paper was to evaluate sewage and waster oil sludge derived materials as antibiotic removal media. Two anticonvulsants (carbamazepine and primidone) that are barely removed during wastewater treatment were also included here, as adsorption might be an effective method of their separation. The sludge derived materials were shown previously as excellent adsorbents of dyes [108]. Taking into account the similarity in the sizes and chemistries of dyes and antibiotics, we hypothesized that the surface of sludge derived carbonaceous adsorbents would also be active to retain antibiotics. We measured the adsorption capacities and linked them to the specific surface features of adsorbents and to the properties of adsorbates. Finding applications of the sludge derived materials as adsorbents is an important issue from the point of view of environmental remediation. The process applied has the potential of turning hazardous wastes to adsorbents that could be used in wastewater and drinking water treatment.

3.2 Materials and methods

3.2.1 Adsorbents

The materials used in this study were described previously [108, 124]. They were obtained by pyrolysis of industrial waste oil sludge (WO) from Newport News Shipyard, dewatered sewage sludge from Wards Island Water Pollution Control Plant (SS), or their mixtures (SSWO, 50:50 ratio based on the wet mass), at 950 °C or 650 °C in a nitrogen atmosphere in a fixed bed (horizontal furnace). The materials are referred to as SS, WO and SSWO based on their composition, followed by 950 or 650 reflecting the pyrolysis temperature.

3.2.2 Characterization of adsorbents

Textural characterization was carried out using nitrogen adsorption-desorption isotherms (ASAP 2010, Micromeritics) at -196°C. The isotherms were used to calculate the specific surface areas, micropore volumes, mesopore volumes, total pore volumes, and pore size distributions. The latter was determined using the BJH method.

Potentiometric titration measurements were performed with a DMS Titrino 716 automatic titrator. The instrument was set in the equilibrium mode when the pH was collected. Each sample was titrated with 0.1 M HCl. Experiments were carried out in the pH range 3-10. The experimental data were transformed into a proton binding curves, Q , representing the total amount of protonated sites [125].

Thermal analysis was carried out using a TA Instruments Thermal Analyzer. The pH of water suspension was measured on a 0.4 g sample of dry adsorbent powder dispersed in 20 ml of

distilled water. Infrared spectroscopic measurements were done on Nicolet 380 FTIR spectrophotometer using Attenuated Total Reflectance method (ATR).

3.2.3 Adsorption of pharmaceuticals

Adsorption of pharmaceuticals was measured in closed batch experiments at room temperature. A mixture of pharmaceuticals was used due to the limited amount of the sludge-derived materials available for this work and the fact that many pharmaceuticals co-exist in wastewater. One mL of solution containing a mixture of 11 antibiotics plus 2 anticonvulsants (see Table B1 in Appendix B for the list of compounds) of various concentrations (from 0.1 mg/L up to 200 mg/L; see Table B2 for the concentrations used) was mixed with 0.050 g of a sludge-derived sorbent material in amber glass vials. Later analyses indicated that adsorption maximum was not reached for many compounds. Since the concentrations of the compounds could not be further increased due to solubility limitations, 10 mL of solution (with the highest two concentrations) was used to increase contaminant loadings. Duplicates were prepared for each concentration with each adsorbent. The sample vials were sealed and then shaken on an orbital shaker for 24 hours for the isotherm study. A preliminary study with the SSWO950 material indicated that this time is sufficient to achieve equilibrium (data not shown). After reaction, the adsorbate concentration in the supernatant liquid (C_e , equilibrium concentrations of the remaining antibiotics in the solution) was measured using liquid chromatography/tandem mass spectrometry (LC/MS/MS, described below) and the uptake (q_e) was calculated. The pH of the solution at equilibrium was also measured using an IQ125 miniLab pH meter from IQ Scientific.

The equilibrium data were fitted to the Langmuir-Freundlich (L-F) isotherm model [126] from which the limiting adsorption capacity was calculated. Non-linear regression was used to derive the fitting parameters.

3.2.4 LC/MS/MS method

All samples were analyzed using LC/MS/MS with electron spray ionization (ESI) and multiple reaction monitoring (MRM). A Shimadzu HPLC with an Agilent Eclipse Plus C18 (1.8 $\mu\text{m} \times 4.6 \text{ mm} \times 50 \text{ mm}$) column was used for compound separation. The temperature of the column oven was kept at 40°C. The mobile phase consisted of water (component A) and methanol (component B), each containing 0.1% (v/v) formic acid. The flow rate was 0.4 ml/min, and the following gradient elution program was used: 5% B for 1 min, 95% B from 2 to 5.5 min, and 5% B from 5.6 to 6 min. Ten μl of sample (after proper dilution) was injected through the autosampler, and the needle was automatically rinsed with 0.2 ml methanol between injections.

Mass spectrometry was performed with an ABI 4000 Q-trap mass spectrometer (Applied Biosystems, Carlsbad, CA) with an ESI ion source and N300DR nitrogen generator (Peak Scientific, Billerica, MA). Nitrogen was used as both the collision gas and nebulizing gas. The curtain gas, collision gas, and ion source gas 1 and gas 2 were set at 20, 6, 50, and 50 psi, respectively. The nebulizer current was set at 3 mA and the temperature of the interface heater was maintained at 400°C. Quantitation of all compounds was made by two MRM transitions (see Table B3 in Appendix B for the MRM transitions).

3.3 Results and discussion

3.3.1 Adsorption isotherms and capacities

Examples of the measured isotherms of three compounds (OTC, ENR and ERY, representing high, medium, and low adsorption, respectively) on SS950, WO950, and SSWO950 with the fit to the L-F equation (where possible) are presented in Fig. 3-1. It is noted that most of the compounds at environmentally relevant concentrations (e.g., 0.1 to 1 mg/L, see Fig. 3-1 for an example) were completely removed by the adsorbents. As such, it was necessary to use much higher concentrations to determine the maximum adsorption capacities. For the majority of adsorbents, the shape of isotherms indicates the existence of high energy adsorption sites on the sorbent surfaces. For some compounds (e.g., ERY and PRM), the uptake (q_e) by the adsorbents decreased significantly at the two highest contaminant loadings (see Fig. 3-1C for an example), suggesting competitive adsorption among the compounds. The observed adsorption capacities for each compound at the highest contaminant loading are presented in Figure 3-2A. Since the highest contaminant loadings were different for some compounds due to solubility limitations, the removal efficiencies (%) at the highest loading are also presented here (Figure 3-2B).

When the adsorbed amounts of each species are compared, OTC and CTC show highest amounts adsorbed (up to 33 mg/g, or 0.07 mmol/g) with respect to the other pharmaceuticals examined here (Fig. 3-2A). These two compounds are among the three compounds with the largest polar surface areas (close to 200 Å², Table 3-1). Further, over 65% of the OTC molecules and over 82% of the CTC molecules have a positively charged functional group at the solution pH (6.8-8.7, see Tables B4 and B5 in Appendix B). ERY, another antibiotic with a high polar surface area

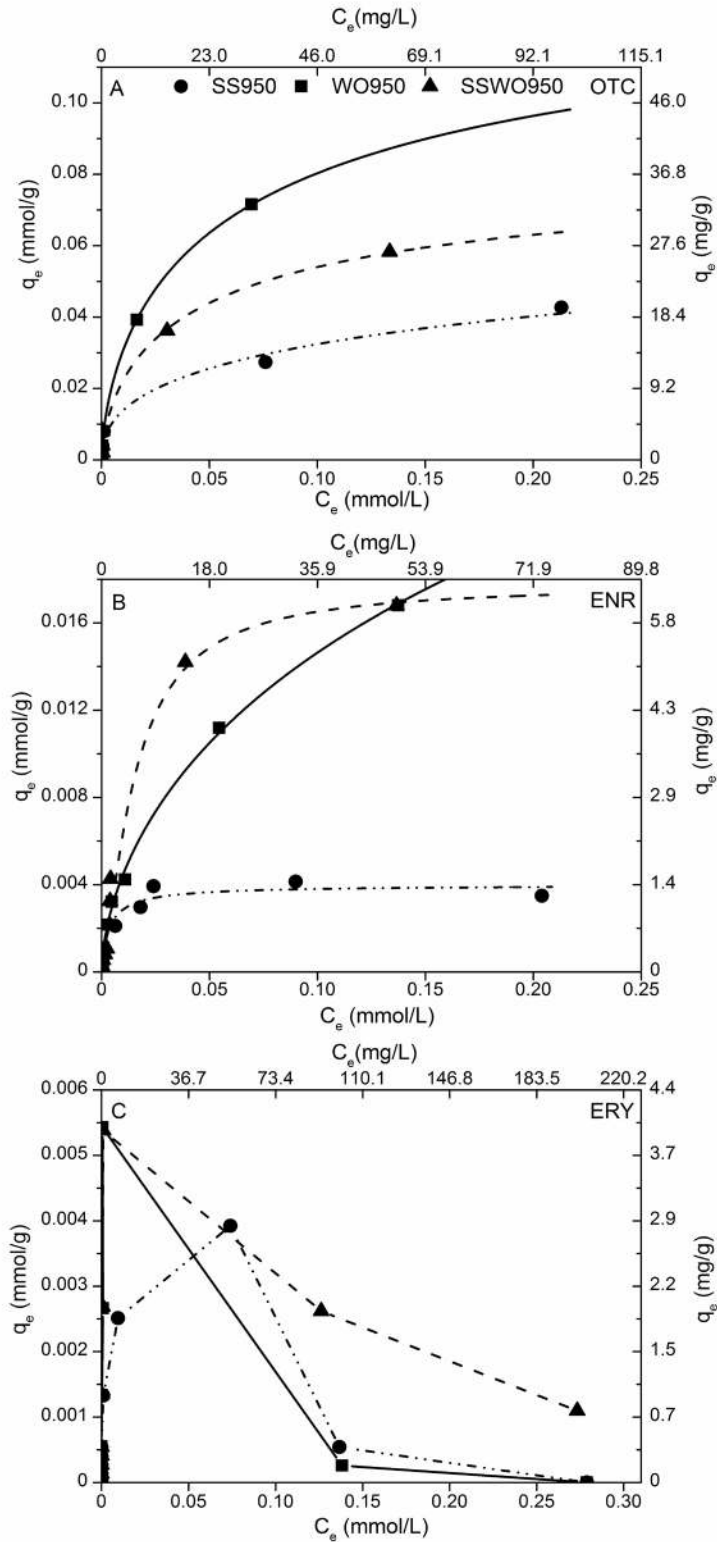


Figure 3-1 Examples of the adsorption isotherms for OTC, ENR, and ERY on the sludge derived adsorbents SS950, WO 950 and SSWO950. The smooth lines represent best fit to the data with the L-F model.

Table 3-1 Some physical properties of the antibiotics and anticonvulsants tested in this study.

Category	Name	Abbr.	Polar surface area (Å ²) ^a	Topological Diameter (Å) ^a	Molar volume (cm ³) ^b
Beta-lactam	Amoxicillin	AMO	158	16.9	236.2
	Penicillin-G K salt	PEN-G	87	15.7	235.2
Fluoroquinolones	Enrofloxacin	ENR	64	16.8	259.3
	Ofloxacin	OFL	73	15.6	243.9
Sulfonamides	Sulfadiazine	SDZ	106	13.2	167.2
	Sulfamethazine	SMZ	106	12.9	199.8
	Sulfamethoxazole	SMX	107	13.2	173.1
Macrolides	Erythromycin	ERY	194	17.6	607.0
Tetracyclines	Oxytetracycline HCl	OTC	202	14.2	268.1
	Chlortetracycline HCl	CTC	182	14.3	270.7
Other antibiotics	Chloramphenicol	CHP	115	14.4	208.8
Anticonvulsants	Carbamazepine	CBZ	46	9.0	186.5
	Primidone	PRM	58	8.9	191.7

^aCalculated by ChemBioOffice 2010 (CambridgeSoft); ^bObtained from SciFinder.

(also close to 200 Å²) and partial positive charges, however, was adsorbed in smaller quantities than were OTC and CTC (Figs. 3-1 and 3-2). It has the highest molar volume and topological diameter among the pharmaceuticals tested (Table 3-1), thus the large molecular size may limit its access to micropores, leading to the small amount adsorbed. Moreover, ERY appeared to be displaced by other molecules such as OTC and CTC as the contaminant loading increased (Fig. 3-1C). Since the three sulfonamides (SDZ, SMZ, and SMX) are among the smallest compounds tested here (Table 3-1), they should have the advantage of entering micropores. Interestingly, they were adsorbed in relatively low quantities (Fig. 3-2). Obviously, the size of the adsorbate is not the only factor affecting the adsorption process. At the solution pH (6.8-8.7), the three

sulfonamides are predominately negatively charged (Table B5), which may have hindered their interactions with the surface of the adsorbents (slightly negative at the solution pH of 6.8-8.7). Among the three neutral compounds, CBZ had higher affinity for adsorption on our materials than CHP and PRM (PRM was displaced by other compounds at the highest contaminant loadings). The physicochemical properties of CBZ and PRM are very similar except for hydrophobicity, i.e., CBZ is more hydrophobic (logKow of 1.51) than PRM (logKow 0.91). CHP is slightly larger and more polar (Table 3-1) than CBZ but less hydrophobic (logKow of 1.14). The difference in hydrophobicity may be an important factor affecting adsorption of neutral compounds by the adsorbents used here.

When the adsorption capacities of our materials are considered, the WO and SSWO materials show similar performance whereas the amounts adsorbed on SS materials are smaller (Fig. 3-2). This difference is more apparent when the total adsorption capacities (sum of adsorption capacities for all compounds tested) are compared (Fig. 3-3). On the WO and SSWO materials about 100 mg of the pharmaceuticals were adsorbed per g of adsorbent at the highest contaminant loading, twice the amount adsorbed on the SS materials. The adsorption capacities for the adsorbents obtained at the two different temperatures (650 °C and 950 °C) appeared to be similar (Fig. 3-3). It is important to mention that the maximum adsorption capacities obtained from fitting the L-F equation to the data for the 6 materials tested here (80 -300 mg/g, Fig. 3-3) are comparable to the adsorption capacities of 3 different activated carbons for nitroimidazole antibiotics (200-400 mg/g) [62].

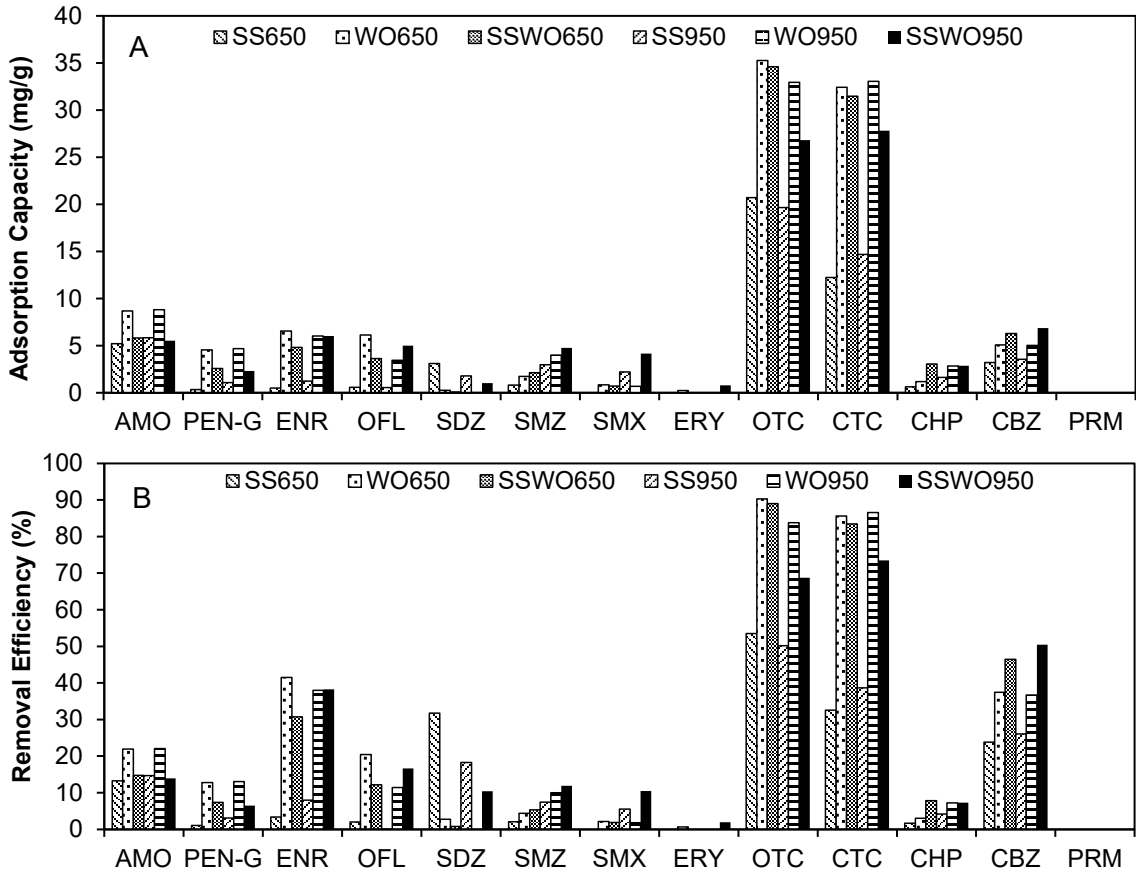


Figure 3-2 Maximum observed adsorption capacities (A) and percent removal of each species at the highest contaminant loading (B).

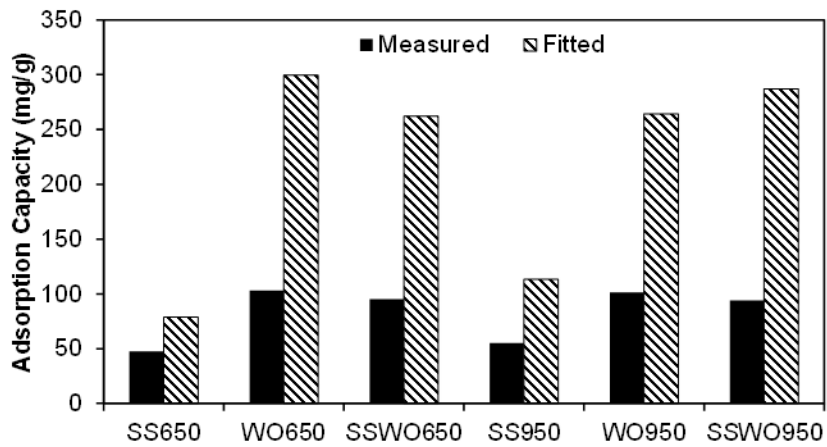


Figure 3-3 Comparison of the total adsorption capacities for the compounds tested on the sludge derived adsorbents. “Measured” represents the amount adsorbed at the highest contaminant loading, whereas “Fitted” represents the values obtained from the L-F model.

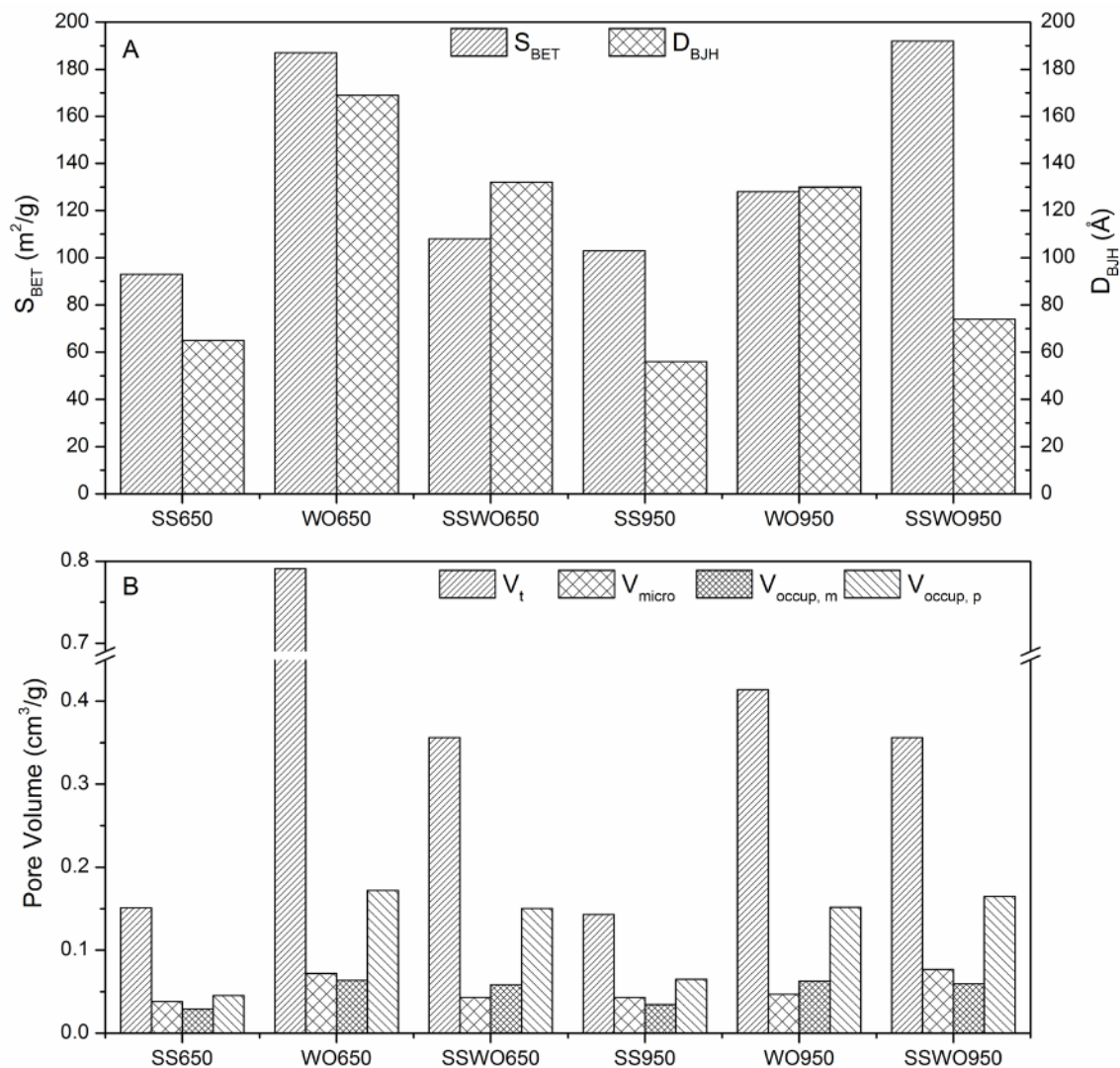


Figure 3-4 A) Surface area (S_{BET}) and average pore sizes (D_{BJH}); B) Total volume (V_t) and volume of the micropores (V_{micro}) of the adsorbents, and the volume occupied by the compounds derived from the amount adsorbed at the maximum contaminant loading ($V_{occup, m}$) and from the maximum capacity predicted from the L-F model ($V_{occup, p}$).

3.3.2 Material characteristics and adsorption performance

In order to understand the complex behavior of our materials, the properties of both adsorbates and adsorbents have to be analyzed. Even though the surface features of the sludge derived materials have been described in detail elsewhere [108, 124], for the sake of clarity and more meaningful data interpretation, we briefly summarize the previously published results here.

Parameters of the porous structure determined from nitrogen adsorption isotherms and pore size distributions are important to evaluate the performance of any adsorbent. They are presented in Fig. 3-4 and Figure B1 of Appendix B, respectively. The porosity of our materials is mainly in the range of mesopores with sizes between 30 and 1000 Å. The surface areas range from 100-180 m²/g (S_{BET}) with the average pore sizes of 50 -150 Å (D_{BJH}) (Fig. 3-4A), which is consistent with the mesoporous nature of our samples. The best performing adsorbents have the highest degree of microporosity and smallest pores. Since the estimated sizes of our adsorbate molecules are smaller than 20 Å (Table 3-1), the micropores should be the high energy adsorption centers, if physical adsorption is the predominant adsorption mechanism [127]. We have to also consider that in our system the compounds of various chemistries and geometries are present and each of them would tend to occupy the most energetically favorable centers. Therefore, the competition for the adsorption centers cannot be ruled out. Moreover, specific adsorption and reactive adsorption mechanisms [128] are also highly probable to take place and they are discussed later in this paper. Nevertheless, for the latter adsorption mechanisms, the molecules have to be first physically attracted to the surface. Based on the volume of micropores the order of the performance should be the following: SSWO950 ≈ WO650 > WO950 ≈ SSWO650 ≈ SS950 ≈ SS650 (Fig. 3-4B). However, the adsorption capacities of the first four materials (WO and SSWO) are similar, and

are more than twice the capacities of the last two materials (SS) (Fig. 3-3). These results suggest that physical adsorption is not the sole mechanism that governs the removal of the pharmaceuticals on our adsorbents. This notion is supported by the comparison of the volume of the species adsorbed and the volume of micropores (V_{micro}) (Fig. 3-4B). The occupied volume derived from the molar volume of each compound and the amount adsorbed under the maximum contaminant loading, $V_{\text{occup, m}}$, was very close to the V_{micro} for the 6 adsorbents (Fig. 3-4B). For the SS650, SS950, and SSWO950 materials more than 50% of the micropores are probably too small ($< 9\text{\AA}$, Fig. B1) for the compounds tested here (topological diameter $>9\text{\AA}$, Table 3-1), thus some adsorption must have occurred in mesopores. The occupied volume derived from the predicted maximum adsorption amount (based on the L-F fits), $V_{\text{occup, p}}$, was 1.2-3.2 times of V_{micro} (Fig. 3-4B), further supporting the notion that mesopores (where specific/chemical interactions can take place) were involved in the adsorption of the compounds.

When chemisorption or reactive adsorption is considered as possible adsorption mechanisms, the sizes of pores and the accessibility/distribution of reactive centers are of paramount importance. For the presence of active centers, the surface chemistry has to be analyzed. The elemental analysis indicated that our materials have up to 20 wt % of carbon (less in high temperature carbonized adsorbents) [106, 129], 3.2-6.1 % of iron, 4-5.1 % of calcium, 0.13-0.25 % of copper, 0.1-0.59 % of zinc and 1.3-11 % of magnesium [108, 124, 129]. The surface pH varies between 9.3 and 10.9, indicating their strong basic character. While there are no significant differences in the amounts of iron or calcium between the adsorbents, magnesium exhibits a very broad range of concentrations. The highest content of this element is found in the waste oil derived adsorbents, especially in WO650 (11%) [124]. When the sludges are pyrolyzed at relatively low

temperature (650 °C) the solid state transformations of an inorganic matter does not occur to a great extent [129] and an inorganic phase is expected to be quite active in chemical reactions. The XRD analysis indicated that in WO650 besides aluminum in the metallic form, huntite ($\text{Mg}_3\text{Ca}(\text{CO}_3)_4$), sapphirine ($(\text{Mg}_4\text{Al}_4)\text{Al}_4\text{Si}_2\text{O}_2$), barringerite, (Fe_2P), goethite ($\text{FeO}(\text{OH})$) and almandine ($\text{Fe}_3\text{Al}_2\text{SiO}_4$) are also present. Heating this material at 950 °C results in the appearance of metallic iron, lepidirocite ($\text{FeO}(\text{OH})$), bornite (Cu_5FeS_4), zincite (ZnO), quartz (SiO_2) and ankerite ($\text{Ca}(\text{Fe}, \text{Mg})(\text{CO}_3)_2$), hibonite ($\text{CaAl}_{12}\text{O}_{19}$) and vaterite (CaCO_3) [129]. From all these compounds, carbonates appear to be the salts which might be involved in chemical exchange reactions with antibiotics having carboxylic acid- or phenol-based acidic groups. Indeed, the affinity of such compounds (e.g., OTC, CTC, AMO, PEN-G, ENR, and OFL) to the adsorbents containing waste oil (WO and SSWO) was the highest among all compounds tested here (Fig. 3-2). It is possible that the salts formed precipitated in the pore system, and the large volume of pores favors this process. The presence of inorganic amorphous oxides from the thermal decomposition of magnesium salts during pyrolysis cannot be ruled out. Carbonates were also found in SS650 (MgCO_3), SSWO950 (vaterite (CaCO_3), smithsonite (ZnCO_3)) [129]. They may contribute to the significant uptake of the majority of our adsorbates on the latter material. In the case of SS650 the presence of small micropores can limit the accessibility of the bulky adsorbate molecules to the reactive sites.

The polarity of adsorbents' surface can also play a crucial role in the specific adsorption, especially where there is some degree of compatibility with the properties of the adsorbate. The polar surface area (PSA) for each antibiotic was calculated using ChemOffice (CambridgeSoft, Cambridge, UK) and the values obtained are listed in Table 3-1. PSA characterizes the polar part

of the molecular surface and is defined as the part of this surface corresponding to oxygen and nitrogen as well as hydrogen heteroatoms attached to these atoms. The biggest polar surface areas are exhibited by OTC, ERY, CTC, and AMO, and three of them (OTC, CTC, and AMO) have the highest adsorption to waste oil derived materials (Fig. 3-2A). Our analysis indicates that in addition to micropores, mesopores also played an active role in adsorption, especially on the surface of the waste oil derived materials (Fig. 3-4B). In those pores the polar mineral phase is the predominant chemical constituent of the pore walls. Therefore, it appears that polar interactions of the adsorbates with the polar mineral phase are another important mechanism of adsorption. The lack of adsorption of ERY could be attributed to its large size (molar volume of 607 cm³, Table 3-1), which may limit its access to the micropores (where physical adsorption occurs) and subsequently to the larger mesopores where chemical adsorption occurs. In contrast to the mesopores in which the polar mineral phase dominates, the micropores are of a carbonaceous or mixed origin and are important sites for the adsorption of non-polar compounds such as CBZ.

The surface chemical reactivity of our adsorbents towards acids is confirmed by the results of potentiometric titration. The proton binding curves presented in Fig. B2 (Appendix B) show the basic character of the surfaces with the highest reactivity of WO650 and SSWO650. SSWO950 becomes reactive in strongly acidic environment. Interestingly, both sewage sludge derived adsorbents appear as the most stable. This is linked to their low content of magnesium, which we hypothesize is the active species enhancing reactive adsorption of antibiotics containing acidic groups on the materials having the waste oil component. Even though the majority of acidic groups present on the surface of our adsorbates cannot be considered as very strongly acidic (Table B1),

one has to take into account the shift in chemical equilibria in confined spaces and thus different behavior of these groups than that in the bulk phase.

3.3.3 FTIR result

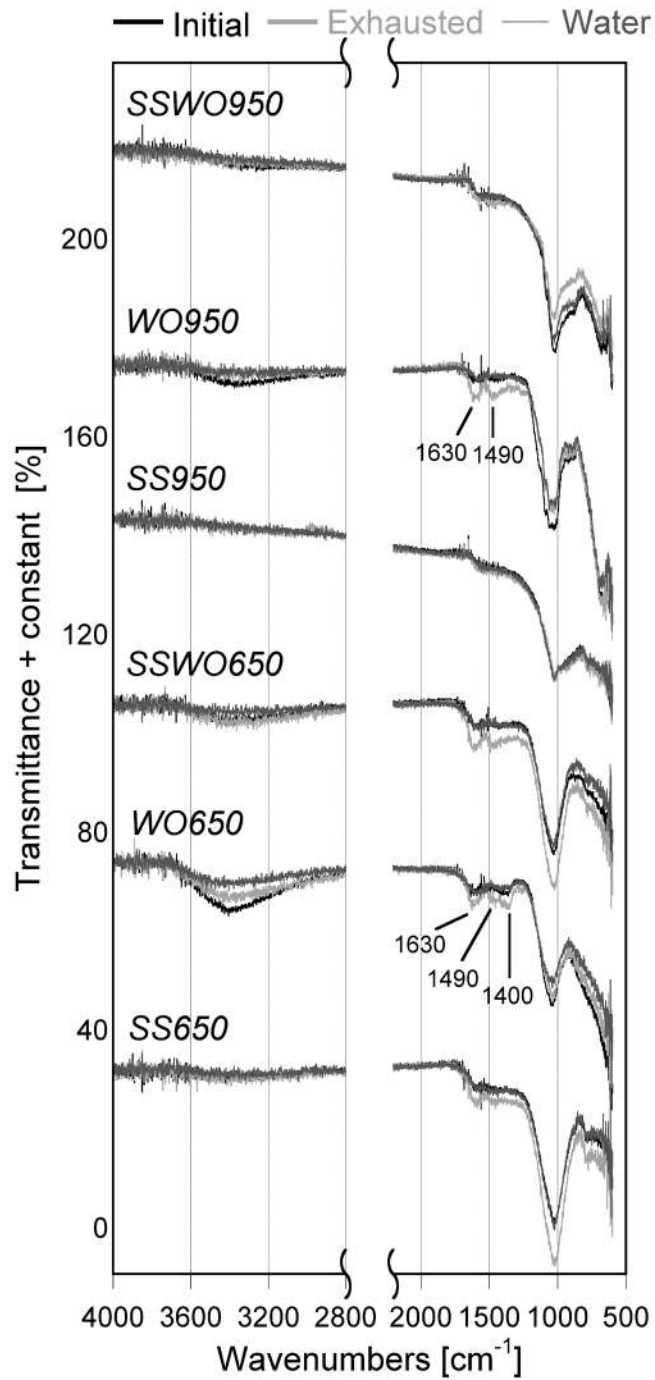


Figure 3-5 FTIR spectra for the initial, water exposed, and exhausted (after adsorption under the highest loading of pharmaceuticals) sludge materials.

The surface chemistry of the adsorbents before and after exposure to antibiotics was also analyzed using FTIR and the spectra are presented in Fig. 3-5. The main difference between the waste-oil- and sewage-sludge-derived adsorbents is the well-defined band in the wavelength range 3200-3600 cm^{-1} representing vibrations of OH groups. This band is even revealed on the spectrum for WO950 indicating the presence of hydroxides (likely magnesium based), which contribute to the reactivity of these adsorbents' surfaces with acidic groups of adsorbates. The intense bands between 800 and 1200 cm^{-1} represent Si-O(Si) and Si-O(Al) from tetrahedral or alumino- and silico-oxygen bridges in aluminosilicates [130]. The small band between 1400 cm^{-1} and 1700 cm^{-1} are more visible for samples heated at 650 °C than for their high temperature counterparts. This might be related to the oxygen groups incorporated to the carbonaceous phase and might include vibrations from carboxylic groups at about 1100 and 1650 cm^{-1} or C-O groups at about 1400 cm^{-1} . Some of these groups are destroyed when heated at high temperature. The band at 800 cm^{-1} is attributed to the vibration of quartz [130]. Exposure of the adsorbents to high concentrations of pharmaceuticals causes visible changes in the region between 1250 cm^{-1} to 1700 cm^{-1} . Thus, the visible new bands at 1630 cm^{-1} and 1490 cm^{-1} and 1400 cm^{-1} (Fig. 3-5B) are the results of vibrations of various bonds in the adsorbates associated with benzene rings, double bonds, and heteroatoms in the functional groups. Owing to the variety of the adsorbates used and their complex chemistries, a more precise assignment of the bonds is not possible. Interestingly, for the samples obtained at 650 °C the intensity of the bands at about 1000 cm^{-1} increase after adsorption of pharmaceuticals whereas the opposite effect is revealed for the high temperature treated samples. While the decrease in the intensity can be caused by adsorption of organic molecules on the surface, an increase for SS650-E and SSWO650-E can be linked to the formation of salts on the surface with the involvement of organic moieties. To account for the effect of water on the surface

chemistry changes, the FTIR spectra were also collected for the samples exposed to pure water only for the same period of time as that in the adsorption experiments. As seen from Figure 3-5, this treatment does not result in any changes in the spectral range between 1250 and 1700 cm^{-1} . On the other hand, the intensity the band related to $-\text{OH}$ groups decreases, especially for WO650. We link it to the instability of this adsorbent and dissolution of some hydroxide in water. Adsorbed organic molecules likely screen $-\text{OH}$ groups and/or limit their dissolution and thus this effect is smaller.

3.3.4 Thermal analysis result

Valuable information about the surface reactivity and organic compounds adsorbed on the surface of the exhausted materials can be also derived from the analysis of the weight lost as a result of heat treatment in an inert atmosphere. The DTG curves measured in nitrogen for the initial samples, those exposed to water only (W) and after adsorption of pharmaceuticals (E) are presented in Fig. 3-6. As seen, exposure to water resulted in hydration of the samples, especially those obtained at low temperature and those obtained from waste oil. This is the result of formation of hydroxides and hydrated salts, which decompose during heating. After adsorption of pharmaceuticals more complex weigh loss patterns are revealed. The first peak centered at about 110 $^{\circ}\text{C}$ represents removal of physically adsorbed water. Then for the initial samples the continuous small weight loss between 200 and 600 $^{\circ}\text{C}$ is assigned to the decomposition of various inorganic salts as carbonates and oxy(hydroxides). Although for the sample exposed to pharmaceuticals, the weight loss in all cases differ and is related to the surface reactivity and the

capacity, a common feature is the presence of peaks of various intensities at about 180 °C, 250 °C, and 400 °C. For the WO950-E also the weight loss between 500 and 800 °C is clearly visible. The

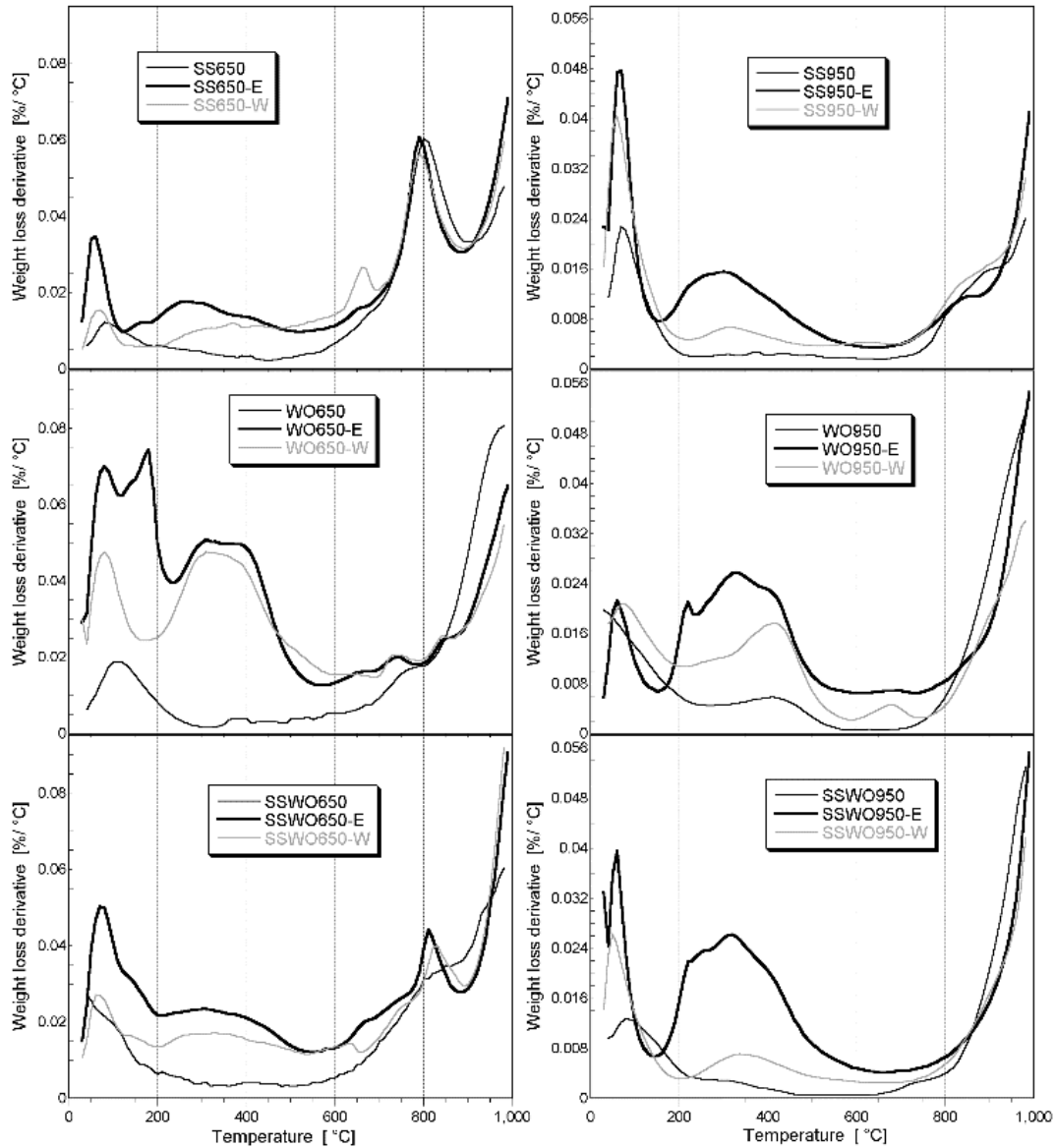


Figure 3-6 DTG curves for the initial, water exposed (-W), and exhausted (-E, after adsorption under the highest loading of pharmaceuticals) sludge materials.

peaks at these temperatures are also revealed for the other oil sludge derived samples but since the samples were exposed only to 650 °C their interpretation is rather problematic. The most heterogeneous surface and the most pronounced changes in the weight loss are observed for WO650, WO950 and SSWO950 and, as discussed above, these samples exhibit relatively high capacities for antibiotics with acidic groups and those with large sizes of the molecules. The TA results support the hypothesis that the addition of sewage sludge favors the adsorption of smaller molecular weight species, which are desorbed at lower temperatures. This is consistent with smaller pores introduced in the sewage sludge component. For the water-stable SS950 and SSWO950 samples a broad peak between 200 and 600 °C is found representing removal/decomposition of various antibiotics adsorbed, likely via physical adsorption. That weight loss pattern for WO950-E is much more complex. A few maxima are noticed on the weight loss with the higher temperature desorption range. This supports formation of salts on this material with the involvement of an inorganic matter.

3.3.5 Environmental Implications

Industrial and municipal sludge and other industrial wastes can be used as precursors for new materials, thus environmental pollution caused by accumulation of those wastes will be eliminated. The materials obtained will create a new class of inexpensive adsorbents for the removal of not only pharmaceuticals but also metals, dyes, and other contaminants from water. This would certainly lead to a healthier, more sustainable environment. Applications of these materials to water reuse would lead to more sustainable water resources.

3.4 Conclusions

Even though the systems presented in this study are very complex, the objective of this research was accomplished by demonstrating the high potential of the sludge derived materials as adsorbents of trace amounts of antibiotics. On their surface, significant quantities of antibiotics of various topographies and chemistries were retained. Physical adsorption, reactive adsorption and specific polar interactions were indicated as the mechanisms of the separation process. The variety of antibiotics was adsorbed on the surface of the sludge derived adsorbents owing to its high degree of heterogeneity linked to the pores of specific sizes of hydrophobic nature and existence of the reactive/polar phase dispersed in the pore walls. It ensured not only the accessibility of the high-energy adsorption centers but also the possibility of precipitation of surface reaction products within the pore system. Further studies on model systems are needed to identify the adsorption centers for particular molecules and the mechanism of specific adsorption/reactive adsorption processes.

Acknowledgements

This work was partially supported by a STAR grant from the United States Environmental Protection Agency (US EPA, RD835178). Any opinions, findings, and conclusions or recommendations expressed in this material are those of the authors and do not necessarily reflect the views of the US EPA. R. Ding would like to acknowledge a graduate fellowship from the Dean's Office.

Chapter 4 Leaching of heavy metals from sewage sludge/fish waste based composite adsorbents and the effects of post carbonization acid wash

4.1 Introduction

Municipal sewage sludge, often referred to as biosolids, is one of the byproduct wastes produced by wastewater treatment plants in large quantities. It is estimated that the United States and the European Union each produces about 10 million tons of dry sewage sludge annually [5, 131]. China adds another 6 million tons of dry sludge per year [6], and this number is likely to grow in the near future. Sewage sludge typically contains high levels of nutrients, metals, persistent organic pollutants, pathogens, etc. [1-3], and requires proper treatment and disposal.

Like sewage sludge, fish waste is also being generated in large quantities. The world fish production in 2010 was 114.5 million tons, and up to 50% ended up as waste [7]. Over the past years, commercial fish waste was usually landfilled or discharged as processing effluents into water bodies. The processing effluents are highly likely to produce adverse effects on the receiving coastal and marine environments [132].

Traditional methods to dispose of sewage sludge such as utilization as fertilizer, incineration, and landfilling have been limited by either regulations or cost [1]. Carbonization of sludge to produce adsorbents becomes an especially promising approach at present because of the potential to valorize sewage sludge. There has been a wealth of research showing that sewage sludge based adsorbents (SBAs) are capable of removing contaminants such as Cu^{2+} , Hg^+ , Cd^{2+} , dyes, phenolic compounds and pharmaceuticals from water [1, 63, 133].

In order to further diversify the surface features of SBAs and explore more options of waste reclamation, fish waste which is a source of carbonaceous material and elements such as P, Ca, and Mg that could form catalytic centers after pyrolysis, was added to sewage sludge as a

secondary component to produce a new type of SBAs. It has been proven that these SBAs with fish as additives work effectively in removing pharmaceuticals such as carbamazepine, sulfamethoxazole and trimethoprim from water [34, 35].

Before the practical applications of SBAs in wastewater or drinking water treatment, however, it is necessary to evaluate whether SBAs can cause secondary pollution. There exists a general fear of the use of sewage sludge derived materials in drinking water treatment due to the presence of toxic biological and chemical components in the raw materials. The presence of heavy metals in the raw sludge is one of the main issues potentially preventing applications of SBAs [134]. While all of the toxic organic compounds and pathogens could be destroyed during pyrolysis (up to 900 °C), heavy metals still remain. Although thermal treatment can significantly stabilize heavy metals in sludge [135, 136], there is evidence that some of the metals such as Cr and Cu are leachable even after 900 °C treatment [133, 136]. Acid washing may be used as a method to reduce the leachable components and to increase the BET surface areas and porosity of SBAs by dissolving basic oxides [1, 133].

Thus, the purpose of this paper is to investigate the heavy metal leaching behavior of sludge and fish waste based adsorbents, and to evaluate acid washing on minimizing metal leaching while enhancing the capacity of adsorption for organic pollutants.

Three organic compounds (atenolol (ATN), carbamazepine (CBZ), and N-nitrosomethylethylamine (NMEA)) were selected to represent the potential target contaminants in order to evaluate the adsorption performance of the SBAs. ATN and CBZ are pharmaceutical compounds ubiquitous in natural water bodies and drinking water sources [137]. NMEA belongs

to nitrosamines, a family of potent carcinogens and widespread disinfection by-products [138] included in the USEPA's second Unregulated Contaminant Monitoring Rule [139].

4.2 Materials and Methods

4.2.1 Materials

The adsorbents were prepared by pyrolysis of dewatered sewage sludge (SS) from Wards Island Water Pollution Control Plant in New York, or fish waste (F) from a seafood market in New Jersey, or their mixtures (ratio of 75:25 and 90:10 based on dry mass), at 650 °C or 950 °C in nitrogen atmosphere in a horizontal furnace. The name of a composite material has the following format: SSf1Ff2_temp where f1 and f2 refer to the fraction (in percentage) of the two end-members, SS and F, respectively, and temp refers to the pyrolysis temperature. For the sewage sludge or fish waste only adsorbents they are simply named SS_temp or F_temp. Trace metal grade acid was purchased from Fisher Scientific.

4.2.2 Acid washing after carbonization

Both hydrochloric acid and acetic acid were tested to investigate the effects of strong and weak acid washing on material properties. Hydrochloric acid washing was done by mixing SBAs and 1N HCl with the solid to liquid ratio of 1:10 and shaking the mixture on an orbital shaker for 2 hours. For weak acid wash, the materials were washed with diluted acetic acid (pH=2.88, solid to liquid ratio of 1:5) for 2~3 times (18 hours each) until pH dropped to about 7. The acid wash was followed by 3 times of pure water (Milli-Q) wash (2 hours each). At the end, the solids were separated and dried in an oven at 120 °C for 16 hours for further use.

4.2.3 Characterization of SBAs

Textural characterization was carried out using nitrogen adsorption-desorption isotherms (ASAP 2010, Micromeritics) at -196 °C. The isotherms were used to calculate the specific surface areas, micropore volumes, mesopore volumes, total pore volumes, and pore size distributions. The latter was determined using the BJH method [35]. Composition of the sludge composites was determined by X-ray diffraction (XRD) and X-ray fluorescence (XRF). XRD data was collected on a Rigaku D/max X-ray Diffractometer, operated at 40 kV tension and 100 mA current to produce CuK α radiation at 1.5418 Å. Scans were taken between 10° and 90° 2 θ at 0.02° step size at 0.03 s/step. Mineral phases were identified using HighScore Plus software. XRF measurement was carried out with a Rigaku ZSX Primus II X-ray Fluorescence Spectrometer. FTIR analysis was performed on Nicolet iS50 FT-IR Spectrometer (Thermo Fisher Scientific).

4.2.4 Leaching test

The following fluids were used to extract the SBAs: 1) pure water (18.2 M Ω Milli-Q), 2) NYC tap water, and 3) extraction fluid (acetic acid, pH 2.88) of the standard Toxicity Characteristic Leaching Procedure (TCLP) [140]. The first two fluids represent different water sources whereas the third fluid would yield the maximum amount of leachable metals due to its acidity. The TCLP also serves the purpose of determining whether the SBAs would be classified as hazardous waste based on metal leaching. All the leaching tests were done by mixing 1 g of adsorbent with 20 mL of extraction solution. Following 18 hours of shaking, the mixture was separated by a glass fiber filter and the leachate was analyzed for metals.

4.2.5 Column leaching with pure water

To mimic the metal leaching behavior under dynamic flow through conditions (e.g., packed filter) column leaching tests were also conducted for acid washed samples. Each selected adsorbent (0.5 g, ~0.7 mL) was packed into a 1 mL syringe of 4 mm ID, with both ends filled with glass wool. Ultrapure water was pumped through the column via a rotary pump at a flow rate of 0.10-0.16 mL/min (corresponding to an empty bed contact time (EBCT) of 4.4-7 min). The effluent was collected with a fractional collector and analyzed for metals.

4.2.6 Metal analysis

Metals were analyzed by inductively coupled plasma – mass spectrometer (ICP-MS, Perkin Elmer) according to EPA standard method 200.8 [141]. The analyzed elements include Ag, Al, As, Ba, Be, Cd, Co, Cr, Cu, Hg, Mn, Mo, Ni, Pb, Ru, Sb, Se, Th, Tl, U, V, and Zn. Internal standard of Ge and Bi were used to correct instrument drift.

4.2.7 Batch adsorption experiment

Adsorption of the nitrosamine and pharmaceutical compounds from aqueous solutions was performed at room temperature in batch experiments. The physical properties of the compounds are listed in Table C1 of Appendix C. The initial concentrations of the organic compounds were 1-100 mg/L for ATN, 0.57-57 mg/L for CBZ, and 1-60 mg/L for NMEA. Ten mL of the target compound solution was mixed with 0.05 g of SBA in an amber glass vial, sealed, and shaken in an orbital shaker for overnight. The mixtures were then filtered by 0.2 μm polyethersulfone syringe

filters and diluted by proper factors. The equilibrium data were simulated using the Langmuir-Freundlich (L-F) isotherm model [142] from which the maximum adsorption capacity was calculated. Non-linear regression was used to derive the fitting parameters.

4.2.8 LC/MS/MS method

ATN, CBZ and NMEA in the batch absorption experiment were analyzed by liquid chromatography tandem mass spectrometry (LC/MS/MS, API 4000, Applied Biosystems) with electrospray ionization (ESI) and multiple reaction monitoring (MRM). Separation of analytes was achieved using a 50×4.6 mm Eclipse plus C18 column with 1.8 µm particle size (Agilent). The oven temperature was kept at 35°C. Ten µL of sample was injected after 3 min equilibrium. A binary gradient of water (component A) and methanol (component B) was pumped at the flow rate of 0.4 mL/min. Both component A and B contain 0.1% formic acid for ATN and CBZ analysis, and 4mM ammonia formate for NMEA analysis. All the compounds were analyzed under positive ESI. Nitrogen was used as both the collision gas and nebulizing gas. Identification of all compounds was made by two MRM transitions and quantitation was made by the more abundant one.

4.3 Results and Discussion

4.3.1 Metal leaching before acid wash

The levels of metals from leachates were compared to the US drinking water standard [143, 144], or European Union (EU) standard if the metals are not regulated in the US (e.g., V and Ni).

Co, Mo, Ru and Th are not regulated in either US or EU and the results of these metals are not discussed here.

Of the remaining 18 elements examined (Ag, Al, As, Ba, Be, Cd, Cr, Cu, Hg, Mn, Ni, Pb, Sb, Se, Tl, U, V, Zn), 10 do not exceed the US or EU drinking water standards (even with acetic acid leaching) so only those exceeded the standards are presented in Table 4-1 below (the full results can be found in Table C2 in Appendix C). Of those eight elements, As, Mn and Ni do not exceed the US or EU standards during either DI or tap water leaching in any of the materials examined (Table 4-1). Hg levels are all below the US drinking water standard of 2 µg/L but are slightly above the EU standard of 1 µg/L in the SS_950 sample during DI and tap water leaching. Likewise, Se levels are all below the US standard of 50 µg/L but are up to 3 times of the EU standard of 10 µg/L for the sludge only samples (Table 4-1). Pb levels are within the US or EU standards except for the F_950 sample where the Pb level is about 2-3 times of the standards (Table 4-1). Sb levels in the SS_950 sample are about 3 times the standard and Sb levels in the SS90F10_950 sample are slightly above the standard during DI and tap water leaching.

Al levels are extremely low (below detection in most cases) in the fish waste only samples even with acetic acid leaching. In contrast, Al concentrations in the sludge containing materials are rather high during DI and tap water leaching, up to 25 times the drinking water standard of 200 µg/L (Table 4-1). Al in the sludge may come from the alum flocculant often used during wastewater treatment [145]. Al-phosphates, evident in the XRD patterns of the sludge composites (Figure C1 in Appendix C), are insoluble at neutral pH but soluble at alkaline conditions, such as those resulting from the dissolution of alkaline phases [146]. The pH of the DI and tap water leachate of the composite materials is above 11, and in some cases, close to 13 (Table C3 in

Appendix C). The high pH is the result of Ca leached from alkaline minerals calcite, clinopyroxene and calcic feldspar in the composite sludge materials (Table C4 in Appendix C). The high pH of the composite materials would prevent their use in wastewater or drinking water treatment. Therefore, proper acid treatment of the composite materials is necessary to neutralize the materials.

Table 4-1 Leaching of unwashed composite materials by DI water, tap water, and TCLP fluid. Concentrations are in µg/L. Values above the drinking water standards are highlighted in red.

		Al	As	Hg	Mn	Ni	Pb	Sb	Se
Drinking water standards	EU	200	10	1	50	20	10	5	10
	USA	200	10	2	50	-	15	6	50
	TCLP limit	-	5000	200	-	-	5,000	-	1000
SS_650	DI	1461.0	0.0	0.6	1.9	2.6	8.4	5.0	11.2
	TAP	1390.1	0.0	0.5	1.9	2.6	7.2	5.0	11.9
	TCLP	48.4	0.2	0.6	99.1	8.5	3.7	13.9	2.1
SS_950	DI	3069.2	1.5	1.4	2.6	0.0	3.5	14.5	23.2
	TAP	2825.9	1.3	1.2	2.5	0.0	3.5	14.1	27.5
	TCLP	5.7	9.5	0.3	815.2	7.6	3.5	10.2	2.7
SS90F10_650	DI	2626.3	0.1	0.4	2.0	3.3	5.4	2.8	2.8
	TAP	4574.3	0.1	0.4	1.9	2.8	4.9	3.1	3.1
	TCLP	82.0	11.4	0.1	1477.4	56.7	7.4	6.7	1.3
SS90F10_950	DI	3803.9	0.0	1.0	2.2	0.9	4.0	7.4	2.4
	TAP	3777.0	0.0	1.0	2.1	0.7	3.9	7.5	2.5
	TCLP	5.9	10.6	0.2	4196.0	64.2	3.5	28.6	0.0
SS75F25_650	DI	3229.7	0.0	0.3	2.0	1.0	4.0	2.1	1.6
	TAP	3390.5	0.0	0.3	2.0	1.1	4.0	2.0	1.4
	TCLP	21.0	3.8	0.1	610.7	18.9	4.8	4.0	3.0
SS75F25_950	DI	3730.5	0.0	0.8	2.1	1.1	3.9	3.1	1.3
	TAP	3362.7	0.0	0.9	2.0	0.7	3.7	3.4	0.7
	TCLP	0.0	8.0	0.2	1545.0	39.3	3.5	11.8	0.0
F_650	DI	0.0	0.4	0.1	3.2	9.0	3.5	1.2	3.8
	TAP	6.0	0.5	0.1	2.2	8.6	3.5	1.2	4.3
	TCLP	0.0	0.0	0.1	1.9	15.5	4.8	1.2	1.1
F_950	DI	0.0	0.7	0.1	2.2	15.4	33.7	1.2	5.2
	TAP	0.0	0.8	0.1	2.2	15.7	28.5	1.2	5.2
	TCLP	0.0	0.0	0.1	2.0	27.2	25.2	1.2	1.1

In acetic acid leaching, As, Mn and Sb exceeded the drinking water standards while the remaining elements were within their allowable limits (if any). As levels are slightly above the drinking water standard in the SS90F10 samples whereas the Sb levels are as high as 5 times the drinking water standard. Mn levels in sludge containing samples all exceed the drinking water standard (up to 80 times). Mn is present in clinopyroxene and in phosphates such as hydroxyapatite/chlorapatite, which are present according to XRD results (Figure C1 in Appendix C). Clinopyroxene, in particular, is soluble under acidic conditions. None of the metals exceeded the TCLP limits (if any).

4.3.2 Metal leaching after acid wash

4.3.2.1 HCl wash

Hydrochloric acid was first tried to neutralize the composite materials. HCl with concentration from 0.1 N up to 5 N was used to wash SBAs in many studies [1, 133, 147-149] for the purpose of decreasing ash content and increasing porosity and specific surface area. HCl wash may also enhance metal uptake because H^+ could replace exchangeable cations and thus increase cation exchange capacity [150]. When the HCl washed, DI rinsed and oven dried SBAs were subject to DI water leaching, the pH of the resultant leachate is around 3 for most of the materials except for the fish waste only samples where the pH is around 6 (Table C3 in Appendix C). More metals (Ni, Cu, Zn, Pb) which were not shown in the previous leaching test of unwashed materials were released in concentrations far over the allowable limits (Table C5 in Appendix C). The low equilibrium pH (~3) of water extraction may have contributed to the rising in released metals as metals are generally more mobile under acidic pH [151]. It was also possible that the 1N HCl used

here destructed relatively stable minerals formed during pyrolysis and resulted in the release of more metals. In fact, the HCl wash resulted in 30-50% weight loss of the raw materials, indicating that a significant amount of the mineral phases was dissolved. As such, HCl is not recommended for the pre-treatment of the SBAs examined here.

4.3.2.2 Weak acid wash

In contrast to the significant material loss (30-50%) with HCl wash, the weak acid (acetic acid) wash only led to about 10% material loss at the most. When the acetic acid washed, DI rinsed, and oven dried SBAs were subject to DI and tap water leaching, the pH of the resultant leachate is between 6 and 8 except for the fish waste only materials where the pH is still above 9.5 (Table C3 in Appendix C).

The metal leaching behavior of the weak acid washed SS75F25_650, SS75F25_950, SS90F10_650, and SS90F10_950 materials are examined here because 1) fish waste was only considered as a secondary component, and 2) previous studies showed that these composite materials have the best adsorption properties.

When the weak acid-washed samples were subject to DI or tap water leaching, only four (As, Mn, Ni, and Sb) out of the 22 elements in the leachate exceeded the drinking water standards (see Table 4-2 below, full results in Table C6 in Appendix C). As in the leachate of the SS90F10_950 and SS75F25_950 samples is about twice the drinking water standard, whereas As in the SS90F10_650 and SS75F25_650 samples is below the limit. Mn in the leachate of the SS90F10_650, SS90F10_950, and SS75F25_950 samples is 2-18 times the drinking water

standard whereas Mn in SS75F25_650 is below the standard (Table 4-2). Mn levels in the leachate of the weak acid washed samples are much higher than those in the unwashed samples. This is likely due to the increased solubility of Mn-bearing minerals clinopyroxene and chloroapatite as pH decreases. Only Ni in the leachate of the SS90F10_950 sample exceeded the EU standard (~twice). Sb in the leachate of all four samples exceeded the drinking water standard (up to four times).

Table 4-2 Leaching of metals from acid washed composite materials (in µg/L). Be, Ru, Th, Tl, U were all below detection and therefore are not tabulated. Metals in the Milli-Q (DI) and tap water (TAP) leachate that exceeded MCLs are highlighted in red.

		Al	As	Hg	Mn	Ni	Pb	Sb	Se
Drinking water standards	EU	200	10	1	50	20	10	5	10
	US	200	10	2	50	-	15	6	50
	TCLP limit	-	5000	200	-	-	5,000	-	1000
SS90F10_650	DI	10.9±2.2	6.5±0.1	0.18±0.03	102.0±1.5	2.22±0.03	0.53±0.23	12.5±0.2	19.8±0.3
	TAP	10.4±2.8	6.9±0.2	0.15±0.01	111.6±1.2	2.6±0.2	0.10±0.17	12.9±0.2	21.2±0.7
	TCLP	144.5±11.7	24.7±0.4	0±0	1293.0±14.5	34.9±0.7	5.8±0.2	13.2±0.1	54.3±2.7
SS90F10_950	DI	7.3±1.8	18.8±0.6	0.01±0.01	879.5±15.6	38.0±1.0	0.24±0.41	24.5±0.7	37.8±0.8
	TAP	7.9±1.7	18.5±0.6	0±0	924.0±10.4	36.9±0.4	0±0	24.7±0.5	40.9±1.5
	TCLP	45.8±2.5	40.2±0.1	0±0	3040.7±34.0	119.9±1.0	0.52±0.15	21.6±0.4	85.2±2.6
SS75F25_650	DI	33.9±14.4	1.9±0.1	0.20±0.01	23.9±1.5	0±0	1.8±1.7	9.0±0.1	7.5±0.3
	TAP	18.8±2.3	2.13±0.02	0.17±0.02	27.5±1.2	0±0	0.10±0.16	9.3±0.2	8.0±0.2
	TCLP	20.5±2.9	12.1±0.2	0±0	637.8±29.4	9.9±0.2	1.92±0.05	10.3±0.3	31.6±0.4
SS75F25_950	DI	7.4±1.9	16.5±0.5	0.04±0.02	263.1±9.0	8.5±0.2	0±0	22.8±0.8	34.9±1.4
	TAP	5.6±0.8	15.4±1.2	0.01±0	278.9±7.5	8.0±0.3	0±0	22.9±0.2	34.4±0.8
	TCLP	41.7±0.9	39.7±0.9	0±0	2059.6±79.1	70.8±0.9	0.25±0.24	18.1±0.6	77.4±1.2

The TCLP extraction showed somewhat higher amounts of metals leached, especially for Mn (Table 4-2). Nonetheless, most of the elements in the TCLP leachate did not exceed drinking

water standards. For those few elements (As, Mn, Ni, Sb, and Se) did exceed drinking water standards, none exceeded TCLP limits (if any).

The most promising result obtained by the acetic acid wash was that Al content dropped significantly to below the drinking water standard with all three extraction fluids. This is likely due to the effective neutralization of the materials by the acetic acid (Table C3 in Appendix C). The solubility of Al oxide/hydroxide and Al-phosphate is low near neutral pH [146].

The metal leaching behavior of the acetic acid washed SBAs was further evaluated by column leaching test with DI water. At the flow rate of 0.1 mL/min (EBCT of ~7 min), the effluent concentrations of the 5 elements exceeded drinking water standards during batch leaching tests (As, Mn, Ni, Sb, and Se) rapidly dropped to constant levels that are well below drinking water standards (Figure 4-1), for at least 2000 bed volumes (where experiments ceased).

The leaching behavior for Al is somewhat surprising. In batch tests, Al concentrations in the leachate never exceeded the drinking water standard for all four materials. This is consistent with the initial Al concentrations in the column effluent (Fig. 4-1). However, Al concentration gradually increased over time. For the SS75F25_650, SS75F25_950, and SS90F10_650 samples the effluent concentration reached a steady state level below the standard at ~250-500 bed volumes. However, the effluent Al concentration from the SS90F10_950 column slightly exceeded the drinking water standard until the flow rate was increased to 0.15 mL/min at 1000 bed volumes, where the effluent concentration dropped below the drinking water standard. The four acid-washed sludge composites exhibit similar Al concentrations with values of 2.45 wt. % to 3.18 wt. %, however, the difference in Al leaching behavior between batch and column tests may be attributed

to the different dissolution dynamics of the Al-bearing minerals, plagioclase feldspar ((Ca,Na)AlSi₂O₈) and berlinite (AlPO₄), and other acid-soluble minerals such as clinopyroxene (Ca,Mg,Fe)₂Si₂O₆ and calcite (CaCO₃). Destabilization of these phases at pH < 4 during acid wash leads to an initial strong leaching of Al³⁺, Ca²⁺, and H₂PO₄⁻/HPO₄²⁻. Leached Ca slowly increased the alkalinity of the solution, resulting in recrystallization of berlinite as a mineral coating and effectively reducing the amount of Al in solution [146].

In the batch experiments, this complex equilibration and redistribution of Al, Ca and P among the mineral phases is dictated by the buffering effects of Ca and phosphate species. Both SS75F25_950 and SS90F10_950 exhibit much stronger barringerite (Fe₂P) peaks than the samples pyrolyzed at 650 °C, however, the difference in the effect on effluent Al concentration for sample SS90F10_950 in the column experiment can be explained by a combination of pyrolysis temperature, composition of the composite, and pH. A somewhat higher Fe concentration in SS90F10_950, 8.67 wt. % compared to 7.07 wt. % average concentration in the other three acid-washed samples, coupled with phosphorus stemming from the loss in stability of hydroxyapatite/chlorapatite after heating above 900 °C [152], causes barringerite to effectively scavenge enough P from the effluent to delay the buffering effect of phosphate. Once Fe no longer competes with Al for P, the pH begins to rise and berlinite can recrystallize. This results in an initial increase in Al concentration followed by decrease and stabilization in the column experiments.

This result suggests that the acetic acid washed SBAs could be potentially used in packed filters to treat wastewater or even drinking water without the concern of metal leaching.

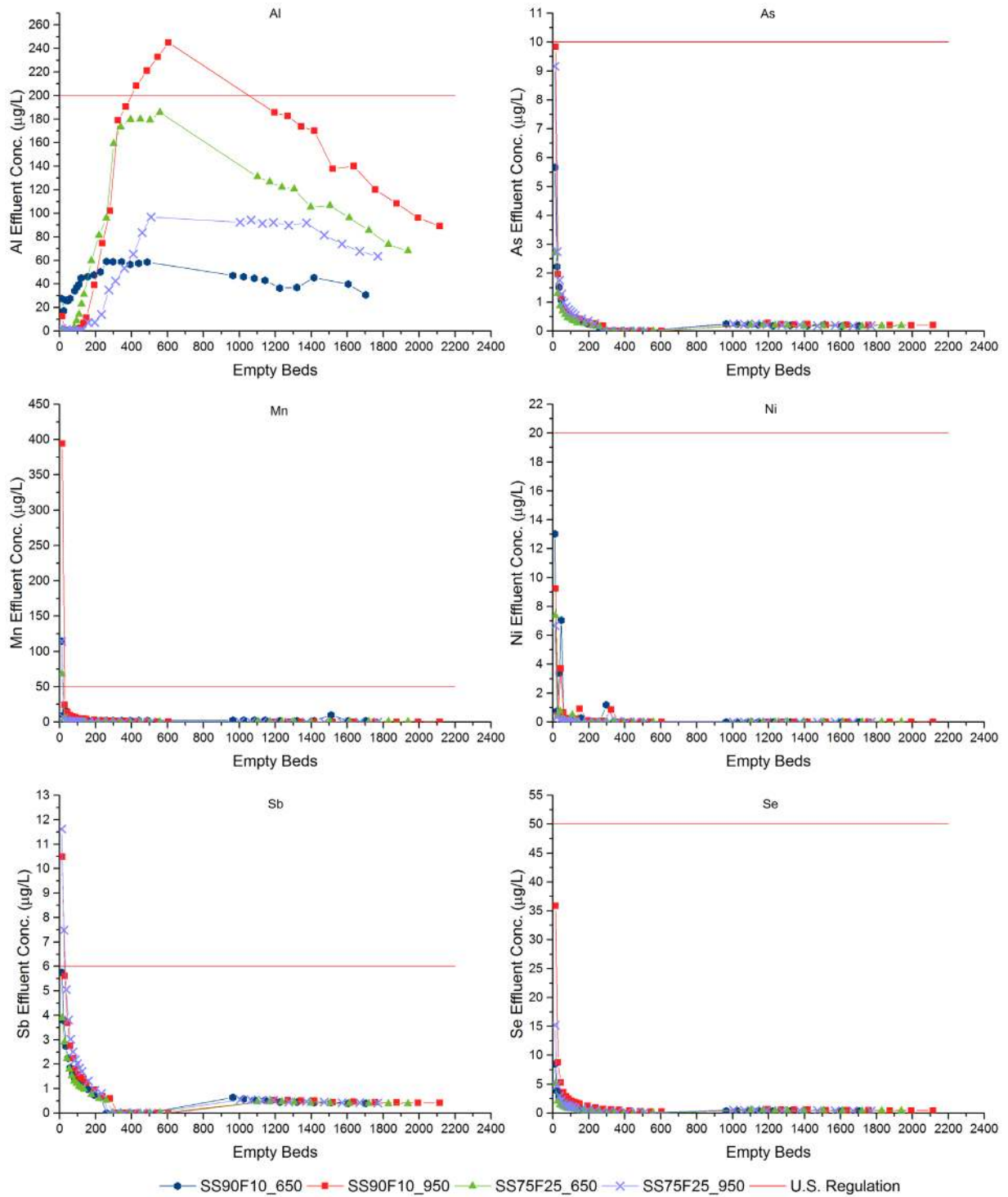


Figure 4-1 Leaching of metals with DI water from acetic acid washed SBAs under dynamic flow through conditions.

4.3.3 Characterization of SBAs before and after acetic acid wash

For unwashed SBAs with the same composition, those pyrolyzed at 950 °C usually have higher surface area and total pore volume than those pyrolyzed at 650 °C, which is consistent with previous studies [133, 153, 154]. This is especially true for the SS75F25 materials, where the surface area, micropore volume, and total pore volume almost doubled when the pyrolysis temperature increased from 650 °C to 950 °C (Figure 4-2). This is because thermally unstable contents would decompose and act as pore formers at high temperatures. A slight drop of micropore volume for SS90F10 material at 950 °C was observed. It was reported that long pyrolytic time at high temperature may destroy micropores in sludge based adsorbents [155]. High burn-off rate of initial materials would also result in a decrease in microporosity as pore widening would become predominant [154].

Acid wash appeared to have positive effects on the physical properties of SBAs. Except for SS90F10_650, the other three adsorbents all have their pore volume and surface area increased by acid wash. The acid wash could remove the tarry residues which may block the accesses to pores. Further, basic oxides such as CaO could be dissolved from adsorbents, generating extra pores [149]. Sample SS90F10_650 contains significantly less Ca, 4.88 wt. % compared to a range of 6.1 to 6.9 wt. % in the other acid-washed samples. This supports the hypothesis that micropores were transformed into mesopores through dissolution induced by acid wash, thus decreasing surface area without significantly changing the pore volume.

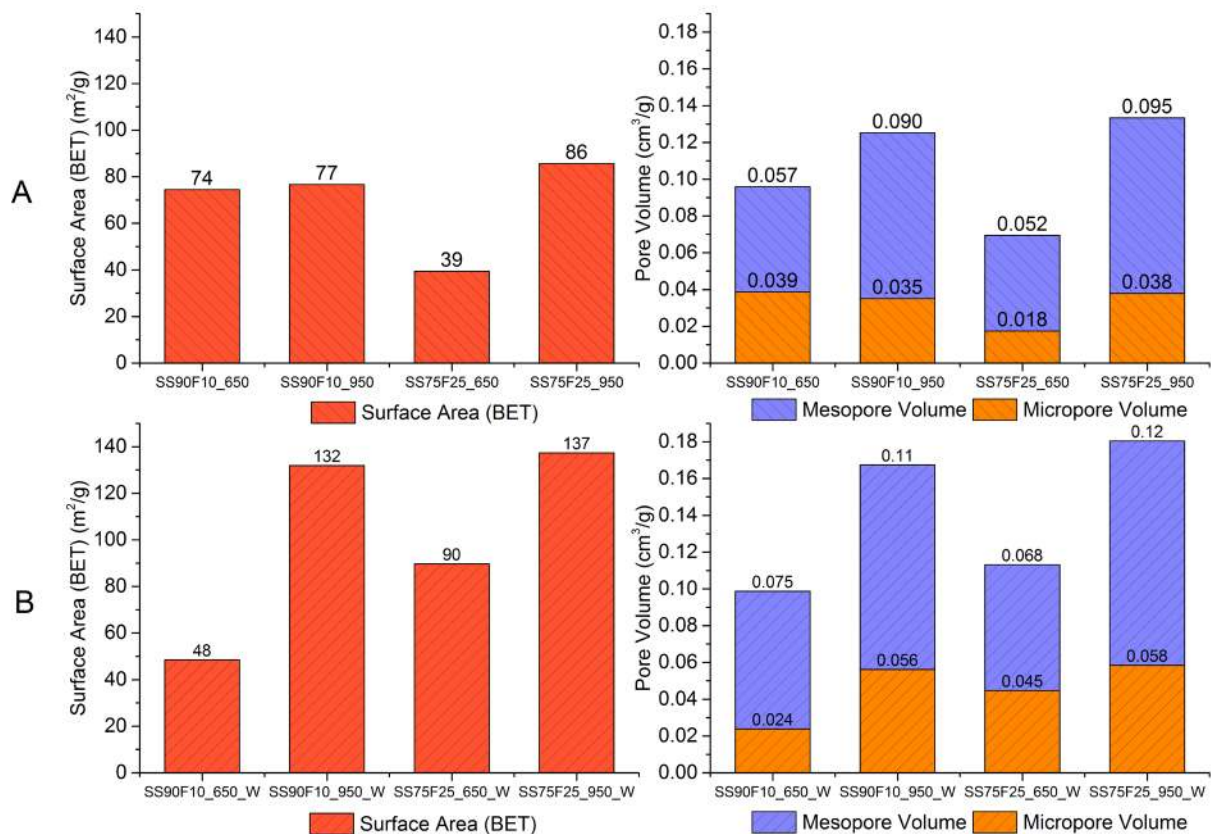


Figure 4-2 Surface area and pore volume of SABs before (A) and after (B) acetic acid wash. “_W” indicates acid wash.

The pore size distribution (Figure 4-3) shows that mesopores contribute to most of the total pore volume in the SBAs. Acetic acid wash has significantly increased the volumes of both micropores and mesopores, especially the volume of pores with a width less than 10 nm.

BJH Desorption Pore Distribution

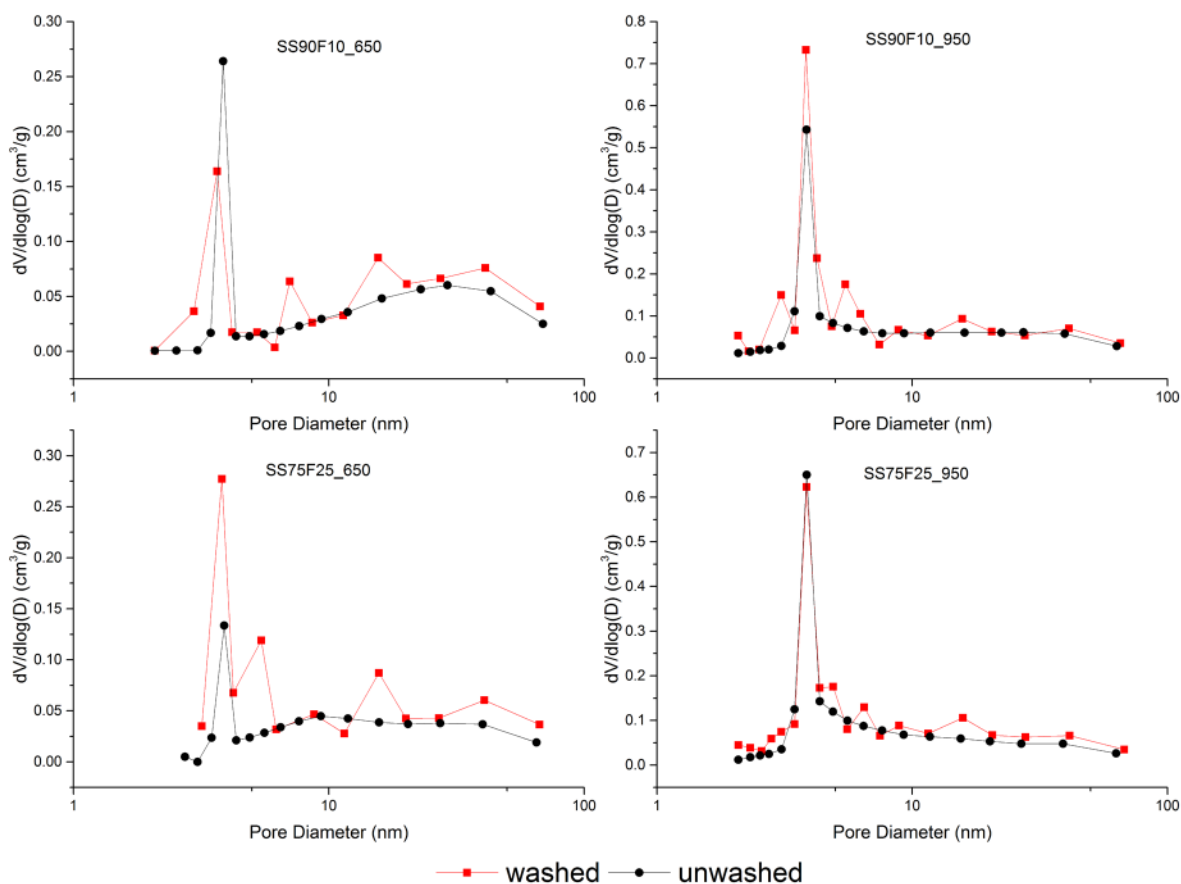


Figure 4-3 BJH Pore size distribution

4.3.4 Batch adsorption before and after acetic acid wash

SS75F25_650 was selected as the representative material to evaluate the adsorption capacity before and after acetic acid wash. Figure 4-4 shows the adsorption isotherms of ATN, CBZ and NMEA with both the experimental and simulated (L-F model) data. The observed and simulated maximum adsorption capacities for each compound are presented in Figure 4-5. Since the input concentrations were different due to solubility limitations, the removal efficiencies (%) at the highest compound loading were also presented in Figure 4-5.

Figure 4-4 shows that acid wash has significantly increased the adsorption capacity of the material. After acid wash the observed maximum adsorption increased from 3.37 to 8.18 mg/g for ATN, from 2.19 to 4.06 mg/g for CBZ, and from 0.41 to 2.12 mg/g for NMEA. Similar trends could be found for the simulated maximum adsorption and removal efficiencies (Figure 4-5). This could be primarily due to the increased surface area and pore volumes. Acid wash may also have increased the ion exchange capacity of the material by replacing metals with H^+ . In addition, solution pH and the pKa values of adsorbates may be an important factor affecting the adsorption. The pH for solutions of acid washed materials is around 8.0-8.7, while that of the unwashed material is around 11.3.

Since all the three compounds have a molecular size smaller than 20 Å, they all have accesses to the micropores which should be the high-energy adsorption center for physical adsorption. In addition to micropores, in SBAs it is very likely that mesopore which is predominant by sludge derived minerals plays an important role in adsorption [63]. The larger polar surface may also contribute to the polar interaction between adsorbent surface and the compounds.

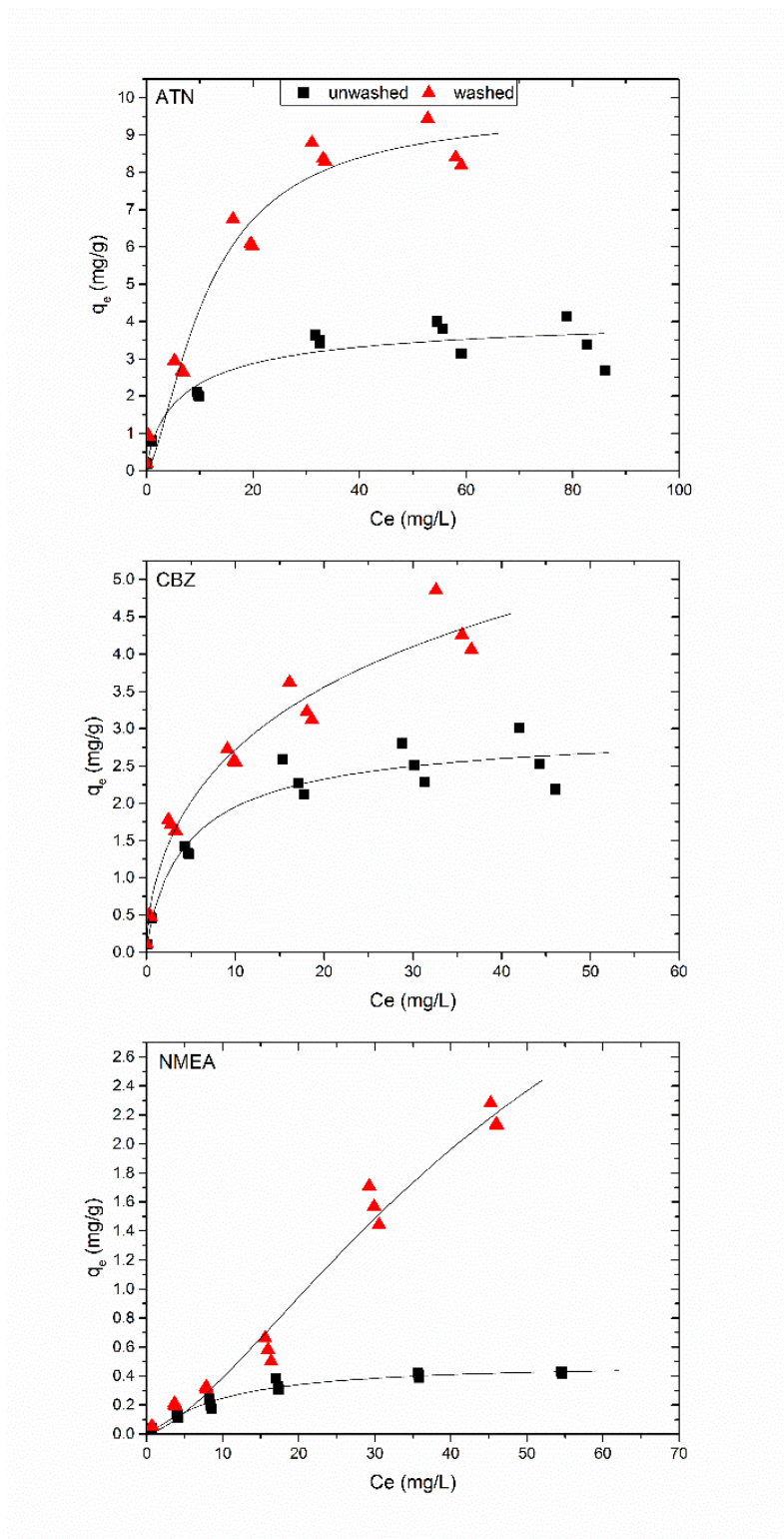


Figure 4-4 Adsorption isotherms of ATN, CBZ and NMEA.

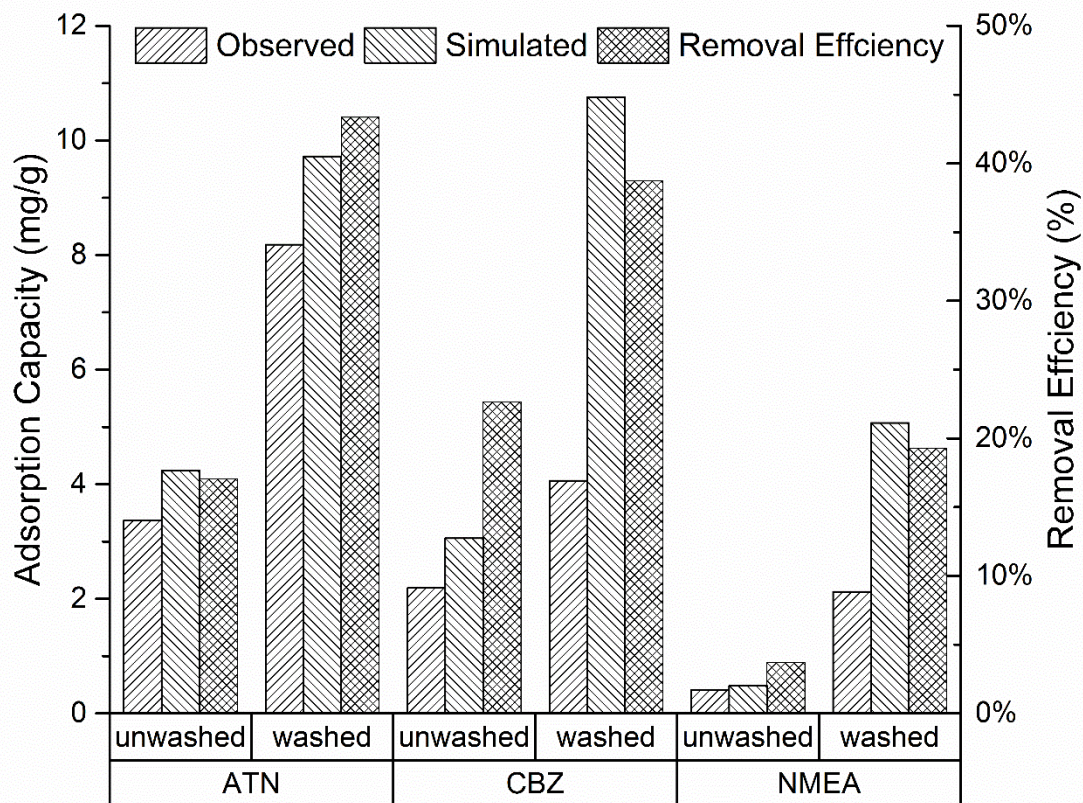


Figure 4-5 Observed and simulated adsorption capacity and removal efficiency.

Overall, the adsorption capacities of the three compounds increased in the order of NMEA, CBZ and ATN. In general, nitrosamines are all difficult to remove by adsorption to activated carbon due to its low K_{ow} value [138]. It was also reported as zero adsorption by 4 types of zeolites with different hydrophobicities [156]. ATN was reported to be adsorbed at the amount of 10 mg/g by natural zeolite [157] and up to 100 mg/g by powdered activated carbon [158]. For CBZ, the reported amount is about 0.14 mg/g by modified zeolite [159] and above 40 mg/g by GAC [160].

NMEA is the smallest molecule of the three and can enter micropores easily. However, the lowest amount of adsorption comparing to other compounds suggests molecular size is not the

controlling factor in the current adsorption process. The poor adsorption is probably because NMEA is neutral (pK_a of -3.39) under the experimental condition and very hydrophilic ($\log K_{ow}$ of -0.15). According to literature, hydrophobicity plays an important role in adsorption of nitrosamines by both zeolite and GAC [156, 161, 162]. The adsorbent SS75F25_650 contains about 25% carbon. The low $\log K_{ow}$ value makes it thermodynamically less favorable for NMEA to expulse from water phase onto the adsorbent surface.

CBZ ($pK_a < 1$, 13.9) also existed as neutral form under solution pH. However, it is much more hydrophobic ($\log K_{ow}$ of 1.51) than NMEA ($\log K_{ow}$ of -0.15), which may contribute to the hydrophobic interaction with carbon contents in the material. The benzene rings in the structure of carbamazepine may also be involved in the cation- π interaction with varieties of minerals on the surface of adsorbent [163].

At the solution pH of 8.7 (washed adsorbent), 89% of ATN (pK_a of 9.6) is protonated at the basic amine group, whereas 98% is neutral at pH of 11.3 (unwashed adsorbent). The positive charges could help ATN molecules get close to the adsorbent's surface because of the original material's basic nature (pH_{PZC} of 9-10) [35]. Elemental analysis indicates the adsorbent consists of 6-8% Ca, 2.5% Mg and 6% Fe. The minerals presented in the adsorbent could be involved in the cation exchange reaction with positively charged ATN, not only in the micropores but also mesopores. Thus, the acid washed material exhibited a much higher adsorption ability against ATN than that of unwashed adsorbent. ATN also has a much larger polar surface area (Table C1 in Appendix C) and more functional groups than NMEA and CBZ, which may help to interact with minerals and lead to specific or reactive adsorption.

4.4 Conclusions

The composite materials obtained from the pyrolysis of sewage sludge and fish waste had high pH and some metals (Al in particular) were leached out at levels above the maximum contaminant levels (MCLs, or drinking water standards). Wash the composite materials with acetic acid (pH 2.88) effectively neutralized the materials and significantly reduced metal leaching, with only 5 metals exceeded their MCLs during batch leaching tests. When column leaching tests were conducted with an empty-bed contact time (EBCT) of ~5 min (i.e., similar to conditions used in packed carbon filters), the concentrations of all the 5 metals dropped to below their respective MCLs within 10 bed volumes. Acid wash also significantly increased the surface area and pore volumes of the materials, and enhanced the adsorption of the three organic compounds (ATN, CBZ, and NMEA) by 2-5 times.

**Chapter 5 Adsorption of multiple pharmaceuticals and endocrine
disrupting compounds (EDCs) from water by sewage sludge-fish
waste based adsorbents**

5.1 Introduction

The global pharmaceuticals market revenue is almost one trillion dollars [164]. While there is no data for the total use of pharmaceuticals, it is estimated that the annual worldwide antibiotics consumption lies between 100,000 and 200,000 tons [165]. Some of the pharmaceuticals are used as human medication while others, especially antimicrobials, are used in animal husbandry for veterinary purposes or as growth promoters, particularly in intensive livestock farming [166]. Many pharmaceuticals undergo structure changes in the bodies of human and animals, but others are only moderately or poorly metabolized and excreted. For example, 21% of the oxytetracycline by sheep and 17-75% of chlortetracycline by young bulls (orally feed) were excreted in the form of their parent compounds [167]. It was also reported that up to 10% of ibuprofen, 76% of gemfibrozil, 31% of carbamazepine, 10% of naproxene, 30% of sulfamethoxazole and 43% of trimethoprim are excreted in the free form by human [168, 169]. Some of the human metabolized compounds such as sulfonamides could even retransform to their parent forms in surface water [170, 171].

Municipal and hospital wastewater usually contain high concentrations of pharmaceuticals. However, the removal efficiencies of pharmaceuticals by wastewater treatment plants (WWTPs) vary significantly depending on compounds and treatment methods. It has been widely reported that conventional biological treatment processes are usually ineffective for many of these compounds [172-175]. In some cases, the effluent may even yield higher concentrations of pharmaceuticals than influent [172, 176], which may be due to the dissociation of these compounds from bile and feces during biological treatment [177]. These organic contaminants have entered the environment through pathways such as applications of animal waste as fertilizers and discharge

of inefficiently treated wastewater. As a result, pharmaceuticals are present ubiquitously in soils, surface and ground waters, and even drinking water nowadays [137, 178].

The information about the effects of pharmaceuticals on organisms in the aquatic and terrestrial environment is still limited. However, it has been demonstrated that blue-green algae are sensitive to trace amount of antibiotics and would be inhibited at the level of a few $\mu\text{g/L}$ [179]. The microbial populations and communities would be affected by chronic exposure to environmentally relevant concentrations, in terms of reproduction [180]. The greater concern of pharmaceutical contamination is the potential development of antibiotic resistant bacteria (ARB) and antibiotic resistant genes (ARGs). Antibiotic resistances may primarily result from the excreted bacteria in patients and animals, and can be easily transferred across different species of bacteria (horizontal gene transfer). There are conflicting evidence about whether WWTPs would increase the concentrations of ARB and/or ARGs in effluent comparing to raw sewage or the reverse [181-184], but analyses showed that the majority of the ARGs and ARB coming into the WWTPs might eventually present in the sludge [183]. Thus the traditional disposal pathway of biosludge from WWTPs such as landfill and agricultural application would be a significant source of ARB and ARGs into the environment [185].

Sewage sludge is one of the byproducts of activated sludge process. It is produced in abundant quantity and is rising accompanied with growing population and amount of processed wastewater. Because of the negative effects of traditional methods to dispose of sewage sludge, scholars have been searching for an alternate pathway. Pyrolyzing the sewage sludge to produce porous adsorbents has a promising prospect. Their adsorption performance against Hg^{2+} [186], dyes [187], phenol [25], phosphates [188] and antibiotics [63] have been reported. In this study,

the sewage sludge was mixed with fish waste to further add diversities to the surface features of adsorbents. The fish bone and scales have been proven effective adsorbents against metals and dyes [189, 190]. Similar to sewage sludge, fish waste is another type of potential resource which is being discharged at considerable quantities annually. Currently, the commercial fish waste was usually either landfilled or discharged into water bodies as processing effluent. The effluent which is high in BOD (biological oxygen demand), COD (chemical oxygen demand), TSS (total suspended solid) and fat-oil-grease could very likely produce adverse effects on the receiving environments [10]. Most of current technologies to reutilize fish waste are either not economically attractive or odoriferous [7]. In this regard, pyrolysis together with sewage sludge can be an alternative.

Thus, the main objective of this study is to investigate the adsorption performance of the newly developed sewage sludge-fish waste adsorbents on removing multiple pharmaceuticals and endocrine disrupting compounds (EDCs) from water. It was found that 11 pharmaceuticals and EDCs were frequently detected in 19 U.S. water utilities [137]. Eight (atenolol, atrazine, carbamazepine, gemfibrozil, naproxen, phenytoin, sulfamethoxazole, and trimethoprim) of the 11 compounds were examined here since they can be analyzed simultaneously with one method.

Typically, batch equilibrium tests (12-24 hours) with high input sorbate concentrations are performed in order to quickly assess the maximum adsorption capacity of an adsorbent. High input concentrations are needed to ensure that the amount remaining in the aqueous phase after adsorption could still be detected. A constant critique of such an approach is that the concentrations used are unrealistically high and therefore the results are of little use in predicting real flow through applications (e.g., packed columns). Column tests with more realistic input sorbate concentrations

would be an ideal choice but such tests often require a large volume of solution and long duration (e.g., weeks) to reach full breakthrough (saturation). A secondary objective of the study is therefore to compare adsorption capacities determined from batch equilibrium tests to those obtained from rapid flow through column tests. A pilot scale column test was also performed in a drinking water treatment plant with real source water to evaluate the performance of the composite material.

5.2 Materials and Methods

5.2.1 Adsorbents

The detailed method to prepare adsorbents was described previously [35]. Briefly, anaerobically digested sewage sludge from a wastewater treatment plant in New York City and fish waste from a local fish market in New Jersey were dried and grounded individually or as homogeneous mixtures in the ratio of 90:10 or 75:25 (sludge:fish waste, by dry weight). Then the mixtures were carbonized in a horizontal furnace under nitrogen atmosphere at the temperature of 650 °C or 950 °C. The materials are finally referred to as SS, F and SSF based on their composition, followed by 650 or 950 reflecting the pyrolysis temperature.

5.2.2 Acid wash of sludge based adsorbents

Acid wash may be a method to cut down the leachable components in sludge based adsorbents while increasing the BET surface area and porosity and hence the adsorption capacities. A preliminary study indicated that HCl wash would destroy the crystalline structure within the adsorbent and result in leaching of heavy metals, so in this work weak acid (acetic acid) was employed. The materials were washed with diluted acetic acid (pH=2.88) with a solid to liquid

ratio of 1:5 for 18 hours at room temperature for 2~3 times until the solution pH dropped to about 7. The materials were then washed by DI water with the same solid to liquid ratio for 3 times (2 hours each), and dried in an oven for future use.

5.2.3 Batch adsorption experiment

Both acid washed and unwashed materials were evaluated in batch adsorption experiments. A mixture solution containing the 8 compounds (atenolol, atrazine, carbamazepine, gemfibrozil, naproxen, phenytoin, sulfamethoxazole, and trimethoprim) was prepared. The physical properties of the compounds are summarized in Table D1 in Appendix D. Ten mL of mixture solution of various concentrations (from 1 mg/L to 100 mg/L) was mixed with 0.05 g of an adsorbent in an amber glass vial at room temperature. Triplicates were prepared at each concentration. The sample vials were sealed and shaken for 18 hours for isotherm studies. A previous kinetics study indicated that the time is sufficient to achieve equilibrium [191]. After filtration and proper dilution, the equilibrium concentrations (C_e) of adsorbates in the liquid phase were analyzed using liquid chromatography-tandem mass spectrometry (LC/MS/MS). The equilibrium data were simulated using the Langmuir-Freundlich (L-F) isotherm model [192] from which the maximum adsorption capacity was calculated. Non-linear regression was used to derive the fitting parameters. The pH of the solution at equilibrium was also measured.

5.2.4 Column transport experiment

Based on the performance in batch adsorption experiments, SS90F10_950 and SS75F25_950 (both acid washed) were selected for the column transport experiments. Duplicate

columns were prepared by packing 0.5 g adsorbent (~0.7 mL) into a mini-column of 4 mm ID, with both ends filled with glass wool. Influent solution with the 8 compounds (1 mg/L each) was pumped through the columns by a peristaltic pump at a flow rate of 0.15 mL/min (corresponding to an empty bed contact time (EBCT) of 4.7 min). The effluent was collected with a fraction collector and analyzed using LC/MS/MS, described below. The effluent concentrations were plotted over time to obtain the so-called breakthrough curves (BTCs), and the final adsorbed amount for each compound was calculated by integrating its BTC using the software OriginPro.

5.2.5 Field Experiment

The source water of the Little Falls Water Treatment Plant in New Jersey (Passaic River) contains pharmaceuticals and EDCs and hence the Plant was selected to conduct the large size column experiments (with the SS90F10_950 material). The field tests were carried out from Oct 29th to Dec 4th 2015 in the pump house using the raw water without any pre-treatment. The acid washed adsorbent SS90F10_950 was filled into duplicate glass columns with i.d. of 4.8 cm and length of 30 cm. Guard columns filled with glass wools were employed to remove particulates in the feeding water. The effluent was sampled every day and influent was sampled twice a week. All of the samples were preserved with sodium omadine and stored at 4 °C after sampling. Samples were analyzed by online SPE coupled with LC-MS-MS at Eurofins Eaton Analytical laboratory (Monrovia, CA).

5.2.6 LC/MS/MS method

All the compounds except samples from field experiment were analyzed by LC/MS/MS (API 4000, Applied Biosystems) with ESI and MRM in our own laboratory. Separation of analytes was achieved using a 50×4.6 mm Eclipse plus C18 column with 1.8 μm particle size (Agilent). Oven temperature was kept at 35°C. Ten μL sample was injected after 3 min equilibration. A binary gradient of water (component A) and methanol (component B) both consisting of 0.1% formic acid was pumped at a flow rate of 0.4 mL/min. Gemfibrozil and naproxen were analyzed under negative ESI while all the other compounds were under positive ESI. Nitrogen was used as both the collision gas and nebulizing gas. Identification of all compounds was made by two MRM transitions and quantitation was made by the more abundant one.

5.3 Results and Discussion

5.3.1 Material properties

The micromeritics results are summarized in Table 5-1. Before the acid wash, the carbonized sludge materials have BET surface area ranging from 39 to 86 m²/g, where materials produced at 950 °C have higher BET surface area than those produced at 650 °C. This is consistent with other reports that higher pyrolysis temperature will endow adsorbents with higher surface area [1]. The micropores account for a small portion of the porosity which is similar to other sludge based adsorbents [63]. The 950 °C pyrolytic temperature also generated higher pore volumes. Typically, higher temperature would result in more micropores due to gasification of thermally decomposable contents [154]. This is true for the SS75F25 material, but for SS90F10 the micropore volume dropped slightly after pyrolyzed at 950 °C. It was reported that long

pyrolytic time at high temperature may destroy micropores in sludge based adsorbents [155]. Microporosity would decrease if the burn-off rate exceeds a certain threshold value [154]. Another reason could be the limited carbon phase in sludge based materials and thus fewer pore formers [35].

Table 5-1 BET surface area and pore volume of unwashed and acid washed materials.

		Surface Area (BET) (m²/g)	Micropore Volume (cm³/g)	Mesopore Volume (cm³/g)	Total pore Volume (cm³/g)
Unwashed	SS90F10_650	74	0.039	0.057	0.096
	SS90F10_950	77	0.035	0.090	0.13
	SS75F25_650	39	0.018	0.052	0.069
	SS75F25_950	86	0.038	0.095	0.13
Acid washed	SS90F10_650_W	48	0.024	0.075	0.099
	SS90F10_950_W	132	0.056	0.11	0.17
	SS75F25_650_W	90	0.045	0.068	0.11
	SS75F25_950_W	137	0.058	0.12	0.18

Acetic acid wash has produced noteworthy positive effects. Both BET surface area and pore volumes have been enlarged after acid wash except in one case (SS90F10_650). The acid wash could remove the tarry residues that may block the accesses to pores. Another reason is that basic oxides such as CaO formed during pyrolysis could be dissolved, generating extra pores [149]. The surface area of SS90F10_650 decreased after acid wash, concurrent with a decrease in micropore volume and an increase in mesopore volume (Table 5-1), suggesting that the acid may have destroyed some micropores and transformed them into mesopores and thus led to a reduction in surface area. For all the other samples both the micropore volume and mesopore volume increased after acid wash (Table 5-1).

5.3.2 Batch adsorption experiment

5.3.2.1 Unwashed materials

Examples of selected adsorption isotherms of unwashed materials (SS_950, SS90F10_950, SS75F25_950 and F_950) are presented in Figure 5-1. At low contaminant loadings, the adsorbents could remove more than 99% of the compounds. As such, it is necessary to apply concentrations much higher than environmentally relevant levels to examine the maximum adsorption capacities. For most of the compounds the uptake by the adsorbents increased as the input concentrations increased. However, it is observed that for some compounds (e.g., CBZ and SMZ) the amount adsorbed started to decrease at higher contaminant loadings, suggesting competitive adsorption among the compounds.

The observed adsorption capacities for each compound and their sum at the highest contaminant loading are presented in Figure 5-2. TMP, ATN, and SMX have equal initial concentrations (100 mg/L at the highest loading), while the initial concentrations of the other compounds were lower due to solubility limitations. Therefore, the removal efficiencies of all compounds at the highest contaminant loading were also calculated and presented in Figure 5-3. The observed total adsorption capacities of the materials varied slightly (20-23 mg/g) with the addition of fish component. However, the addition of fish waste enabled the adsorbent to uptake more types of contaminants. As shown in Figures 5-2 and 5-3, GFB, NAP, PHT and SMX were poorly removed by the sludge only adsorbents, but their adsorption was enhanced as a small amount of fish waste was added. This is probably because the fish waste could bring in more functional groups to the composite materials [35].

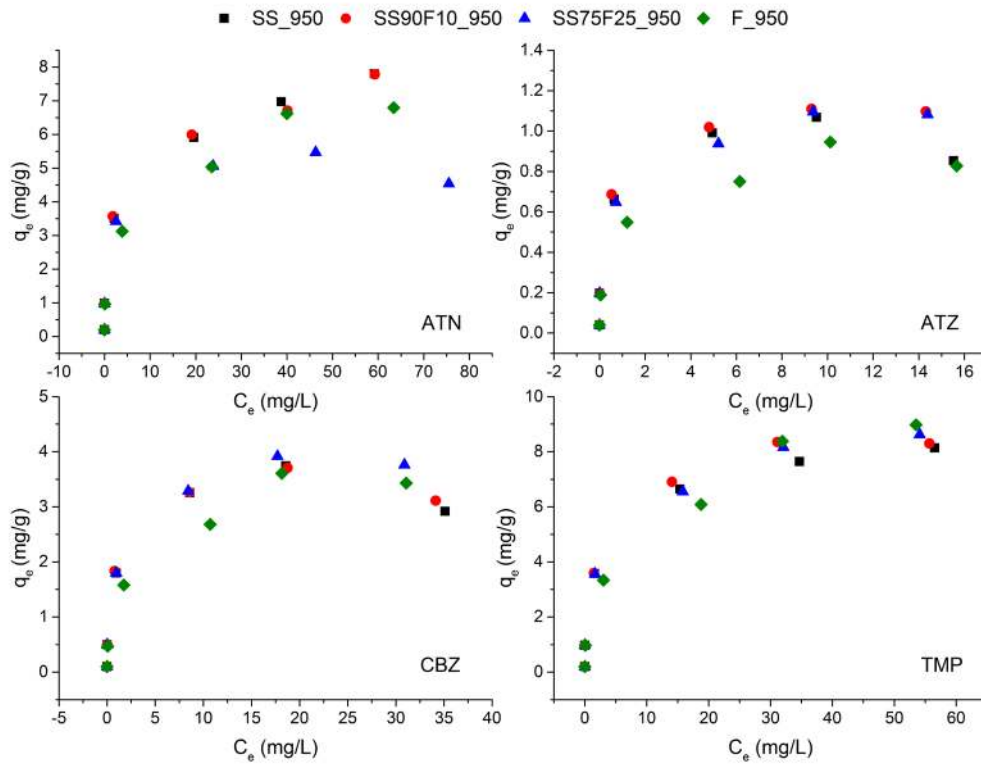


Figure 5-1 Examples of adsorption isotherms of unwashed materials.

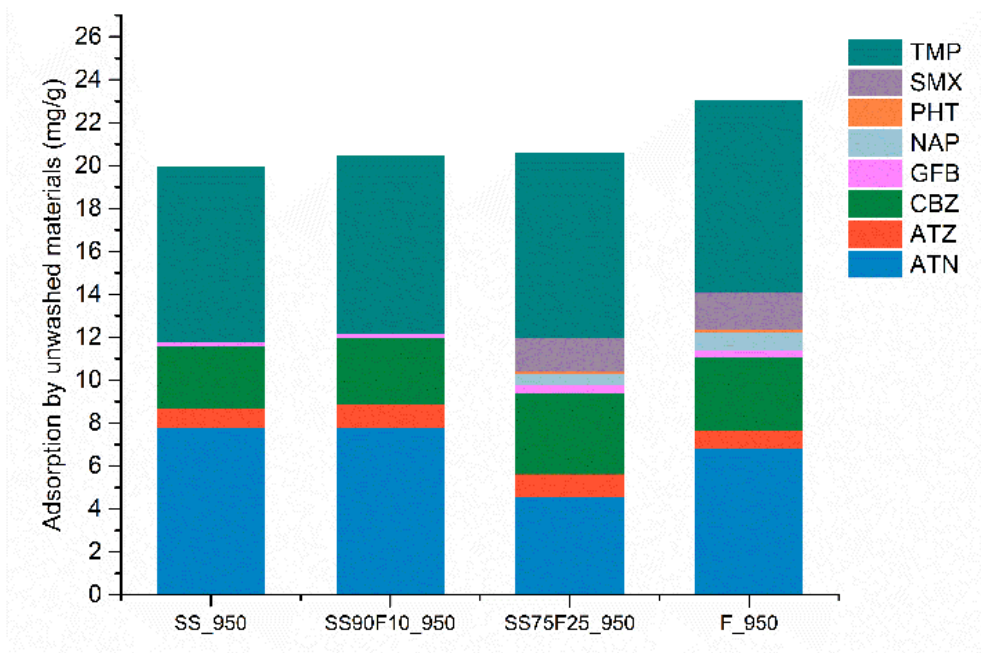


Figure 5-2 Adsorption on unwashed materials at the highest contaminant loading. Triplicate tests were performed with each adsorbent.

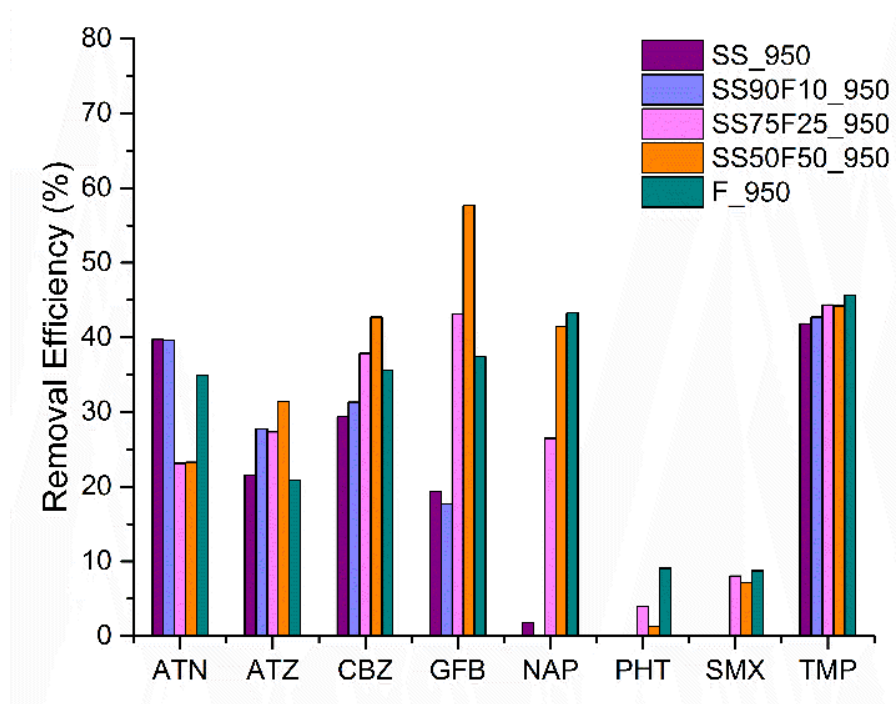


Figure 5-3 Removal efficiency of unwashed adsorbents at the highest contaminant loading.

5.3.2.2 Acid washed material

Figure 5-4 shows the isotherms of some selected compounds absorbed by acid washed materials. Unlike the adsorption on the unwashed materials, the phenomenon that the uptake of compounds decreased at high contaminant loadings was not observed here. This is probably because the competition among compounds was not prominent due to the improved adsorption capacity. The shape of isotherm and the fitting parameters obtained by L-F model indicate that the adsorbents were not saturated yet even at the highest contaminant loading.

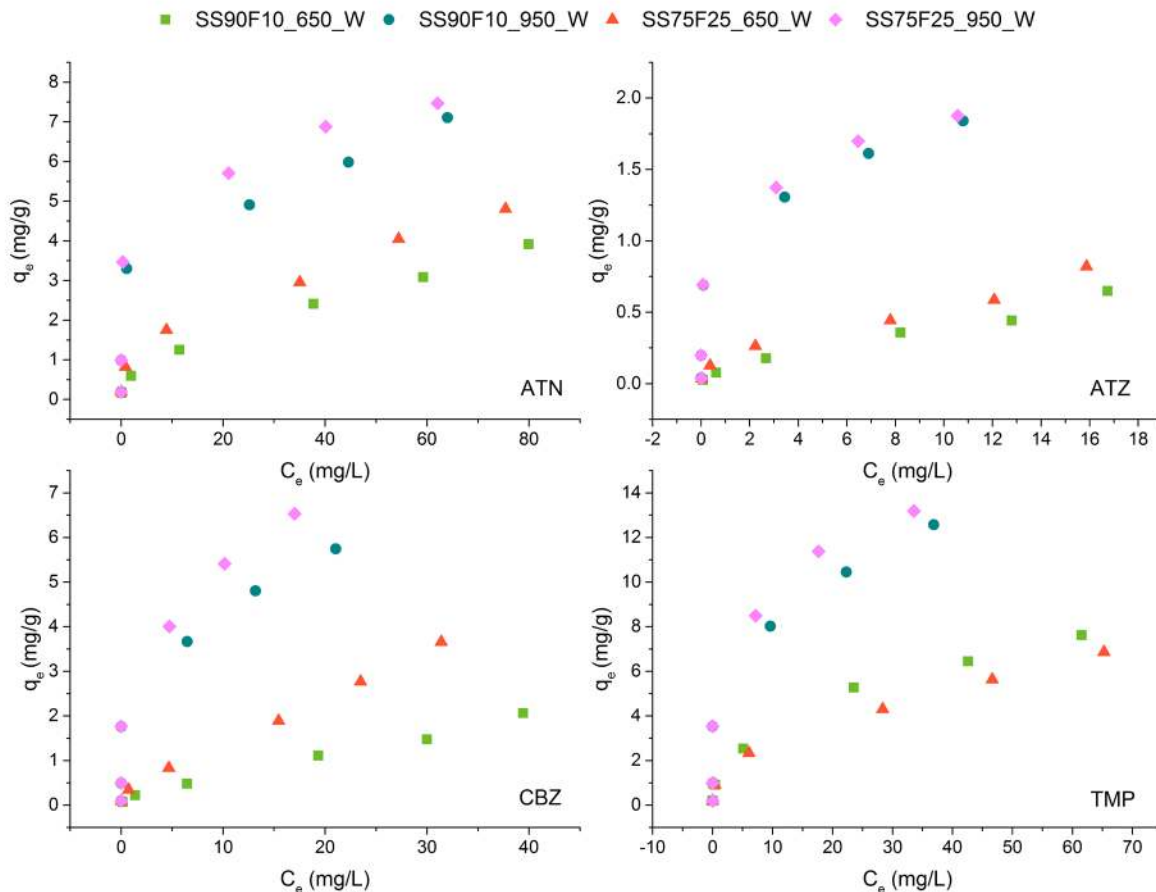


Figure 5-4 Examples of adsorption isotherms of acid washed materials.

When the materials with different pyrolysis temperatures are compared, those obtained at 950 °C have almost twice the adsorption capacity (~ 40 mg/g) as the materials obtained at 650 °C (Figure 5-5). Similar results were also obtained in previous reports [34, 35]. Generally speaking, higher pyrolysis temperatures would result in higher surface area and porosity (almost doubled from 650 to 950 °C for the SS90F10 and SS75F25 materials, see Table 5-1) which would apparently benefit adsorption. Higher pyrolysis temperatures would also lead to a higher level of carbonization which may lead to stronger dispersive attraction between the adsorbent and

adsorbate, and a higher degree of aromatization [35] which would attract more benzene rings in the target compounds through π interactions.

The commercially available activated carbon (WVA 900) demonstrated better adsorption towards the pharmaceuticals and EDCs examined here, probably because of the higher surface area (1025 m²/g) and pore volume (0.36 and 1.24 cm³/g for micro- and total pore volume, respectively) [193]. Comparing to activated carbon, the acid washed SS90F10_950 and SS75F25_950 adsorbents exhibited about half of the maximum adsorption capacity of the activated carbon (Figure 5-5).

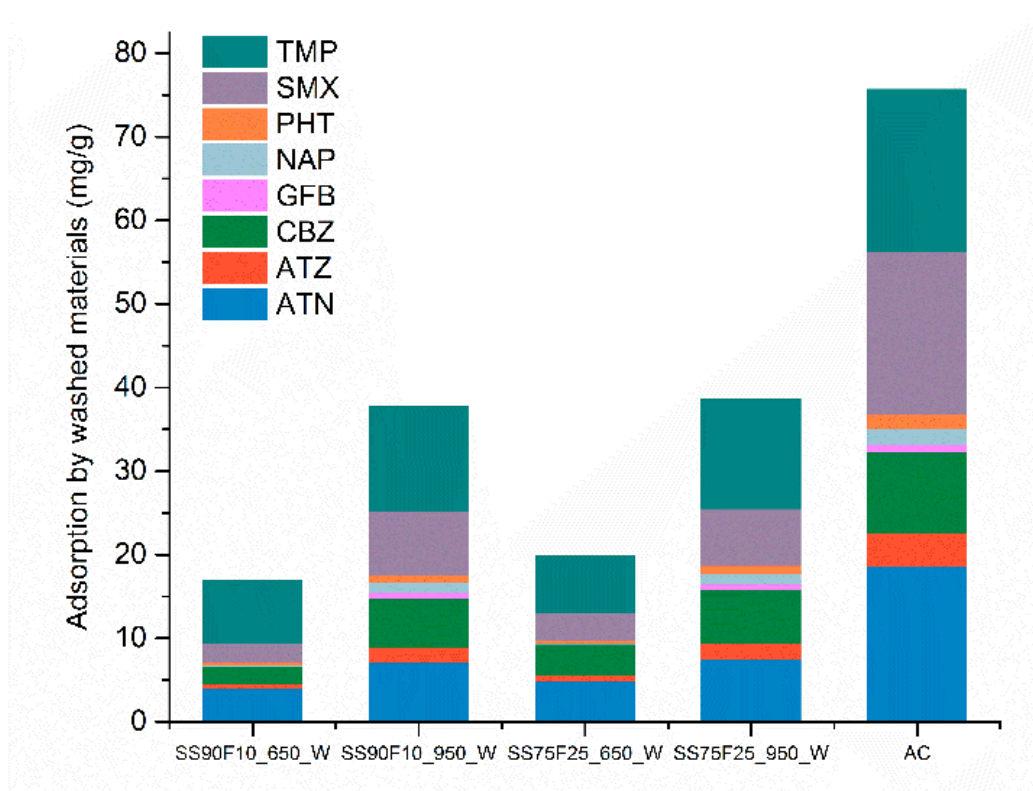


Figure 5-5 Adsorption on acid washed materials and activated carbon (AC) at the highest contaminants loading, each represents the average of triplicate tests.

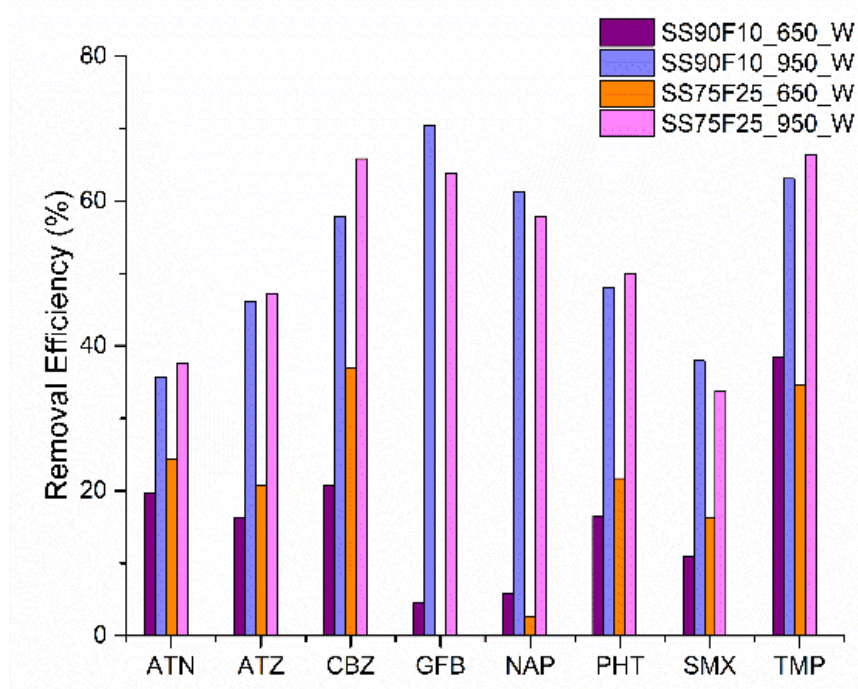


Figure 5-6 Removal efficiency of acid washed adsorbents at the highest contaminants loading.

When the unwashed and acid washed materials (SS90F10_950 and SS75F25_950) are compared (cf. Figure 5-2 and 5-5), the acid washed materials have almost double the adsorption capacity than the unwashed materials. Some compounds such as SMX and PHT which were poorly adsorbed previously are now removed at a higher percentage (cf. Figure 5-3 and 5-6). The performance enhancement could be attributed to the improvement in surface area and porosities from acid wash (Table 5-1).

5.3.2.3 Adsorption related to the physicochemical properties of different compounds

When looking at the removal efficiencies of individual compounds (Figures 5-3 and 5-6), GFB and TMP appeared to be removed most effectively by the sludge based materials. GFB exists

as negative species because the carboxylic acid group is ionized under the solution pH of ~6. The negative charge may contribute to adsorption because it may form complexations with numerous cations in the mineral phase of adsorbent. More importantly, it is very hydrophobic ($pK_a=4.77$), thus strong hydrophobic interactions with the carbon phase in the adsorbent are expected. Similar chemical properties could also be found on NAP which is also removed at a high efficiency. TMP has a very different chemical structure with respect to GFB. It carries positive charges (80% positively charged and 20% neutral) at the solution pH. The positive charges would help when cation exchange occurs between the analytes and materials which contain high content of Ca, Mg and Al. Besides, it is relatively hydrophilic ($pK_a=0.91$) and has the largest polar surface area among all of the adsorbates, so interactions with the polar mineral surface of the adsorbents would be stronger than others.

ATN is the other compound that carries a positive charge at solution pH. The positive charge would act similarly as in TMP. Besides, the presence of N–H dipoles allows the amide group to function as H-bond donors. It has only one amine group and the polar surface area is less than that of TMP (Table D1 in Appendix D), which may be the reasons for less amount of ATN adsorbed.

ATZ, CBZ and PHT are all neutral compounds at the solution pH, but CBZ appears to be the most favorably adsorbed compound, probably due to its smallest molecular size and high hydrophobicity.

SMX is the least removed compound especially for unwashed materials. A previous study also reported that SMX would not be efficiently adsorbed by sludge based adsorbents [63]. SMX

should be able to interact with the mineral phase of the adsorbents because its polar surface area is high (Table D1 in Appendix D). Obviously, polarity is not the only factor controlling the adsorption here. SMX is 72% negatively charged and 28% neutral. However, unlike GFB, the negative charge is on the acid amide group which is hidden in the middle of the molecular structure. Thus, spatial access to the negative charge by other ions/species would be limited.

5.3.3 Rapid Small Scale Column Test (RSSCT)

Acetic acid washed materials (SS90F10_950 and SS75F25_950) were selected to evaluate the adsorption performance in rapid small scale column test (RSSCT) and the breakthrough curves (BTCs) of selected compounds are presented in Figure 5-7. The empty bed contact time (EBCT) is 4.7 minutes. From Figure 5-7 it is observed that the duplicate columns generated very similar output data. The discontinuities at some parts of the BTCs were caused by the change of input solution (freshly made every 3 days to minimize the slow decay of the compounds in the input solution). With influent concentration of 1 mg/L for each compound, PHT and SMX reached full breakthrough (i.e., effluent concentration = input concentration) first, followed by ATZ, NAP, and then ATN and CBZ. Concentrations of GFB and TMP in the effluent were still well below the influent at the end of the experiments. In general, the order of breakthrough in RSSCT is consistent with the affinity determined via the batch tests, i.e., the ones with higher amounts adsorbed generally broke through at later times. The maximum amount adsorbed for each compound obtained from RSSCT is identical to or less than that obtained from the batch tests (Figure 5-8). This is expected because the RSSCT adsorption process might be kinetically limited (i.e., adsorption equilibrium may not have been reached during the short contact time). The only

exception is the compound gemfibrozil, whose adsorbed amount during RSSCT increased by almost 5-fold with respect to the batch tests. This may be due to the faster adsorption kinetics of gemfibrozil, or less competition during RSSCT with respect to the batch tests. In the batch tests, the concentration of gemfibrozil was about 1/20 of the other ones due to its low solubility whereas in RSSCT all compounds have the same concentrations of 1 mg/L.

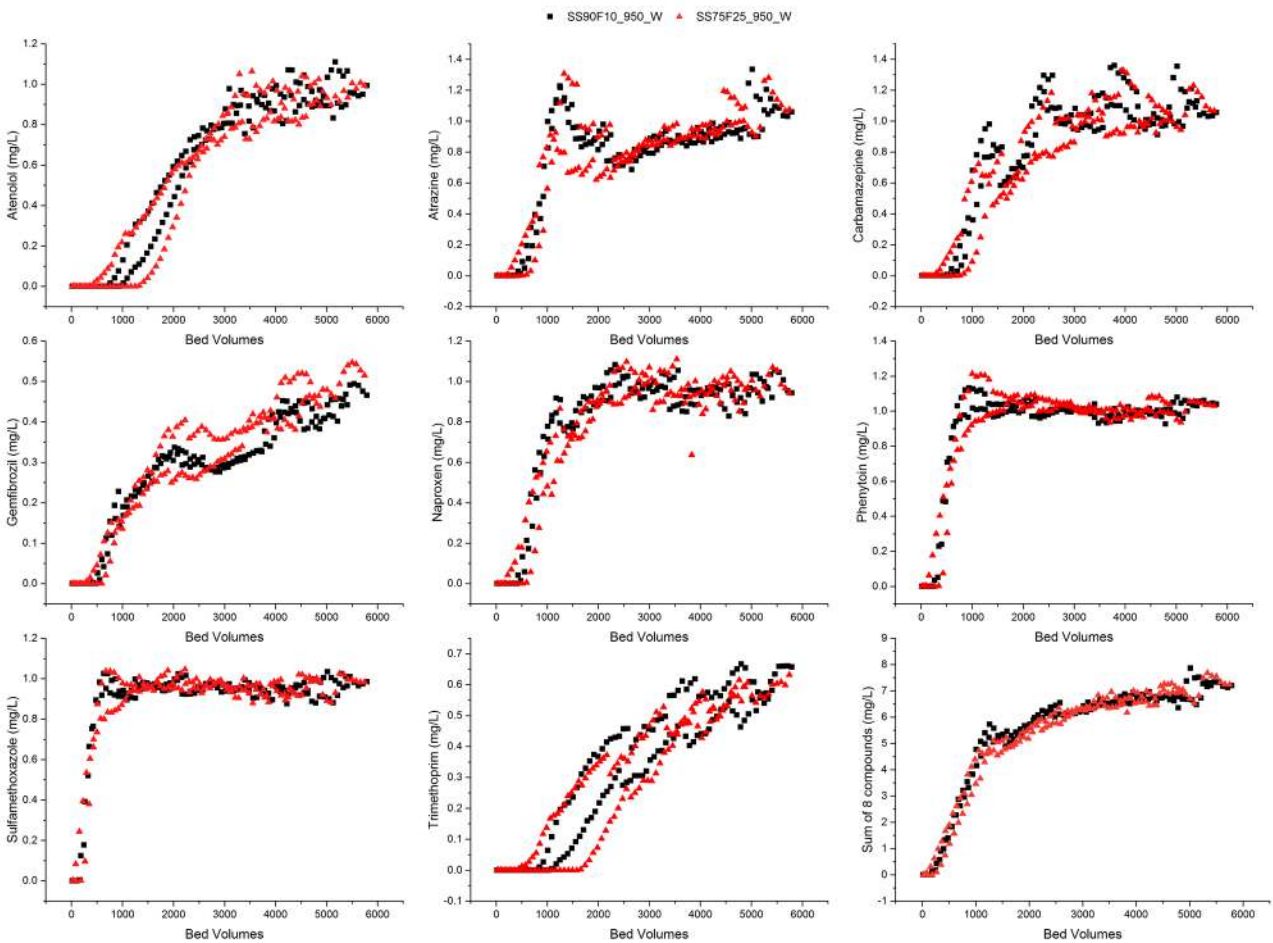


Figure 5-7 Total concentration of 8 contaminants in the effluent of column transport experiment of acid washed materials.

The overall amount of the pharmaceuticals and EDCs removed during RSSCT was about one half of the maximum amount adsorbed during the batch tests (Figure 5-9), despite the fact that the input concentrations in RSSCT (1 mg/L each) was much lower than those in the batch tests (up to 100 mg/L each) and the contact time during RSSCT (EBCT of ~5 min) was much shorter than that in the batch tests (16 hours). In order to quickly assess the maximum adsorption capacity of an adsorbent, batch equilibrium tests (typically 12-24 hours) with high input sorbate concentrations are often conducted. The high input concentrations are needed to ensure that the amount remaining in the aqueous phase after adsorption could still be detected. A constant critique of such an approach is that the concentrations used are unrealistically high and therefore the results are of little use in predicting real flow through applications. Column tests with more realistic input sorbate concentrations would be an ideal choice but such tests require a large volume of solution and long duration (for instance, for our RSSCT tests each 1 mL column needed over 3000 mL of solution and the tests lasted for 16 days to reach full breakthrough). Our results here demonstrate that for compounds and adsorbents similar to those tested here, the maximum adsorption capacities obtained from batch tests would be very relevant to the design of the experiments or the prediction of a performance under rapid flow conditions.

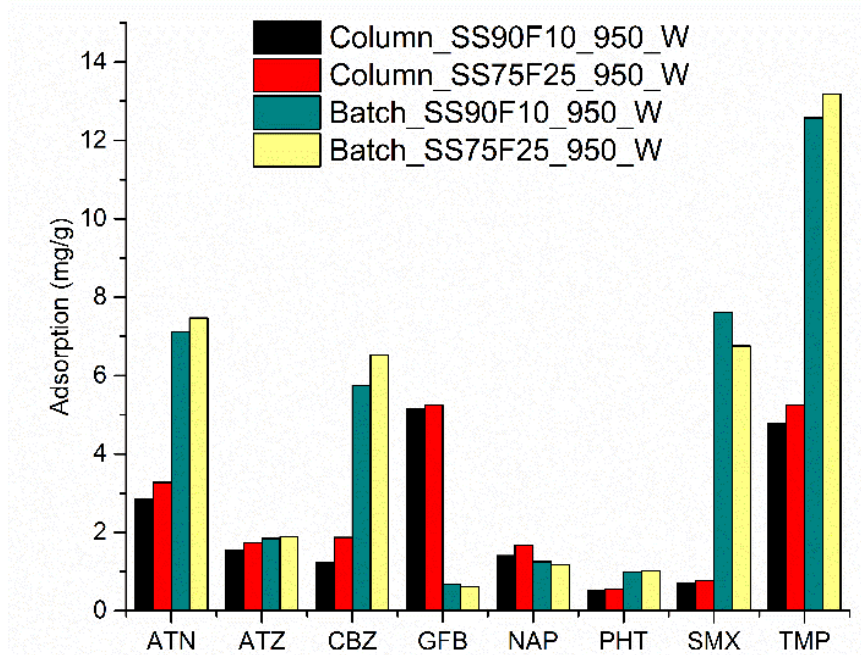


Figure 5-8 Comparison of maximum adsorption of individual compound by acid washed materials, tested in batch adsorption and column transport experiment

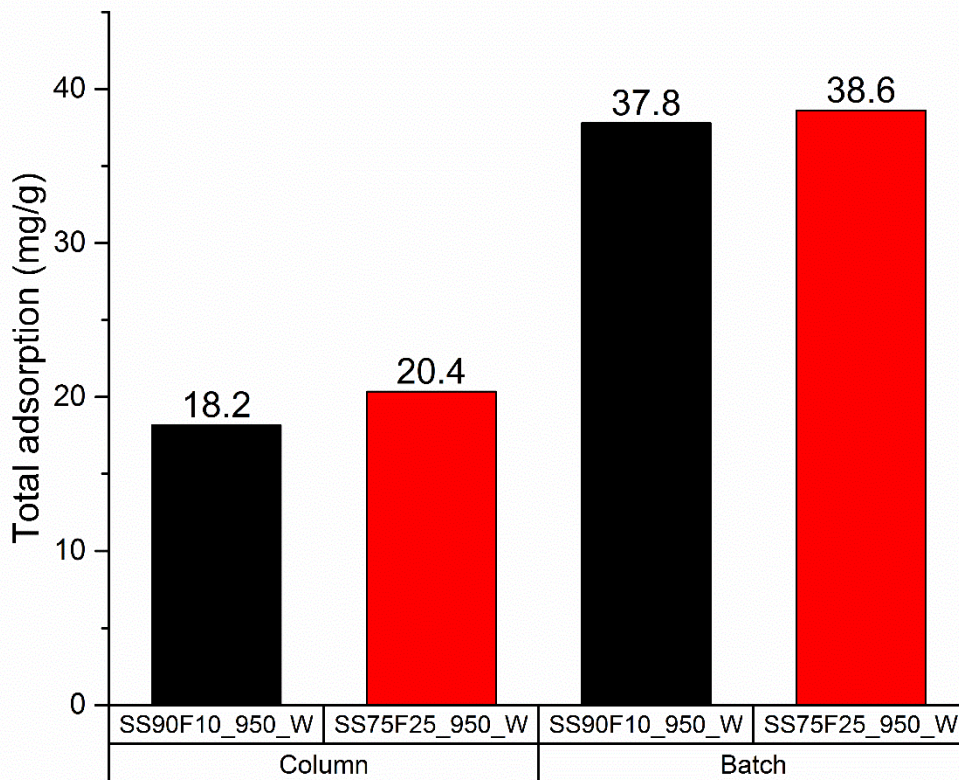


Figure 5-9 Comparison of total adsorption capacities of acid washed materials measured in batch adsorption and column transport experiment.

5.3.4 Field Column Test

Due to the variation in influent pressure, the EBCT fluctuated between 8 to 22 minutes. The experiment lasted for about one month when the columns were gradually clogged by sediment from source river water. Sixty-eight types of PPCPs were screened in both the influent and effluent and 14 were frequently detected, including Atenolol, Caffeine, Carbamazepine, Cotinine, Cyanazine, DEET, Diltiazem, Erythromycin, Lidocaine, Lopressor, Primidone, Sulfamethoxazole, TCP and TDCPP. The BTCs of the total pharmaceuticals and EDCs, together with precipitation amounts, are presented in Figure 5-10. The input concentrations varied significantly (from 200 ng/L to 1000 ng/L), and appeared to be positively correlated to the precipitation amount, likely due to combined sewer overflow (CSO) from wastewater treatment plants upstream of the Passaic River. The two duplicate columns were able to consistently remove 85-90% of the input pharmaceutical compounds and did not show any degradation of performance at the end of the test.

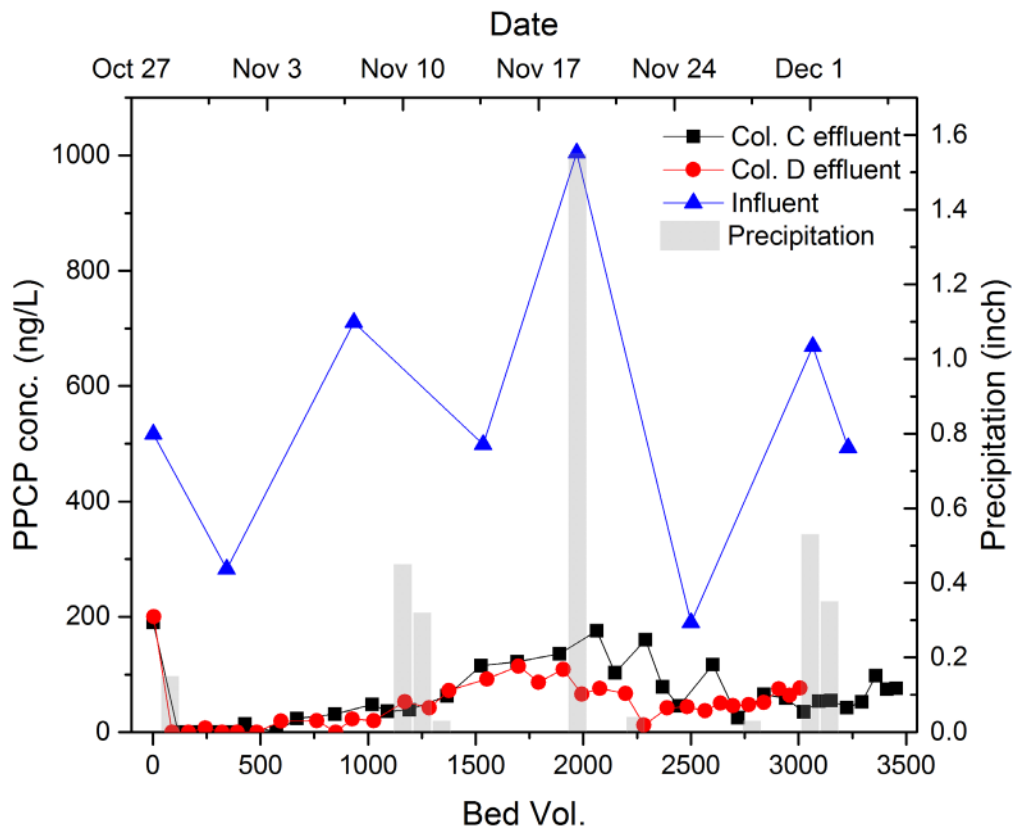


Figure 5-10 Results from the field column test at the Little Falls Water Treatment Plant in New Jersey.

5.4 Conclusions

Sewage sludge and fish waste based materials were tested as adsorbents to remove pharmaceuticals and EDCs from water. Increasing the pyrolysis temperature from 650 °C to 950 °C almost doubled the adsorption capacities of the materials towards the pharmaceutical and EDCs, and dilute acetic acid wash of the materials resulted in another 2-fold increase in adsorption capacities. The maximum adsorption capacities for these materials ranged from 16.9 mg/g to 38.6 mg/g, and the best performer achieved 50% of the capacity of a commercial activated carbon. The

adsorption capacities for these materials under rapid flow through conditions are about 50% of those obtained in batch equilibrium tests, demonstrating that for compounds and adsorbents similar to those tested here, the maximum adsorption capacities obtained from batch tests would be very relevant to the design of the experiments or the prediction of performances under rapid flow conditions. During the field experiment, 14 pharmaceutical compounds were detected in the source water of the Little Falls Water Treatment Plant. The large size columns were able to consistently remove 85-90% of the input pharmaceutical compounds and did not show any degradation of performance after a month of operation (~3500 bed volumes).

**Chapter 6 Adsorption of aqueous nitrosamines by sewage sludge
and fish waste based adsorbents**

6.1 Introduction

N-nitrosamines are a family of extremely potent carcinogens. Some nitrosamines have been classified as B2 carcinogens by the Integrated Risk Information System (IRIS) of the US Environmental Protection Agency (USEPA) and as 2A carcinogens by the World Health Organization's International Agency for Research on Cancer [38, 39]. Six nitrosamine disinfection byproducts are listed in the USEPA's second Unregulated Contaminant Monitoring Rule (UCMR 2) [194] and cited in USEPA's Drinking Water Strategy as a group of contaminants to be addressed in the near-term. These nitrosamines include N-nitrosodiethylamine (NDEA), N-nitrosodimethylamine (NDMA), N-nitrosodinbutylamine (NDBA), N-nitrosodinpropylamine (NDPA), N-nitrosomethylethylamine (NMEA), and N-nitrosopyrrolidine (NPYR).

Nitrosamines, particularly NDMA, were detected in drinking water worldwide, [138, 195-197]. The concentration of NDMA is typically in the low ng/L range in source and effluent of drinking water treatment plants, but it could be up to hundreds of ng/L occasionally [138]. In chloraminated raw water or wastewater effluent, this number could be above 1000 ng/L [198]. Moreover, NDMA may only account for a small portion of total nitrosamines, endangering the populations with these carcinogens.

The primary source of nitrosamines in drinking water treatment plants is disinfection, as nitrosamines present in influent water could be effectively removed by biological treatment [199]. Currently, chloramination is increasingly applied as an alternative to chlorination because chloramine is much more stable and does not dissipate as rapidly as free chlorine. Despite the fact that chloramine could limit the formation of by-products such as trihalomethanes (THM) and

haloacetic acids (HAA), it has been suspected that chloramination may generate more nitrosamines than traditional chlorination [138]. Other processes such as ozonation, catalytic reaction on activated carbon and UV photolysis may also contribute minor amounts of nitrosamines.

Removal of nitrosamines from water could be achieved by adsorption to activated carbon or by UV photolysis. Nitrosamines are decomposed when exposed to UV irradiation at the wavelength of ~230 nm and ~340 nm [200, 201]. The degradation rate is usually very fast, following pseudo-first-order kinetics with half-lives less than 10 minutes [200, 202]. However, some toxic degradation products such as methylamine, dimethylamine and N-methylformamide still remain in treated water [201-203]. Therefore, adsorptive removal of nitrosamines is preferable in this respect. Adsorption of nitrosamines by various materials has been reported. The adsorption by zeolite appeared to be dominated by the extent of geometric matching between adsorbate and adsorbent [204, 205]. The smaller compounds may favor the micropores while the bulkier ones would be attracted by mesopores. Activated carbon and modified activated carbon were also tested on the adsorption of nitrosamines [206, 207]. Besides the effects of pore size and volume, the surface features of adsorbents also play important roles during the adsorption. Metal impregnated activated carbon exhibited better performance than plain activated carbon because of the electrostatic attraction between the N-N=O group and cations [206].

Since adsorptive methods have been proved efficient, we are interested in applying adsorbents reclaimed from sewage sludge as alternatives to remove nitrosamines from water. Sewage sludge is one of the byproducts of active sludge technology in wastewater treatment industry. It is produced daily in abundant quantity and the amount is rising accompanied with growing population. Proper disposal of sewage sludge has been a worldwide problem, and

traditional pathways of disposal such as landfill and conversion to fertilizers have many negative effects [185]. Pyrolyzing the sewage sludge to produce porous adsorbents has a promising prospect. Their adsorption performance against Hg^{2+} [186], dyes [187], phenol [25], phosphates [188] and antibiotics [63] have been reported.

In this study, sewage sludge was mixed with fish waste to further improve diversities to the surface features of the adsorbents. The fish bone and scales have been proven effective adsorbents against metals and dyes [189, 190]. Similar to sewage sludge, fish waste is another type of potential resource which is being discharged at considerable quantities annually. Currently, commercial fish waste was usually either landfilled or discharged into water bodies as industrial effluent. The effluent which is high in BOD, COD, TSS and fat-oil-grease could very likely produce adverse effects on the receiving environments [10]. Most of the current technologies to reutilize fish waste are either not economically attractive or odoriferous [7]. In this regard, pyrolysis together with sewage sludge provides another option.

6.2 Materials and Methods

6.2.1 Adsorbents

The detailed method of preparing adsorbents was described previously [35]. Briefly, anaerobically digested sewage sludge (from a wastewater treatment plant in New York City) and fish waste (from a local market in New Jersey) were dried and grounded individually or as homogeneous mixtures in the ratio of 90:10 or 75:25 (sludge:fish waste by dry weight). Then the mixtures were carbonized in a horizontal furnace under nitrogen atmosphere at the temperature of

650 °C or 950 °C. The materials are finally referred to as SS, F and SSF based on their composition, followed by 650 or 950 reflecting the pyrolysis temperature.

6.2.2 Acid wash

The materials were washed in the solid to liquid ratio of 1:5 with diluted acetic acid (pH=2.88) for 18 hours at room temperature, for 2~3 times until the solution pH dropped to about 7. After that, it was followed by 3 times DI water wash with the same solid to liquid ratio (2 hours each). At the end, the solid was dried in an oven for future use. The letter W was added to the sample names of the acid washed adsorbents to differentiate them from the unwashed samples.

6.2.3 Batch adsorption experiment

Both acid washed and unwashed materials were evaluated in batch adsorption experiments. The 6 compounds N-nitrosodiethylamine (NDEA), N-nitrosodimethylamine (NDMA), N-nitrosodinbutylamine (NDBA), N-nitrosodinpropylamine (NDPA), N-nitrosomethylethylamine (NMEA), and N-nitrosopyrrolidine (NPYR) were purchased as neat compounds and prepared as a mixture in water. The physical properties of the compounds are summarized in Table E1 in Appendix E. Ten mL of a mixture solution with various concentrations (from 1 mg/L to 100 mg/L) was mixed with 0.05 g of an adsorbent in an amber glass vial at room temperature. Triplicates were prepared at each concentration. The samples were sealed and shaken for 18 hours for isotherm study. After filtration and proper dilution, the equilibrium concentrations (C_e) of adsorbates in the liquid phase were analyzed using liquid chromatography-tandem mass spectrometry (LC/MS/MS). The pH of the solution at equilibrium was also measured.

6.2.4 Column transport experiment

Based on the performance in batch adsorption experiments, SS90F10_950-W and SS75F25_950-W (both acid washed) were selected for the transport experiments. Duplicate columns were prepared. The adsorbent (0.5 g, ~0.7 mL) was packed into a mini-column of 4 mm ID, with both ends filled with glass wool. The influent solution with 0.5 mg/L of each compound was pumped through the columns via a peristaltic pump at the flow rate of 0.15 mL/min (corresponding to an empty bed contact time (EBCT) of 4.7 min). The effluent was collected with a fraction collector and analyzed with LC/MS/MS, described below.

6.2.5 LC/MS/MS analysis

The compounds were analyzed by LC/MS/MS (API 4000, Applied Biosystems) with ESI (electrospray ionization) and MRM (multiple reaction monitoring). Separation of analytes was achieved using a 50×4.6 mm Eclipse plus C18 column with 1.8 μm particle size (Agilent). Oven temperature was kept at 35°C. Twenty μL sample was injected after 3 min equilibration. A binary gradient of water (component A) and methanol (component B) both consisting 4 mM ammonia formate was pumped at the flow rate of 0.4 mL/min. All compounds were ionized in positive mode. Nitrogen was used as both the collision gas and nebulizing gas. Identification of all compounds was made by two MRM transitions and quantitation was made by the more abundant one.

6.3 Results and Discussion

6.3.1 Batch adsorption

6.3.1.1 Unwashed materials

Figure 6-1 shows the adsorption isotherms of the 6 nitrosamines by unwashed sludge derived materials, and Table 6-1 presents the observed adsorption capacity at the highest contaminant loading.

NDBA and NMEA could be adsorbed by all four materials (maximum adsorbed amount of 6.1 mg/g and 7.2 mg/g, respectively), and the amount adsorbed increased as the input concentration increased (i.e., a “normal” adsorption isotherm, Figure 6-1). NDMA and NDPA could be removed by the three sewage sludge containing materials (maximum adsorbed amount of 1.4 mg/g and 2.2 mg/g, respectively) but not the F_950 material. The amount of NDPA adsorbed by the SS75F25_950 material actually decreased at the highest two contaminant loadings, suggesting competitive adsorption among the nitrosamines (Figure 6-1). NDEA and NPYR could be barely removed by the SS_950 and SS90F10_950 materials (maximum adsorbed amount ≤ 0.7 mg/g) and could not be adsorbed by the SS75F25_950 or F_950 materials at all.

As far as the different adsorbents are concerned, the SS_950 material (sewage sludge only) could remove all of the 6 nitrosamines and the total capacity is 11.8 mg/g. The F_950 material (fish waste only) could only remove 2 out of the 6 nitrosamines with the total capacity of 9.2 mg/g (Table 6-1). Adding 10-25% of fish waste to the composite materials (i.e., the SS90F10_950 and SS75F25_950 materials) lead to slightly increased capacities (13.2-14.9 mg/g) with respect to the two end members, suggesting some synergistic effects. For the two composite materials, the

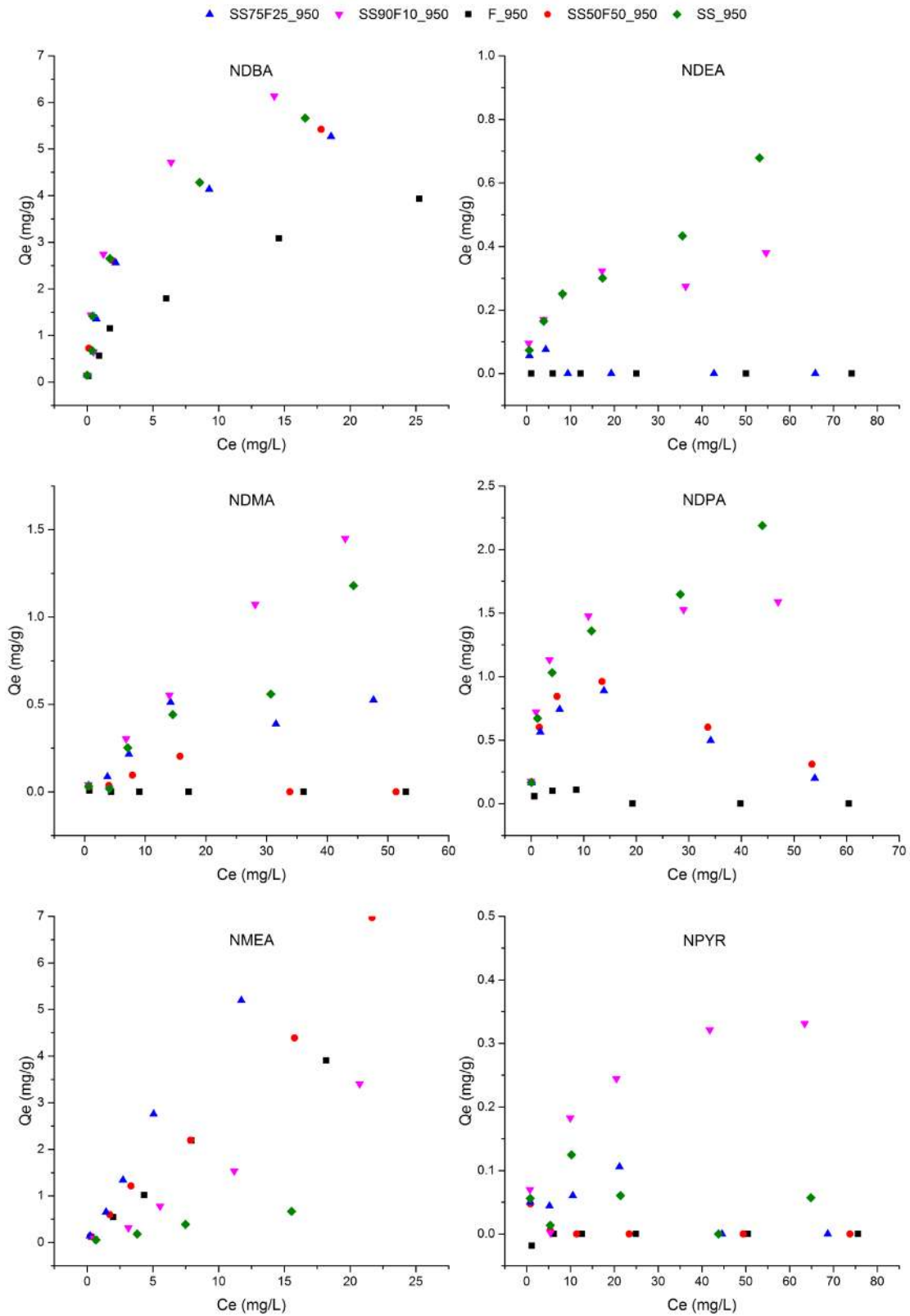


Figure 6-1 Adsorption isotherms of the 6 nitrosamines by the unwashed materials

SS90F10_950 performed better on the adsorption of NDBA and NDPA (with the maximum adsorbed amount of 6.1 mg/g and 1.6 mg/g, respectively) than SS75S25_950, whereas the latter adsorbed more NMEA (with the maximum adsorption of 7.2 mg/g) than the former (Figure 6-1 and Table 6-1).

Table 6-1 Adsorption at the highest contaminant loading for unwashed materials

		NDBA	NDPA	NDEA	NPYR	NMEA	NDMA	SUM
Maximum adsorption (mg/g)	F_950	3.9	0.0	0.0	0.0	5.3	0.0	9.2
	SS75F25_950	5.3	0.2	0.0	0.0	7.2	0.5	13.2
	SS90F10_950	6.1	1.6	0.4	0.3	5.0	1.4	14.9
	SS_950	5.7	2.2	0.7	0.1	2.1	1.2	11.8
	AC	11.0	10.6	6.2	5.2	3.1	2.5	38.7

6.3.1.2 Acid washed materials

Figure 6-2 shows the adsorption isotherms of the 6 nitrosamines by four acid-washed composite materials and Table 6-2 presents the observed adsorption capacity at the maximum contaminant loading. As seen in Figure 6-2, NDBA, NEDA, NDMA, and NMEA could be adsorbed by the four materials tested here to various degrees, whereas NPYR could be adsorbed by 3 materials and NDPA could only be adsorbed by 2 materials. Some competitive adsorption was evident for NDPA where the adsorbed amount dropped as the input concentration increased.

For the two materials obtained at 950 °C, SS90F10_950_W adsorbed more NDPA than SS75F25_950_W (2.0 mg/g vs. 1.2 mg/g), while the latter adsorbed more NDEA, NPYR, and NMEA than the former (Table 6-2), suggesting that the addition of 10 or 25% of the fish waste

produced composite materials with somewhat different surface features and adsorption towards different nitrosamines.

Total adsorption capacity toward the 6 nitrosamines is 14.0 mg/g and 17.0 mg/g for SS90F10_950_W and SS75F25_950_W, respectively. These amounts are 2-3 times the adsorption capacities of the corresponding materials obtained at 650 °C (4.3 mg/g for SS90F10_650_W and 6.8 mg/g for SS75F25_650_W). It was reported previously that higher pyrolysis temperatures would benefit the development of pore structure and surface area of adsorbents [133, 153]. For the acid washed SS90F10 and SS75F25 materials the surface area and pore volumes almost doubled when the pyrolysis temperature increased from 650 °C to 950 °C (see Table 5-1 in Chapter 5), leading to much improved adsorption for the nitrosamines.

Acid wash significantly increased the adsorption for NDBA but drastically reduced the adsorption for NDEA, and slightly improved the total adsorption capacity (cf. Table 6-1 and 6-2 for the SS90F10_950 and SS75F25_950 materials). As seen Table 5-1, the surface area and pore volumes increased significantly after acid wash for these two materials as the result of dissolution of some basic oxides such as CaO formed during the pyrolysis and removal of tarry residues formed during pyrolysis [1, 133]. While acid wash significantly enhanced the adsorption of pharmaceuticals and EDCs (Chapter 5), the improvement for nitrosamine adsorption was marginal.

Compared with the activated carbon employed in this study (WVA-900), the total capacity of the best performed sludge derived material (SS75F25_950-W) was close to one half of that of the activated carbon, even though its surface area and pore volume are only about 1/7 of those of the activated carbon. The adsorption capacities towards nitrosamines (14.0-17.0 mg/g) for the acid

washed materials are better than or comparable to those of many other materials such as modified zeolite, mesoporous silica, and metal impregnated activated carbons [206-208].

Table 6-2 Adsorption at the highest contaminant loading (acid washed materials)

		NDBA	NDPA	NDEA	NPYR	NMEA	NDMA	SUM
Batch maximum adsorption (mg/g)	SS90F10_650_W	1.4	0.0	1.5	0.0	0.5	0.8	4.3
	SS90F10_950_W	9.0	2.0	0.5	1.0	0.6	0.8	14.0
	SS75F25_650_W	1.7	0.0	0.9	2.5	1.2	0.4	6.8
	SS75F25_950_W	8.9	1.2	1.4	2.7	1.9	0.9	17.0
	AC	11.0	10.6	6.2	5.2	3.1	2.5	38.7

Figure 6-3 presents the plots of amount adsorbed vs. $\log K_{ow}$ of the nitrosamines for the acid washed composite materials and activated carbon. It appears that the adsorption of nitrosamines is dominated by the hydrophobicity ($\log K_{ow}$) of the compounds, especially for the adsorption to the activated carbon ($R^2=0.92$, Figure 6-3). The correlation coefficients for SS90F10_950-W and SS75F25_950-W are a bit lower (0.61-0.73), suggesting that factors other than hydrophobicity may also play some roles in the adsorption. For instance, it was reported that the adsorption of nitrosamines was strongly affected by the size matching between the compounds and pore sizes of zeolites [204, 206].

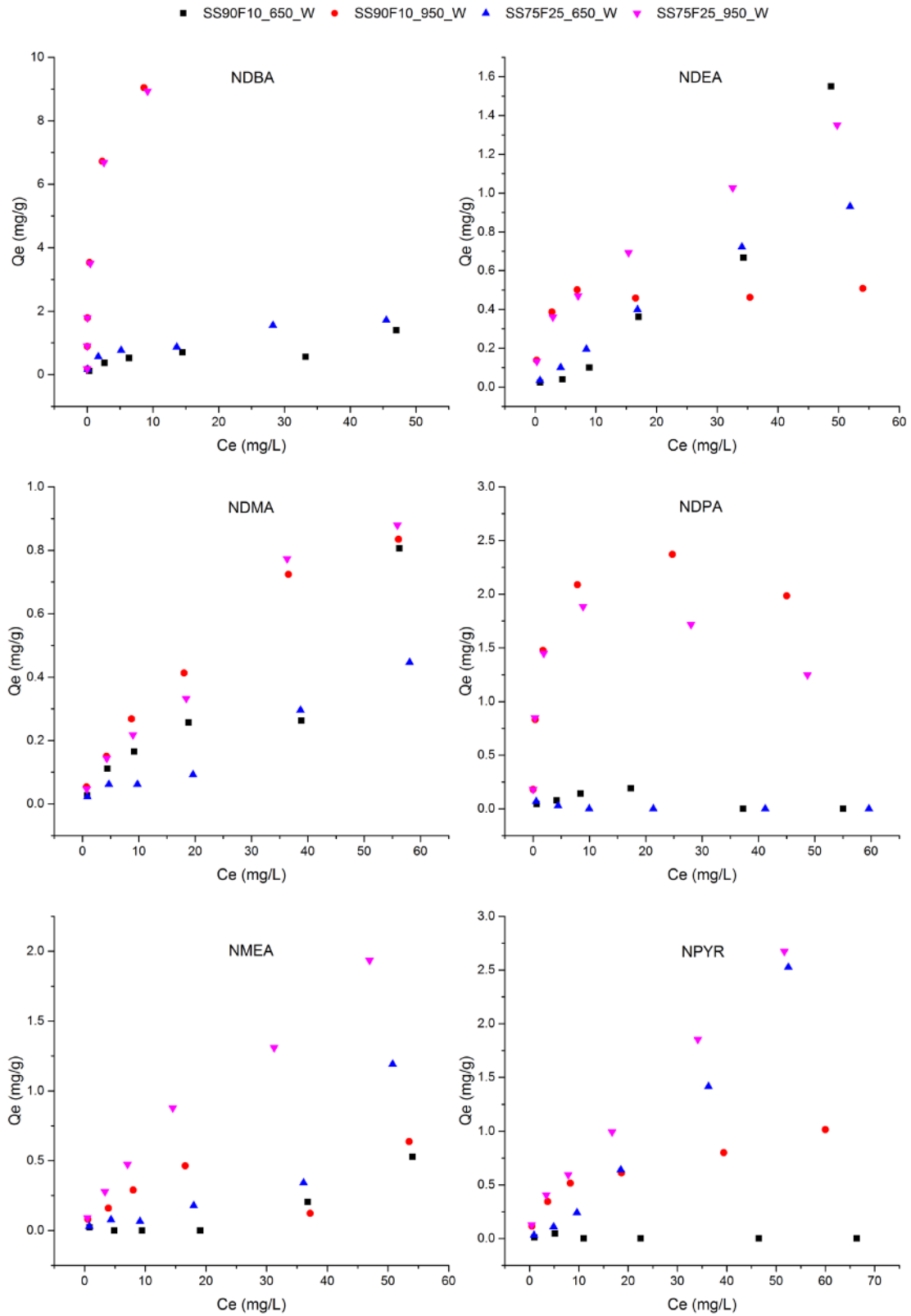


Figure 6-2 Adsorption isotherms of the 6 nitrosamines by the acid-washed materials.

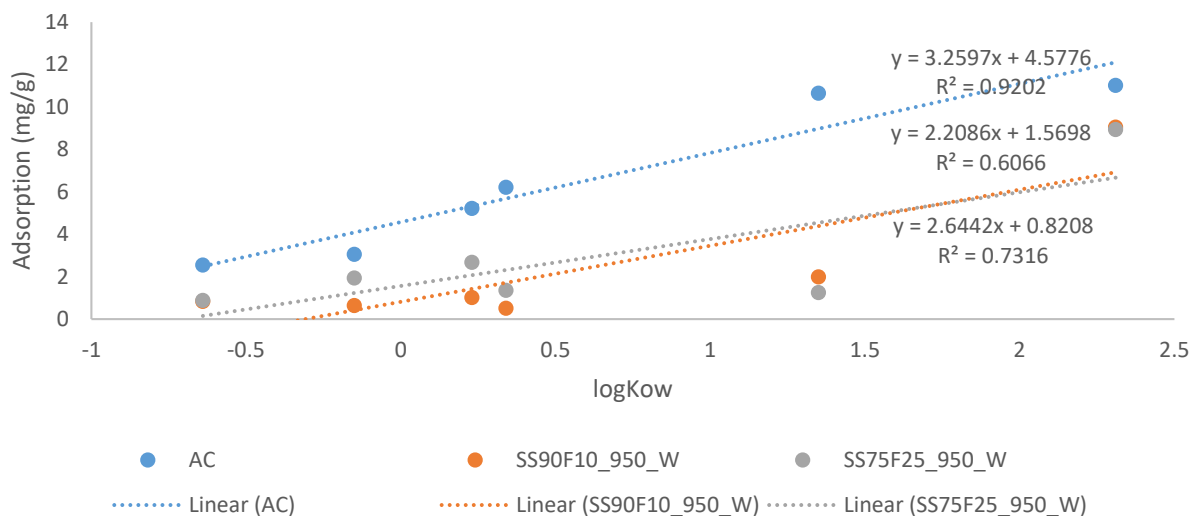


Figure 6-3 The correlation between hydrophobicity (logKow) of nitrosamines and adsorption.

As previously described, the sludge based adsorbents contain many metals such as Ca, Fe, Cu and Zn [34]. The cations in the adsorbents took charge in attracting nitrosamines because electrostatic attraction could be established between the N-N=O group and cations [206]. There were evidence that Cu impregnated zeolite could improve the overall adsorption of nitrosamines even though the impregnation might negatively affect the pore volume of the host [209]. In our case, the metal oxides contained in the raw sludge could play a similar role as the impregnated copper. This may be the reason that sludge based adsorbents could adsorb more nitrosamines than activated carbon per unit surface area.

6.3.2 Column transport experiments

Column transport experiments were also carried out to evaluate the performance of the adsorbents under dynamic flow through conditions. Based on the performance in batch adsorption, SS90F10_950_W and SS75F25_950_W were selected for rapid small scale column test (RSSCT). Figure 6-4 shows the breakthrough curves of the 6 nitrosamines as well as the sum of the 6 compounds. The duplicate columns generated very similar results, indicating good reproducibility. The jumps in the breakthrough curves were probably generated by the temporary suspension and resume of pumping while refilling the input reservoir.

The order of nitrosamines reaching a full breakthrough during column transport was similar to their extent of being adsorbed during batch experiments, i.e., the compounds which were poorly adsorbed in batch experiments broke through the columns faster, and vice versa. With influent concentration of 0.5 mg/L each, NDMA, NMEA, NPYR reached full breakthrough between 300 and 500 bed volumes, closely followed by NDEA at about 1000 bed volumes. Only about 30-40% of the NDBA broke through the columns at the end of the experiments (~ 6000 bed volumes). It is worth noting that NDPA achieved a full breakthrough at about 4000 bed volumes, however, its concentration in effluent kept rising and slightly exceeded the input concentration. This is probably because NDBA was competing with NDPA and has partially replaced NDPA from its adsorption sites, similar to the competition observed in batch adsorption experiments.

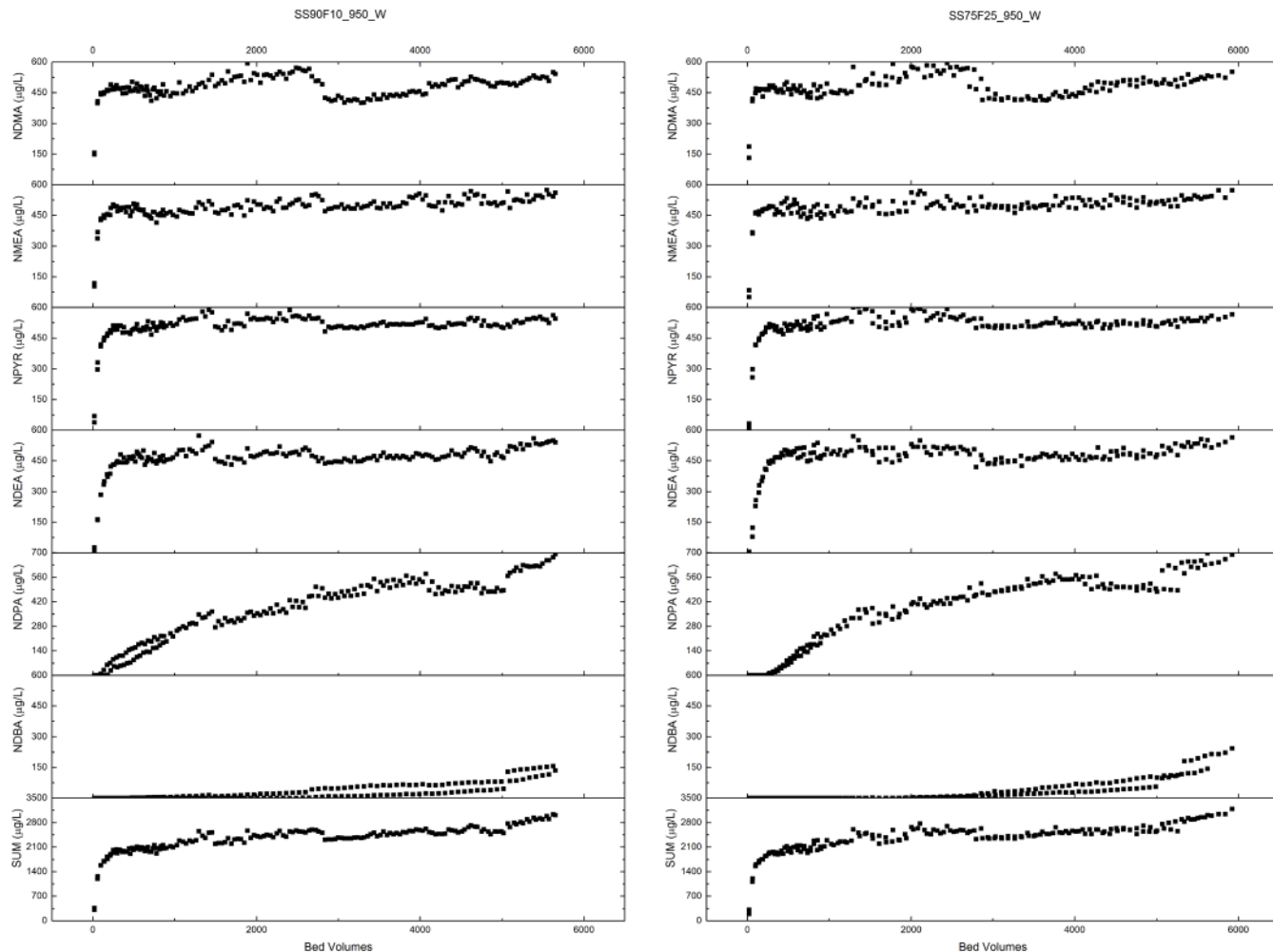


Figure 6-4 Breakthrough curves of the 6 nitrosamines as well as the sum of the 6 compounds

Table 6-3 Nitrosamines adsorbed in batch (at highest loading) and column transport experiment

Qe (mg/g)	Column		Batch	
	SS90F10_950_W	SS75F25_950_W	SS90F10_950_W	SS75F25_950_W
NDBA	3.06	3.23	9.04	8.93
NDPA	0.68	0.66	1.98	1.25
NDEA	0.19	0.17	0.51	1.35
NPYR	0.00	0.00	1.01	2.67
NMEA	0.02	0.01	0.64	1.93
NDMA	0.13	0.12	0.83	0.88
SUM	4.09	4.18	14.02	17.02

The adsorbed amount of each compound in the RSSCT was calculated by integrating its breakthrough curve using the OriginPro software and the results are summarized in Table 6-3. NPYR and NMEA were barely removed from the solution. NDMA and NDEA were also not retained much by the columns. NDPA was removed at the amount about 0.7 mg/g by the sludge derived adsorbents. Similar to what was observed in batch experiment, NDBA was the most effectively removed compound. The amount adsorbed was around 3.5 mg/g, accounting for 77% of the total amount of nitrosamines removed by the columns at the end of the experiments.

From Table 6-3 it is seen that NDPA was the most adsorbed nitrosamine in both batch and column experiments. NPYR and NMEA were adsorbed to a moderate degree in the batch tests but were barely removed in the column experiments. Overall, the amount of nitrosamines removed during batch tests was 3 to 4 times higher than the amount removed during column tests (Figures 6-5 and 6-6). This difference could be attributed to the significantly lower input concentration and shorter residence time in the column tests (0.5 mg/L each and 4.3 min empty bed contact time) with respect to those in the batch tests (up to 100 mg/L per compound and 18 hours of equilibrium time). Short contact time may significantly reduce the amount adsorbed if the adsorption process is somewhat kinetically limited.

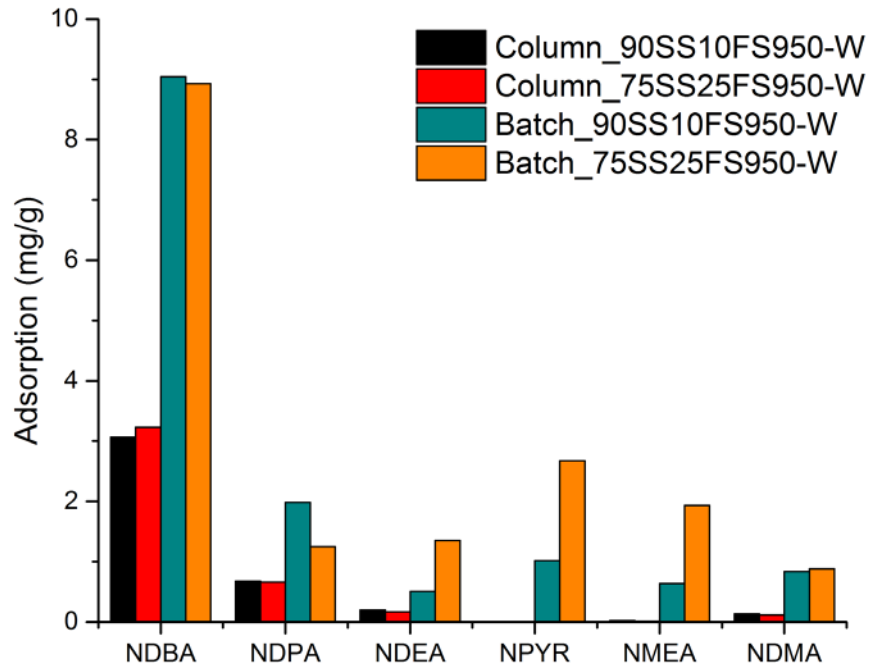


Figure 6-5 Comparison of maximum adsorption of individual analyte by acid washed materials, tested in batch adsorption and column transport experiment.

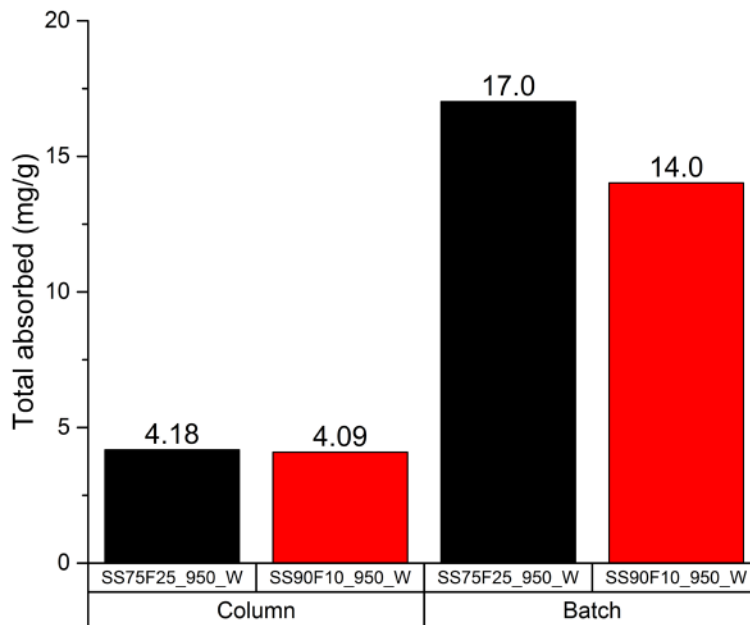


Figure 6-6 Comparison of total adsorption capacities of acid washed materials measured in batch adsorption and column transport experiment

6.4 Conclusions

The performance of sewage sludge and fish waste based composite materials on the removal of 6 nitrosamines from water was evaluated under batch equilibrium and dynamic flow through conditions. The adsorption capacity of the composite materials increased as the pyrolysis temperature increased, likely due to the increased surface area and porosity. Acid wash only improved the adsorption marginally. The adsorption capacities towards nitrosamines (14.0-17.0 mg/g) for the acid washed materials are better than or comparable to those of many other materials such as modified zeolite, mesoporous silica, and metal impregnated activated carbons. The strong correlation between the adsorbed amount and $\log K_{ow}$ values of the compounds suggests that hydrophobic interaction plays a significant role on adsorption on the composite materials. Other mechanisms may include the interaction between N=O group with metals presented in the materials. The maximum amount of nitrosamines adsorbed during batch tests is 3-4 times of that obtained from column tests, indicating that the adsorption process is somewhat kinetically limited.

Chapter 7 Future Research

The conversion of sewage sludge and other wastes to composite adsorbents is a promising means of reusing these wastes. However, there are still some drawbacks of sludge based adsorbents (SBAs) comparing to commercial activated carbons, especially in large scale production and applications. More efforts are needed in order to apply these materials in drinking water treatment, but the application in industrial wastewater and toxic gas treatment is tangible.

One drawback of the SBAs is that the content of sewage sludge and other wastes could vary from place to place and from time to time, and the properties of the resultant SBAs would vary depending upon the nature of the raw materials. As such, quality control of the SBAs is expected to be challenging. It would be very helpful if raw materials from WWTPs and other sources could be collected regularly and the properties of the products be compared. Routine tests of the raw materials and SBAs are necessary to ensure consistent material properties.

The leachable metals presented in the sludge derived materials would not be a problem for wastewater or toxic gas treatment, but care needs to be taken for drinking water treatment. The effluent of treated water should be closely monitored. Even though it was proved in this study that acetic acid wash could significantly reduce leachable metals, long-term studies (e.g., a few months) are needed to ensure the safety of these recycled materials in drinking water treatment.

In addition to acetic acid wash, it would be of a great interest to examine if phosphate acid could be used as washing solution. Phosphate, zero valent iron (ZVI) or other modifiers could be used as additives during pyrolysis. Phosphate could form stable minerals with multiple metals such

as manganese, iron and zinc, which is detected in high concentrations in the sludge materials. ZVI has been proved to have a great ability to remove multiple metals from aqueous solution. At least, a subsequent column packed with sand and ZVI could effectively remove leached metals and provide a safety guard [210].

After pyrolysis, the SBAs could be coated with metal oxides or ZVI, which may change their surface features. For example, CuO and TiO₂ coated zeolite have been applied to remove organic contaminants from water [209, 211, 212]. Iron coated zeolite was used to adsorb multiple heavy metals from water [213]. ZVI coated sand was also used to remove As (III) from water [214]. The surface chemistry alternation could produce application-specific adsorbents.

Currently, the SBAs do not have an advantage in surface area and pore volumes in comparison with activated carbons. Due to the low carbon content, physical activation did not yield high surface area [1]. Chemical activation (KOH) seems to work very well on activating SBAs, but resulting highly alkaline adsorbents which would be applicable for waste gas treatment but not water treatment. Utilization of novel activation techniques (e.g., chemical activation under a gasifying atmosphere) could be a future direction. Another feasible way is to mix the raw sludge with other bio-wastes such as sawdust, straws or food scraps to increase the carbon content and produce granular adsorbents.

Exhausted gas produced during pyrolysis is another concern because it may contain toxic contents such as PAHs [215]. There may also be pyrolysis liquid produced which may contain polyaromatic ketones and monoaromatics [216]. In the meanwhile, both the syngas and bio-oils could be used as fuels [217]. With proper designs, the fuel byproducts would greatly reduce the

energy needed to dry and pyrolyze the raw materials, but more efforts are needed to reduce the production of tars and to improve gas yield and quality (i.e., more light gases).

At last, the management of exhausted adsorbents has not been addressed. It is expected that the regeneration of the adsorbents saturated with organic contaminants would produce materials with higher carbon content at much lower energy cost than using raw sewage materials. However, the mechanical strength of the regenerated materials as well as the adsorption capacities for organic contaminants need to be investigated.

Appendix

Appendix A

Table A4 MRM transitions and Mass Spectrometry parameters

Compounds	Primary Transition	Secondary Transition	DP (volts)	CE (volts)	CXP (volts)
AMO	366.1/349.2	366.1/114.1	51	13	20
PEN-G	335.1/91.1	335.1/217.0	91	71	16
ENR	360.2/316.2	360.2/342.1	61	29	22
OFL	362.1/318.0	362.1/261.1	61	27	18
SDZ	251.0/156.0	251.0/108.0	66	21	8
SMZ	279.1/65.1	279.1/124.1	46	75	10
SMX	254.0/65.0	254.0/92.0	61	65	10
ERY	734.5/83.2	734.5/158.2	81	77	14
OTC	461.2/426.2	461.2/443.2	56	29	12
CTC	479.1/462.2	479.1/444.2	66	25	30
CHP	323.0/275.0	323.0/304.9	66	21	14
CBZ	237.0/194.1	237.0/193.2	76	29	12
PRM	219.1/162.1	219.1/106.1	61	19	16

Table A5 R² values of linear fitting of peak area vs. concentration for all of the compounds with or without NOM.

R²	Constant ratio experiments (CC II)				Constant concentration experiments (CC III)			
	Control*	SRNOM	NRNOM	SRFA	Control*	SRNOM	NRNOM	SRFA
AMO	0.996	0.999	0.997	0.999	0.999	0.999	1.000	1.000
PEN-G	0.996	0.995	0.996	0.997	0.999	0.999	0.999	0.999
ENR	0.988	0.979	0.985	0.989	0.947	1.000	0.995	0.978
OFL	0.986	0.980	0.982	0.997	0.971	0.999	0.996	0.977
SDZ	0.993	0.994	0.994	0.992	0.996	0.996	0.996	0.994
SMZ	0.999	0.998	0.998	0.998	1.000	1.000	0.999	0.999
SMX	0.997	0.996	0.996	0.997	0.999	0.998	0.998	0.999
ERY	0.998	1.000	0.999	0.999	0.999	0.998	0.999	0.998
OTC	0.999	0.998	0.998	1.000	0.998	0.996	0.995	0.995
CTC	0.995	0.997	0.998	1.000	0.996	0.999	0.996	0.999
CHP	0.998	0.995	0.996	0.996	0.998	0.999	0.999	0.999
CBZ	0.962	0.964	0.959	0.962	0.969	0.969	0.971	0.971
PRM	0.996	0.997	0.997	0.996	0.998	0.998	0.999	0.999

* Control is the mixture standard in pure water without NOM (CC I).

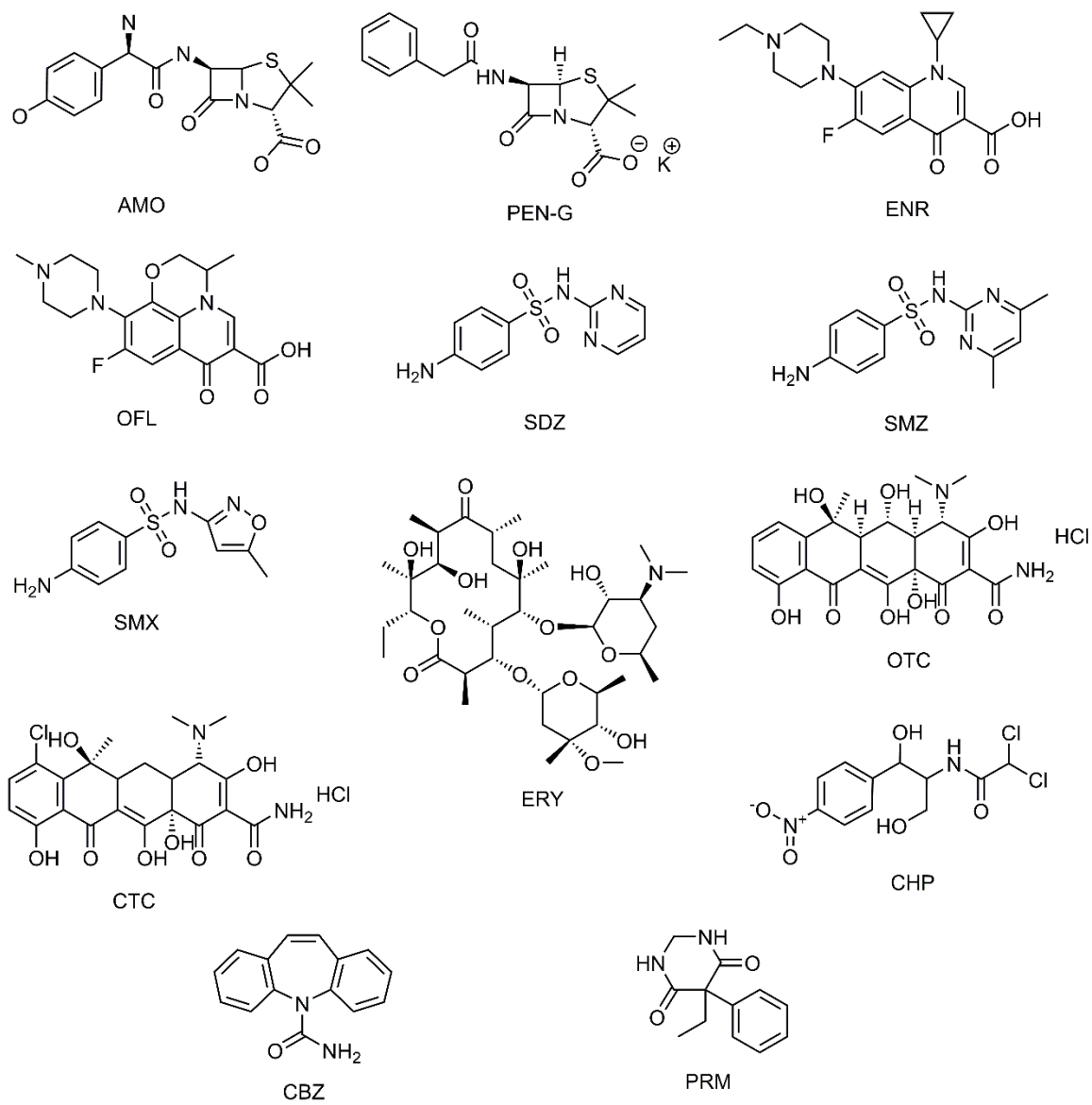


Figure A7 Chemical structures of analytes in this study

Appendix B

Table B6 Formula, molecular weight (MW), pKa, solubility, and logK_{ow} of the antibiotics and anticonvulsants examined in this study.

Compound	Abbr.	Formula	MW	pKa	Solubility (mg/L)	logK _{ow}
Amoxicillin	AMO	C ₁₆ H ₁₉ N ₃ O ₅ S	365.4	2.4 (carboxylic acid group) 7.4 (basic amine group) 9.6 (acidic hydroxide group) [56]	3430 [218]	0.87 [218]
Penicillin-G	PEN-G	C ₁₆ H ₁₇ KN ₂ O ₄ S	372.5	2.8 (free carboxylic acid group) [219]	very soluble	1.83 [218]
K salt						
Enrofloxacin	ENR	C ₁₉ H ₂₂ FN ₃ O ₃	359.4	3.85 (carboxylic acid group) 6.19/7.59/9.86, assigned in order to three basic nitrogen sites starting from ring 1 (nalidixic acid group) to ring 3 (fluoro group) [56, 220]	146 [221]	1.1 [222]
Ofloxacin	OFL	C ₁₈ H ₂₀ FN ₃ O ₄	361.4	5.97 (carboxylic acid group) 8.28 (basic piperazinyl group) [223]	190 [218]	0.35 [222]
Sulfadiazine	SDZ	C ₁₀ H ₁₀ N ₄ O ₂ S	250.3	1.57 (basic amine group) 6.50 (acidic amide group) [224]	67 [225]	-0.092 [226]
Sulfamethazine	SMZ	C ₁₂ H ₁₄ N ₄ O ₂ S	278.3	2.07 (basic amine group) 7.49 (acidic amide group) [220]	451 [225]	0.89 [222]

Sulfamethoxazole	SMX	C ₁₀ H ₁₁ N ₃ O ₃ S	253.3	1.85 (basic amine group)	353 [225]	0.89 [227]
				5.6 (acidic amide group) [220]		
Erythromycin	ERY	C ₃₇ H ₆₇ NO ₁₃	733.9	8.9 (basic dimethylamino group) [220]	19000 [218]	3.06 [226]
Oxytetracycline HCl	OTC	C ₂₂ H ₂₄ N ₂ O ₉ ·HCl	496.9	3.22 (acidic tricarbonyl group)	313 [218]	-1.12 [228]
				7.46 (acidic □-diketone group)		
				8.94 (basic dimethylamino group) [220]		
Chlortetracycline HCl	CTC	C ₂₂ H ₂₃ ClN ₂ O ₈ ·HCl 1	515.3	3.33 (acidic tricarbonyl group)	630 [218]	-0.62 [218]
				7.55 (acidic □-diketone group)		
				9.33 (basic dimethylamino group) [220]		
Chloramphenicol	CHP	C ₁₁ H ₁₂ Cl ₂ N ₂ O ₅	323.1	11 [229]	2500 [222]	1.14 [222]
Carbamazepine	CBZ	C ₁₅ H ₁₂ N ₂ O	236.3	<1, 13.9 (amino group) [230]	78 [218]	1.51 [231]
Primidone	PRM	C ₁₂ H ₁₄ N ₂ O ₂	218.3	12.26 [232]	600 [227]	0.91 [227]

Table B7 Concentrations (mg/L) and corresponding loadings (mg/g) of pharmaceuticals used in the isotherm study. Each of the 12 solutions contains all 13 compounds. ENR, OFL, SZ, and CBZ have solubilities less than 200 mg/L and therefore lower concentrations were used.

Solution No.	#1	#2	#3	#4	#5	#6	#7	#8	#9	#10	#11	#12
Volume of solution	1 mL						10 mL					
AMO, PEN-G, SMZ, SMX, ERY, CHP, PRM	0.1	0.5	1	5	10	15	20	50	100	200	100	200
ENR	0.1	0.5	1	5	10	15	20	40	60	80	60	80
OFL	0.1	0.5	1	5	10	15	20	38	76	151	76	151
SDZ	0.1	0.5	1	5	10	15	20	30	40	50	40	50
OTC	0.1	0.5	1	5	10	14	19	46	93	186	93	186
CTC	0.1	0.5	1	5	9	14	19	47	94	187	94	187
CBZ	0.1	0.5	1	5	10	15	20	30	50	70	50	70

Table B8 MRM transitions used to identify (both transitions) and quantify (primary transition) the antibiotics and anticonvulsants.

Compound	Abbreviation	Primary Transition	Secondary Transition
Amoxicillin	AMO	366.1/349.2	366.1/114.1
Penicillin-G	PEN-G	335.1/91.1	335.1/217.0
Enrofloxacin	ENR	360.2/316.2	360.2/342.1
Ofloxacin	OFL	362.1/318.0	362.1/261.1
Sulfadiazine	SDZ	251.0/156.0	251.0/108.0
Sulfamethazine	SMZ	279.1/65.1	279.1/124.1
Sulfamethoxazole	SMX	254.0/65.0	254.0/92.0
Erythromycin	ERY	734.5/83.2	734.5/158.2
Oxytetracycline	OTC	461.2/426.2	461.2/443.2
Chlortetracycline	CTC	479.1/462.2	479.1/444.2
Chloramphenicol	CHP	323.0/275.0	323.0/304.9
Carbamazepine	CBZ	237.0/194.1	237.0/193.2
Primidone	PRM	219.1/162.1	219.1/106.1

Table B9 Solution pH at adsorption equilibrium.

	SS650	WO650	SSWO650	SS950	WO950	SSWO950
1 mL solution	8.7±0.2	8.6±0.2	8.7±0.1	8.4±0.3	8.4±0.1	8.3±0.2
10 mL solution	7.2	8.6	7.9	6.8	7.1	6.8

Table B10 Fraction of species (%) of the analytes at pH of 6.8 and 8.7

Compounds		Fraction of species (%)				
AMO		○⊕○	⊖⊕○	⊖○○	⊖○○	
	pH 6.8	0.00	79.90	20.07	0.03	
	pH 8.7	0.00	4.26	85.03	10.71	
PEN-G			○	⊖		
	pH 6.8		0.01	99.99		
	pH 8.7		0.00	100.00		
ENR		○⊕⊕⊕	⊖⊕⊕⊕	⊖○⊕⊕	⊖○○⊕	⊖○○
	pH 6.8	0.02	17.43	71.02	11.52	0.01
	pH 8.7	0.00	0.02	6.77	87.18	6.03
OFL		○⊕	⊖⊕	⊖○		
	pH 6.8	12.52	84.67	2.80		
	pH 8.7	0.05	27.53	72.42		
SDZ		○⊕	○○	○⊖		
	pH 6.8	0.00	33.39	66.61		
	pH 8.7	0.00	0.63	99.37		
SMZ	pH 6.8	0.00	83.04	16.96		
	pH 8.7	0.00	5.81	94.19		
SMX	pH 6.8	0.00	5.94	94.06		
	pH 8.7	0.00	0.08	99.92		
ERY		⊕	○			
	pH 6.8	99.21	0.79			
	pH 8.7	61.31	38.69			
OTC		○○⊕	⊖○○	⊖⊖⊕	⊖○○	
	pH 6.8	0.02	81.93	17.92	0.13	
	pH 8.7	0.00	3.52	61.24	35.24	
CTC	pH 6.8	0.03	84.84	15.09	0.04	
	pH 8.7	0.00	5.42	76.62	17.96	
CHP			○	⊖		
	pH 6.8		99.99	0.01		
	pH 8.7		99.50	0.50		
CBZ		⊕	○	⊖		
	pH 6.8	0.00	100.00	0.00		
	pH 8.7	0.00	100.00	0.00		
PRM			○	⊖		
	pH 6.8		100.00	0.00		
	pH 8.7		99.97	0.03		

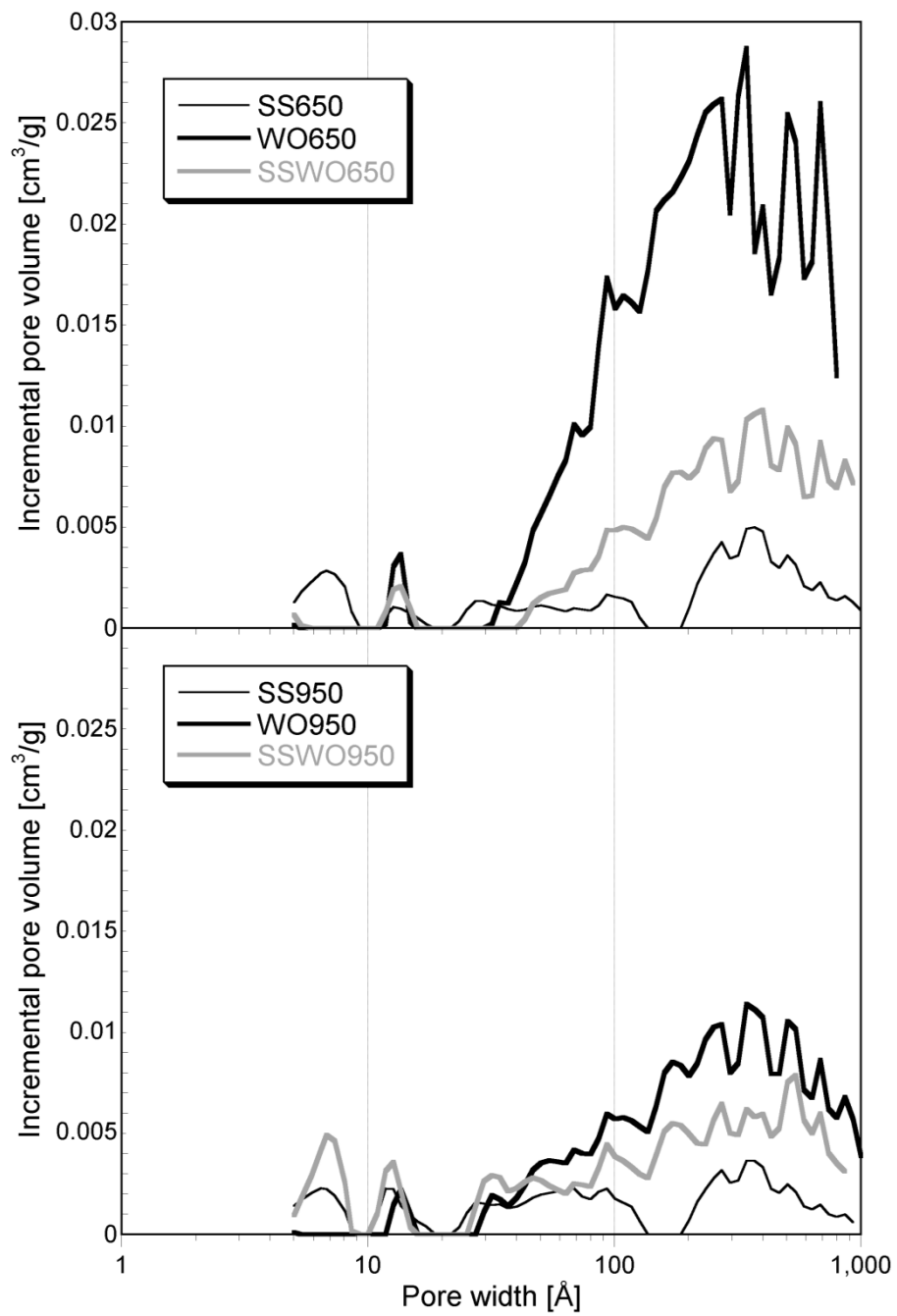


Figure B8 Pore size distributions for the adsorbents studied.

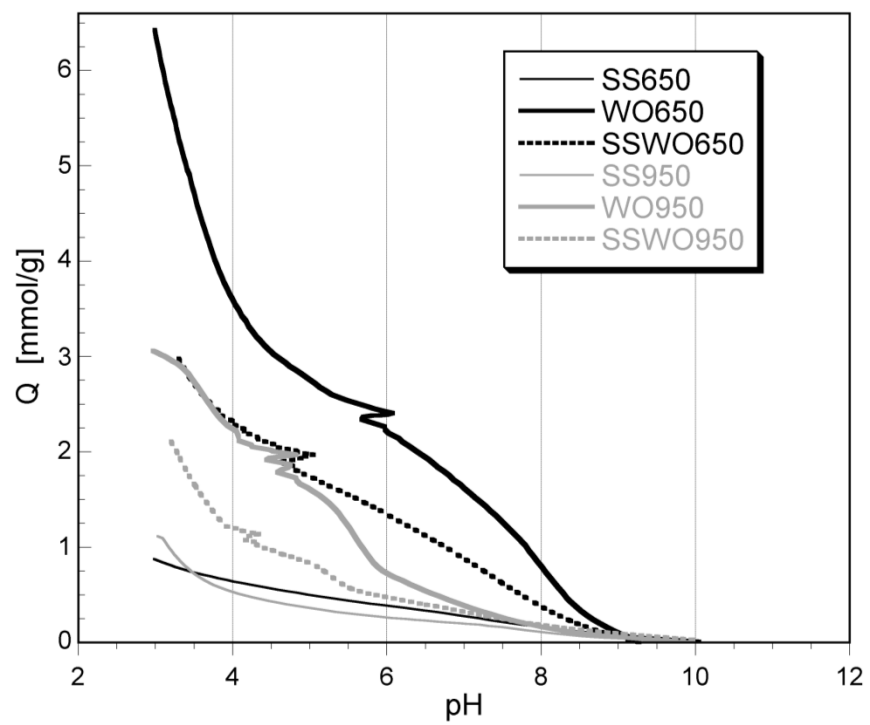
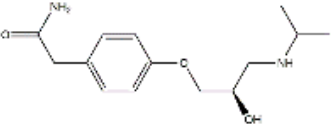
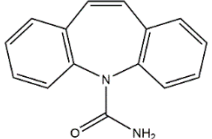
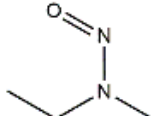


Figure B9 Proton binding curves for the adsorbents studied.

Appendix C

Table C11 physicochemical properties of the adsorbates.

Name	Abbr.	Molecular Structure	Polar surface area (Å ²) ^a	Topological diameter (Å) ^a	Molar volume (cm ³ /mol) ^b	logK _{ow}	pK _a
Atenolol	ATN		85	16	236.6	0.1	9.6 amide group
Carbamazepine	CBZ		46	9	186.5	1.51	<1, 13.9 amine group
N-nitroso-methylethylamine	NMEA		33	5	91.2	-0.15	-3.39 amine group

^aCalculated by ChemOffice (CambridgeSoft)

^bObtained from SciFinder

Table C12 Leaching of unwashed composite materials by DI water, tap water, and TCLP fluid. Concentrations are in µg/L.

		Al	Ag	As	Ba	Be	Cd	Co	Cr	Cu	Hg	Kr	Mn	Mo	Ni	Pb	Ru	Sb	Se	Th	Tl	U	V	Zn
Drinking Water Regulations	EU	200	–	10	–	–	5	–	50	1,000	1	–	50	–	20	10	–	5	10	–	–	–	50	–
	USA	200	100	10	2,000	4	5	–	100	1,000	2	–	50	–	–	15	–	6	50	–	2	30	–	5,000
SS_650	DI	1461.0	0.0	0.0	203.0	0.0	0.0	0.0	1.6	0.0	0.6	0.0	1.9	50.1	2.6	8.4	0.0	5.0	11.2	3.2	0.9	1.3	3.1	6.9
	TAP	1390.1	0.0	0.0	204.2	0.0	0.0	0.0	1.4	0.0	0.5	0.0	1.9	53.4	2.6	7.2	0.0	5.0	11.9	3.0	0.9	1.3	3.2	5.5
	TCLP	48.4	0.0	0.2	248.1	0.0	0.0	0.0	5.8	2.9	0.6	0.0	99.1	48.1	8.5	3.7	0.0	13.9	2.1	3.0	0.9	1.7	3.7	6.4
SS_950	DI	3069.2	0.0	1.5	19.8	0.0	0.0	0.0	7.5	0.4	1.4	0.0	2.6	99.3	0.0	3.5	0.0	14.5	23.2	2.9	0.9	1.3	21.2	4.5
	TAP	2825.9	0.0	1.3	17.3	0.0	0.0	0.0	7.3	0.9	1.2	0.0	2.5	86.6	0.0	3.5	0.0	14.1	27.5	2.9	0.9	1.4	20.1	3.7
	TCLP	5.7	0.0	9.5	80.8	0.0	0.0	0.0	5.4	3.7	0.3	0.0	815.2	46.8	7.6	3.5	0.0	10.2	2.7	2.9	0.9	1.4	5.9	0.0
SS90F10_650	DI	2626.3	0.0	0.1	222.0	0.0	0.0	0.0	1.5	0.0	0.4	0.0	2.0	33.5	3.3	5.4	0.0	2.8	2.8	3.9	0.9	1.3	2.9	8.4
	TAP	4574.3	0.0	0.1	196.9	0.0	0.0	0.0	1.5	0.0	0.4	0.0	1.9	34.4	2.8	4.9	0.0	3.1	3.1	3.2	0.9	1.3	3.0	8.5
	TCLP	82.0	0.0	11.4	65.5	0.0	0.7	17.6	6.7	37.9	0.1	0.0	1477.4	10.8	56.7	7.4	0.0	6.7	1.3	3.3	1.0	1.3	2.8	742.5
SS90F10_950	DI	3803.9	0.0	0.0	60.6	0.0	0.0	0.0	1.5	0.0	1.0	0.0	2.2	109.2	0.9	4.0	0.0	7.4	2.4	2.9	0.9	1.3	8.5	4.9
	TAP	3777.0	0.0	0.0	62.7	0.0	0.0	0.0	1.4	0.0	1.0	0.0	2.1	103.1	0.7	3.9	0.0	7.5	2.5	2.9	0.9	1.3	8.2	4.4
	TCLP	5.9	0.0	10.6	40.9	0.0	0.0	25.3	5.0	0.3	0.2	0.0	4196.0	2.9	64.2	3.5	0.0	28.6	0.0	3.0	0.9	1.2	2.1	83.4
SS75F25_650	DI	3229.7	0.0	0.0	142.1	0.0	0.0	0.0	2.1	0.0	0.3	0.0	2.0	13.0	1.0	4.0	0.0	2.1	1.6	3.6	0.9	1.3	2.6	5.4
	TAP	3390.5	0.0	0.0	146.4	0.0	0.0	0.0	2.2	0.0	0.3	0.0	2.0	12.7	1.1	4.0	0.0	2.0	1.4	3.1	0.9	1.2	2.7	4.3
	TCLP	21.0	0.0	3.8	73.0	0.0	0.0	1.6	5.5	2.3	0.1	0.0	610.7	8.3	18.9	4.8	0.0	4.0	3.0	3.2	0.9	1.3	2.7	91.3
SS75F25_950	DI	3730.5	0.0	0.0	73.9	0.0	0.0	0.0	1.5	0.4	0.8	0.0	2.1	70.7	1.1	3.9	0.0	3.1	1.3	2.9	0.9	1.2	4.9	6.0
	TAP	3362.7	0.0	0.0	59.0	0.0	0.0	0.0	1.6	0.4	0.9	0.0	2.0	68.7	0.7	3.7	0.0	3.4	0.7	2.9	0.9	1.3	5.4	5.2
	TCLP	0.0	0.0	8.0	50.3	0.0	0.0	8.8	3.8	2.9	0.2	0.0	1545.0	28.1	39.3	3.5	0.0	11.8	0.0	3.0	0.9	1.2	2.1	3.5
SS50F50_650	DI	6070.6	0.0	0.2	134.6	0.0	0.0	0.0	3.6	2.0	0.3	0.0	5.8	15.2	1.5	7.5	0.0	1.4	2.5	3.5	0.9	1.3	2.6	19.3
	TAP	17547.6	0.0	0.3	85.8	0.0	0.0	0.0	2.0	0.0	0.4	0.0	2.1	18.2	0.6	3.8	0.0	1.4	2.3	3.1	0.9	1.2	2.6	1.0
	TCLP	0.0	0.0	1.1	86.2	0.0	0.0	0.1	3.7	0.0	0.1	0.0	188.5	9.2	12.2	3.6	0.0	1.8	1.1	3.1	0.9	1.3	2.6	1.4
SS50F50_950	DI	777.4	0.0	0.8	224.0	0.0	0.0	0.0	1.5	0.2	0.4	0.0	2.1	42.6	4.6	10.2	0.0	1.6	12.9	2.9	0.9	1.2	3.1	5.0
	TAP	301.0	0.0	0.6	253.6	0.0	0.0	0.0	1.4	0.0	0.4	0.0	2.1	41.2	5.8	10.4	0.0	1.5	10.1	2.9	0.9	1.2	3.1	4.3
	TCLP	0.0	0.0	0.1	181.9	0.0	0.0	0.4	3.6	5.3	0.3	0.0	219.3	27.6	13.0	3.5	0.0	4.4	1.6	3.0	0.9	1.8	3.8	0.0
F_650	DI	0.0	0.0	0.4	111.7	0.0	0.0	0.0	1.5	0.2	0.1	0.0	3.2	1.5	9.0	3.5	0.0	1.2	3.8	3.3	0.9	1.2	4.6	0.0

	TAP	6.0	0.0	0.5	88.9	0.0	0.0	0.0	1.5	0.3	0.1	0.0	2.2	1.4	8.6	3.5	0.0	1.2	4.3	3.0	0.9	1.2	5.0	0.0
	TCLP	0.0	0.0	0.0	100.1	0.0	0.0	0.5	3.7	0.3	0.1	0.0	1.9	1.0	15.5	4.8	0.0	1.2	1.1	2.9	0.9	1.2	4.2	0.0
F_950	DI	0.0	0.0	0.7	176.5	0.0	0.0	1.3	1.9	0.2	0.1	0.0	2.2	1.9	15.4	33.7	0.0	1.2	5.2	2.9	0.9	1.2	5.2	11.3
	TAP	0.0	0.0	0.8	150.5	0.0	0.0	1.2	1.9	0.4	0.1	0.0	2.2	1.9	15.7	28.5	0.0	1.2	5.2	2.9	0.9	1.2	5.2	8.0
	TCLP	0.0	0.0	0.0	169.1	0.0	0.0	2.6	3.4	0.2	0.1	0.0	2.0	1.6	27.2	25.2	0.0	1.2	1.1	2.9	0.9	1.2	4.2	5.5

Table C13 pH of leachate from composite materials

Unwashed materials

Solution	SS_650	SS_950	SS90F10_650	SS90F10_950	SS75F25_650	SS75F25_950	SS50F50_650	SS50F50_950	F_650	F_950
DI water	12.12	11.3	12.06	11.61	11.68	11.85	12.1	12.59	12.91	12.9
Tap water	12.17	11.33	11.97	11.67	11.79	11.8	11.86	12.69	12.88	12.96
TCLP	7.83	7.41	5.14	5.41	5.33	5.68	5.93	7.92	10.51	12.69

HCl washed materials

Solution	SS_650	SS_950	SS90F10_650	SS90F10_950	SS75F25_650	SS75F25_950	SS50F50_650	SS50F50_950	F_650	F_950
DI water	2.68	3.23	2.5	3.2	2.53	3.3	2.74	3.29	6.31	6

Acetic acid washed materials

Solution	SS_650	SS_950	SS90F10_650	SS90F10_950	SS75F25_650	SS75F25_950	SS50F50_650	SS50F50_950	F_650	F_950
DI water	6.44	6.17	6.5	6.34	7.07	7.14	7.79	8.1	9.52	12.84
TCLP	5.22	5.23	5.3	5.32	5.8	5.88	5.37	5.57	6.1	9.2

Table C14 Major mineral phases present in sludge composites

Silicates	Phosphate/Phosphide	Carbonate/Sulfate	Oxide
Quartz, cristobalite (SiO ₂)	Hydroxy/chlorapatite (Ca ₁₀ (PO ₄) ₆ (Cl,OH) ₂)	Calcite (CaCO ₃)	Brookite, rutile (TiO ₂)
Plagioclase feldspar ((Ca,Na)AlSi ₂ O ₈)	Barringerite (Fe ₂ P)	Hanksite Na ₂₂ K(CO ₃) ₂ (SO ₄) ₉ Cl)	Iron oxide (FeO)
Richterite (Na(NaCa)Mg ₅ Si ₈ O ₂₂ (OH) ₂)	Monetite (CaHPO ₄)		

Table C15 Leaching of HCl washed composite materials by DI water. Concentrations are in µg/L

	Al	Ag	As	Ba	Be	Cd	Co	Cr	Cu	Hg	Kr	Mn	Mo	Ni	Pb	Ru	Sb	Se	Th	Tl	U	V	Zn
EU Limit	200	-	10	-	-	5	-	50	1000	1	-	50	-	20	10	-	5	10	-	-	-	50	-
USA Limit	200	100	10	2000	4	5	-	100	1000	2	-	50	-	-	15	-	6	50	-	2	30	-	5000
SS_650	33974.3	0.0	6.0	183.0	0.0	10.1	34.0	44.1	3655.0	0.0	0.0	505.3	3.4	142.6	578.7	33.5	3.8	0.0	1.9	0.6	1.3	3.6	13239.3
SS_950	9148.6	0.0	6.5	72.7	0.0	0.0	35.5	26.0	2606.1	0.1	0.0	893.4	2.8	175.1	1.7	33.5	1.0	0.0	1.9	0.0	0.8	2.1	745.6
SS90F10_650	40432.9	0.0	11.0	298.0	0.0	120.4	67.4	48.7	8326.4	0.0	0.0	916.8	2.9	200.1	988.5	100.9	2.8	0.0	1.9	0.4	2.0	8.5	20944.2
SS90F10_950	13648.9	0.0	10.1	75.9	0.0	0.0	78.1	29.1	10596.7	0.1	0.0	1151.7	2.9	208.8	5.8	83.3	1.3	0.0	1.9	0.0	0.9	2.9	5015.6
SS75F25_650	26893.8	0.0	11.0	229.4	0.0	38.2	30.8	46.1	4614.7	0.1	0.0	802.2	3.3	149.2	548.2	77.5	3.1	0.0	1.9	0.5	1.6	6.4	16061.4
SS75F25_950	8345.7	0.0	12.5	87.8	0.0	0.0	42.6	20.4	4286.1	0.1	0.0	1121.6	2.9	181.5	4.4	68.7	1.7	0.8	2.0	0.0	0.8	2.2	3887.4
SS50F50_650	14393.6	0.0	8.5	224.2	0.0	23.4	25.1	31.6	610.5	0.1	0.0	737.8	2.7	109.4	223.5	42.3	2.5	0.0	2.0	0.6	0.9	3.7	11687.5
SS50F50_950	7484.7	0.0	16.1	180.3	0.0	0.0	34.0	16.4	4687.1	0.1	0.0	1142.4	2.7	136.8	5.4	98.0	1.4	2.7	2.0	0.0	0.8	2.4	6273.2
F_650	4.7	0.0	0.0	65.2	0.0	0.0	0.0	0.0	0.0	0.1	0.0	12.1	4.3	1.7	1.5	30.5	0.1	0.0	2.3	0.0	0.6	1.7	1.5
F_950	4.8	0.0	0.0	13.4	0.0	0.0	0.0	0.2	0.0	0.1	0.0	8.0	5.2	0.0	8.0	7.1	0.4	0.0	2.0	0.0	0.6	2.3	11.6

Table C16 Leaching of acetic acid washed composite materials by DI water, tap water, and TCLP fluid. Concentrations are in µg/L

		Ag	Al	As	Ba	Cd	Co
	EU	-	200	10	-	5	-
	US	100	200	10	2,000	5	-
	TCLP	5000	-	5000	100,000	1000	-
SS90F10_650	DI Water	0.22±0.3 7	10.9±2.2	6.5±0.1	11.0±0.4	0.31±0.0	1.79±0.0 3
	TAP	0±0	10.4±2.8	6.9±0.2	11.4±0.2	0.35±0.01	1.91±0.0 2
	TCLP	0±0	144.5±11. 7	24.7±0.4	77.5±1.2	3.7±0.4	38.6±3.1
SS90F10_950	DI Water	0±0	7.3±1.8	18.8±0.6	21.9±0.6	0.13±0.03	33.0±0.9
	TAP	0±0	7.9±1.7	18.5±0.6	21.3±0.7	0.12±0.01	31.2±0.3
	TCLP	0±0	45.8±2.5	40.2±0.1	71.6±3.3	0.10±0.01	96.1±1.7
SS75F25_650	DI Water	0±0	33.9±14.4	1.9±0.1	14.3±0.1	0.20±0.01	0.11±0.0 1
	TAP	0±0	18.8±2.3	2.13±0.0 2	15.2±0.2	0.21±0	0.09±0.0 2
	TCLP	0±0	20.5±2.9	12.1±0.2	93.0±4.2	1.33±0.02	2.6±0.1
SS75F25_950	DI Water	0±0	7.4±1.9	16.5±0.5	31.7±0.8	0.19±0.02	1.47±0.0 3
	TAP	0±0	5.6±0.8	15.4±1.2	35.3±2.6	0.16±0.01	1.40±0.0 7
	TCLP	0±0	41.7±0.9	39.7±0.9	76.6±3.2	0.14±0.01	15.8±0.6
		Cr	Cu	Hg	Mn	Mo	Ni
	EU	50	1000	1	50	-	20
	US	100	1000	2	50	-	-
	TCLP	5000	-	200	-	-	-
SS90F10_650	DI Water	1.0±0.1	8.6±0.3	0.18±0.0 3	102.0±1.5	74.9±1.1	2.22±0.0 3
	TAP	1.0±0.1	11.4±2.2	0.15±0.0 1	111.6±1.2	77.6±1.7	2.6±0.2
	TCLP	14.7±0.5	39.3±3.8	0±0	1293.0±14. 5	42.1±1.1	34.9±0.7
SS90F10_950	DI Water	0.62±0.1 2	6.2±0.1	0.01±0.0 1	879.5±15.6	39.8±2.1	38.0±1.0
	TAP	0.54±0.1 0	5.7±0.1	0±0	924.0±10.4	43.2±3.4	36.9±0.4
	TCLP	11.4±0.8	183.8±11. 6	0±0	3040.7±34. 0	22.5±0.6	119.9±1. 0
SS75F25_650	DI Water	4.3±0.3	1.7±0.7	0.20±0.0 1	23.9±1.5	66.1±1.9	0±0
	TAP	4.0±0.2	0.36±0.03	0.17±0.0 2	27.5±1.2	70.5±0.5	0±0
	TCLP	13.2±0.9	8.5±2.8	0±0	637.8±29.4	41.1±1.1	9.9±0.2

SS75F25_950	DI Water	0.67±0.1 0	19.1±2.2	0.04±0.0 2	263.1±9.0	76.4±3.5	8.5±0.2
	TAP	0.73±0.1 0	26.5±11.9	0.01±0	278.9±7.5	76.1±3.4	8.0±0.3
	TCLP	9.4±0.5	99.4±17.0	0±0	2059.6±79. 1	23.4±1.4	70.8±0.9
		Pb	Sb	Se	V	Zn	
	EU	10	5	10	50	-	
	US	15	6	50	-	5000	
	TCLP	5,000	-	1000	-	-	
SS90F10_650	DI Water	0.53±0.2 3	12.5±0.2	19.8±0.3	7.08±0.04	58.7±9.3	
	TAP	0.10±0.1 7	12.9±0.2	21.2±0.7	7.5±0.2	54.6±2.4	
	TCLP	5.8±0.2	13.2±0.1	54.3±2.7	3.9±0.2	1056.6±60. 6	
SS90F10_950	DI Water	0.24±0.4 1	24.5±0.7	37.8±0.8	5.1±0.1	132.5±23.5	
	TAP	0±0	24.7±0.5	40.9±1.5	5.5±0.1	139.3±20.4	
	TCLP	0.52±0.1 5	21.6±0.4	85.2±2.6	3.63±0.02	964.0±264. 7	
SS75F25_650	DI Water	1.8±1.7	9.0±0.1	7.5±0.3	4.3±0.1	20.9±3.1	
	TAP	0.10±0.1 6	9.3±0.2	8.0±0.2	4.73±0.04	12.4±1.1	
	TCLP	1.92±0.0 5	10.3±0.3	31.6±0.4	2.7±0.1	157.4±8.3	
SS75F25_950	DI Water	0±0	22.8±0.8	34.9±1.4	8.8±0.3	1.4±0.2	
	TAP	0±0	22.9±0.2	34.4±0.8	8.5±0.1	1.4±0.1	
	TCLP	0.25±0.2 4	18.1±0.6	77.4±1.2	4.1±0.2	86.6±2.2	

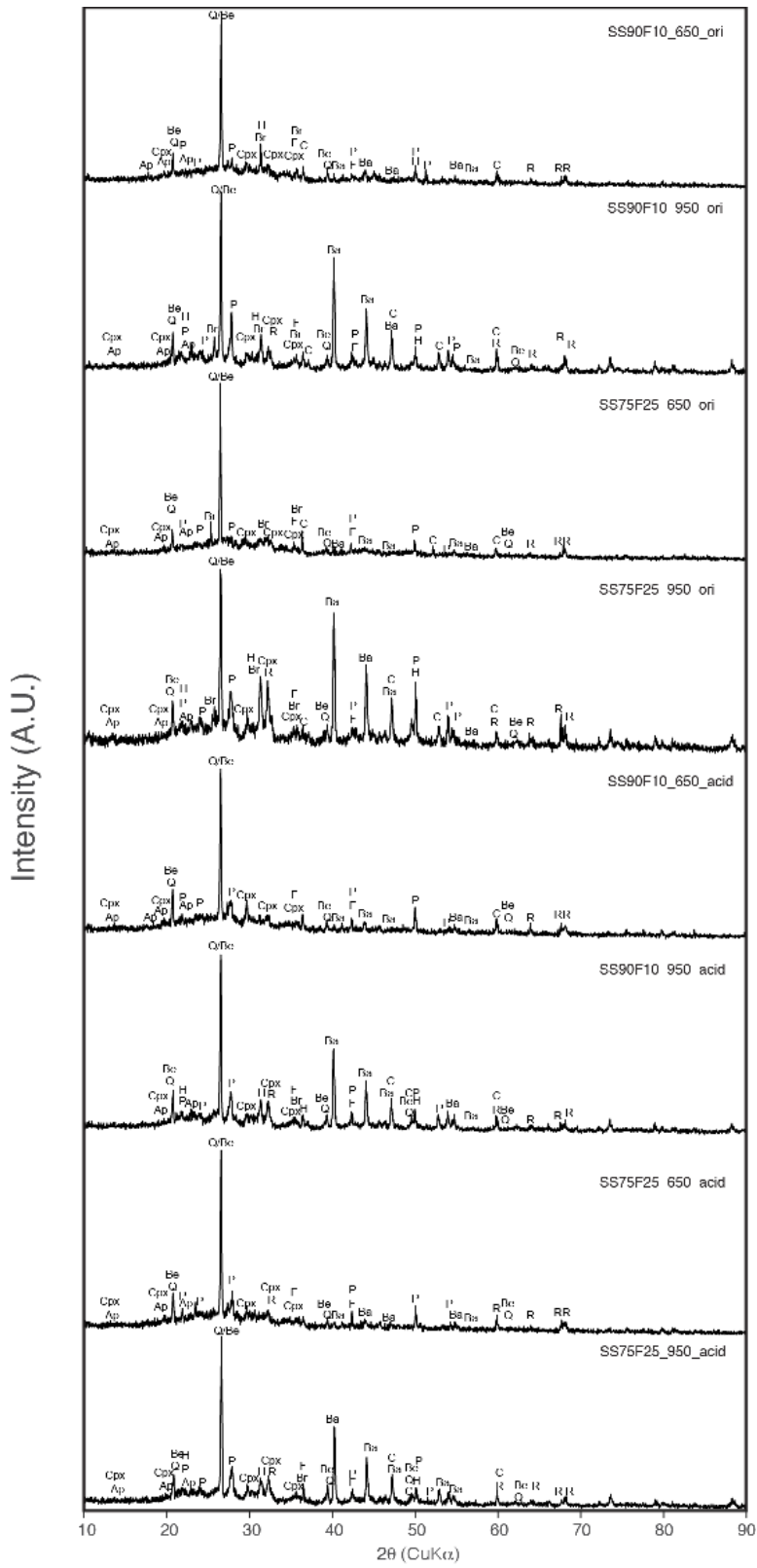
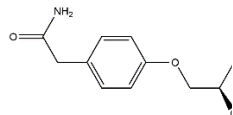
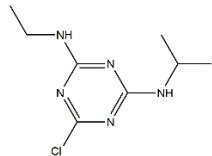
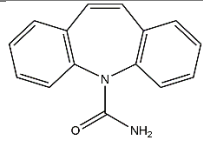
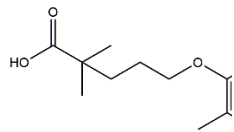
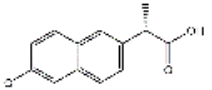
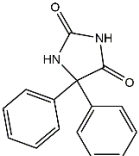
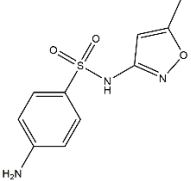
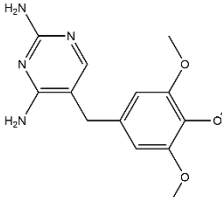


Figure C10 XRD data for original and acetic acid washed materials

Appendix D

Table D17 Properties of pharmaceuticals and EDCs

Name	Abbr.	Structure	Water Solubility 25 °C mg/L *	Polar Surface Area (Å ²) †	Topological Diameter †	logK _{ow}	pKa	Functional group/charge at pH=6	Molar Volume (cm ³ /mol) *
Atenolol	ATN		0.071 M [233]	84.58	16.2	0.1 ± 0.28 [234]	9.57 [235]	Amine/+	236.6
Atrazine	ATZ		35 [236]	61.14	10.2	2.3–2.7 [236]	1.7 [236], 1.61 [237]	Amine/0	169.8
Carbamazepine	CBZ		112 [238]	46.33	8.7	2.45 [239]	<1, 13.9 [230]	Amide/0	186.5
Gemfibrozil	GFB		7.9/10.9	46.53	12.6	4.77 [240]	4.7 [240], 4.42 [241]	Carboxyl ic/-	239.7

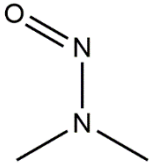
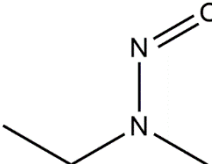
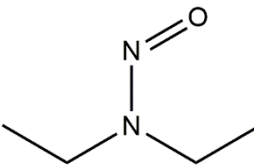
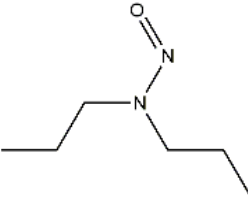
Naproxen	NAP		16 [242]	46.53	12.8	3.18 [240]	4.2 [240]	Carboxylic/-	192.2
Phenytoin	PHT		14 [243]	58.2	10.3	2.47 [238]	8.2 [244]	Amide/0	200.5
Sulfamethoxazole	SMX		610 [245]	93.78	13.2	0.89 [240]	1.85/5.6 [220]	(basic amine group)/ (acidic amide group)/0/-	173.1
Trimethoprim	TMP		1.4 mM [246]	104.45	13.9	0.91 [240]	7.1 [240], 7.16 [241]	Amine/8 0%+ 20% 0	231.8

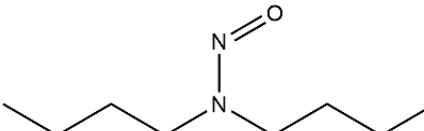
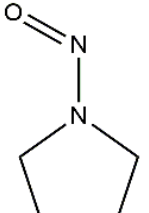
* Data from SciFinder

† Calculated in ChemOffice 2015

Appendix E

Table E18 Properties of nitrosamines

Name	Abbr.	Formula	MW	Structure	K_{oc}	$\log K_{ow}$ [247]	pK_a	Molar Volume (cm^3/mol) *	Density 20 °C
N-nitroso-dimethylamine	NDMA	$(CH_3)_2NNO$	74.08		12.8	-0.64	-3.63 ± 0.70	74.9 ± 7.0	1.0048
N-nitroso-methylethylamine	NMEA	$C_3H_8N_2O$	88.11		24.2	-0.15	-3.39 ± 0.70	91.2 ± 7.0	0.9448
N-nitroso-diethylamine	NDEA	$(C_2H_5)_2NNO$	102.14		45.9	0.34	-3.14 ± 0.70	107.4 ± 7.0	0.9422
N-nitroso-di-n-propylamine	NDPA	$C_6H_{14}N_2O$	130.19		164	1.35	-3.18 ± 0.70	139.9 ± 7.0	0.916

N-nitroso-di-n-butylamine	NDBA	C ₈ H ₁₈ N ₂ O	158.24		589	2.31	-3.14±0.70	172.2±7.0	0.9009
N-nitroso-pyrrolidine	NPYR	C ₄ H ₈ N ₂ O	100.12		21.3	0.23	-3.14±0.20	80.7±7.0	1.085

*Data from SicFinder

Bibliography

1. Smith, K.M., et al., *Sewage sludge-based adsorbents: A review of their production, properties and use in water treatment applications*. Water Research, 2009. **43**(10): p. 2569-2594.
2. Cao, Y. and A. Pawłowski, *Sewage sludge-to-energy approaches based on anaerobic digestion and pyrolysis: Brief overview and energy efficiency assessment*. Renewable and Sustainable Energy Reviews, 2012. **16**(3): p. 1657-1665.
3. Ulrich, H., K.P. Freier, and M. Gierig, *Getting on with persistent pollutants: Decreasing trends of perfluoroalkyl acids (PFAAs) in sewage sludge*. Chemosphere, 2016. **161**: p. 527-535.
4. USEPA, *Biosolids regeneration, Use, and Disposal in the United States*. 1999, United States Environmental Protection Agency.
5. Fullana, A., et al., *Pyrolysis of sewage sludge: nitrogenated compounds and pretreatment effects*. Journal of Analytical and Applied Pyrolysis, 2003. **68-9**: p. 561-575.
6. Yang, G., G. Zhang, and H. Wang, *Current state of sludge production, management, treatment and disposal in China*. Water Research, 2015. **78**: p. 60-73.
7. Wiggers, V.R., et al., *Biofuels from waste fish oil pyrolysis: Continuous production in a pilot plant*. Fuel, 2009. **88**(11): p. 2135-2141.
8. Eiroa, M., et al., *Evaluation of the biomethane potential of solid fish waste*. Waste Management, 2012. **32**(7): p. 1347-1352.
9. FAO, *FAO yearbook. Fishery and Aquaculture Statistics*. 2010, Rome: Food and Agriculture Organization of the United Nations.
10. Islam, M.S., S. Khan, and M. Tanaka, *Waste loading in shrimp and fish processing effluents: potential source of hazards to the coastal and nearshore environments*. Marine Pollution Bulletin, 2004. **49**(1-2): p. 103-110.
11. Lundin, M., et al., *Environmental and economic assessment of sewage sludge handling options*. Resources Conservation and Recycling, 2004. **41**(4): p. 255-278.
12. Wang, K.S., et al., *The thermal conductivity mechanism of sewage sludge ash lightweight materials*. Cement and Concrete Research, 2005. **35**(4): p. 803-809.
13. Piskorz, J., D.S. Scott, and I.B. Westerberg, *Flash Pyrolysis of Sewage-Sludge*. Industrial & Engineering Chemistry Process Design and Development, 1986. **25**(1): p. 265-270.

14. Chiang, P.C. and J.H. You, *Use of Sewage-Sludge for Manufacturing Adsorbents*. Canadian Journal of Chemical Engineering, 1987. **65**(6): p. 922-927.
15. Lewis, F.M., *Method of pyrolyzing sewage sludge to produce activated carbon*. 1977: US.
16. Nickerson, R.D. and H.C. Messman, *Making activated carbon from sewage sludge*. 1975: US.
17. Bandosz, T.J. and A. Bagreev, *Preparation of adsorbents from organic fertilizer and mineral oil and their application for removal of acidic gases from sulfur containing wet gas streams*. 2005: US.
18. Devi, P. and A.K. Saroha, *Utilization of sludge based adsorbents for the removal of various pollutants: A review*. Science of The Total Environment, 2017. **578**: p. 16-33.
19. Bagreev, A., et al., *Sewage sludge-derived materials as efficient adsorbents for removal of hydrogen sulfide*. Environmental Science & Technology, 2001. **35**(7): p. 1537-1543.
20. Bagreev, A. and T.J. Bandosz, *H₂S adsorption/oxidation on materials obtained using sulfuric acid activation of sewage sludge-derived fertilizer*. Journal of Colloid and Interface Science, 2002. **252**(1): p. 188-194.
21. Bagreev, A. and T.J. Bandosz, *Efficient hydrogen sulfide adsorbents obtained by pyrolysis of sewage sludge derived fertilizer modified with spent mineral oil*. Environmental Science & Technology, 2004. **38**(1): p. 345-351.
22. Bashkova, S., et al., *Adsorption of SO₂ on sewage sludge-derived materials*. Environmental Science & Technology, 2001. **35**(15): p. 3263-3269.
23. Seredych, M. and T.J. Bandosz, *Removal of cationic and ionic dyes on industrial-municipal sludge based composite adsorbents*. Industrial & Engineering Chemistry Research, 2007. **46**(6): p. 1786-1793.
24. Rio, S., et al., *Experimental design methodology for the preparation of carbonaceous sorbents from sewage sludge by chemical activation - application to air and water treatments*. Chemosphere, 2005. **58**(4): p. 423-437.
25. Rio, S., et al., *Structure characterization and adsorption properties of pyrolyzed sewage sludge*. Environmental Science & Technology, 2005. **39**(11): p. 4249-4257.
26. Otero, M., et al., *Removal of heavy metals from aqueous solution by sewage sludge based sorbents: competitive effects*. Desalination, 2009. **239**(1-3): p. 46-57.
27. Phuengprasop, T., J. Sittiwong, and F. Unob, *Removal of heavy metal ions by iron oxide coated sewage sludge*. Journal of Hazardous Materials, 2011. **186**(1): p. 502-507.

28. Qian, Q.R., et al., *Removal of copper from aqueous solution using iron-containing adsorbents derived from methane fermentation sludge*. Journal of Hazardous Materials, 2009. **172**(2-3): p. 1137-1144.
29. Rio, S., et al., *Preparation of adsorbents from sewage sludge by steam activation for industrial emission treatment*. Process Safety and Environmental Protection, 2006. **84**(B4): p. 258-264.
30. Bouzid, J., et al., *A study on removal characteristics of copper from aqueous solution by sewage sludge and pomace ashes*. Journal of Hazardous Materials, 2008. **152**(2): p. 838-845.
31. Fang, P., et al., *Carbonaceous Adsorbents Prepared from Sewage Sludge and Its Application for Hg⁰ Adsorption in Simulated Flue Gas*. Chinese Journal of Chemical Engineering, 2010. **18**(2): p. 231-238.
32. Ros, A., et al., *Dried sludges and sludge-based chars for H₂S removal at low temperature: Influence of sewage sludge characteristics*. Environmental Science & Technology, 2006. **40**(1): p. 302-309.
33. Bandosz, T.J. and K. Block, *Municipal sludge-industrial sludge composite desulfurization adsorbents: Synergy enhancing the catalytic properties*. Environmental Science & Technology, 2006. **40**(10): p. 3378-3383.
34. Nielsen, L. and T.J. Bandosz, *Analysis of sulfamethoxazole and trimethoprim adsorption on sewage sludge and fish waste derived adsorbents*. Microporous and Mesoporous Materials, 2016. **220**: p. 58-72.
35. Nielsen, L., P. Zhang, and T.J. Bandosz, *Adsorption of carbamazepine on sludge/fish waste derived adsorbents: Effect of surface chemistry and texture*. Chemical Engineering Journal, 2015. **267**: p. 170-181.
36. USEPA. *Basic Information about the Unregulated Contaminant Monitoring Rule 2 (UCMR 2)*. Aug 2012]; Available from: <http://water.epa.gov/lawsregs/rulesregs/sdwa/ucmr/ucmr2/basicinformation.cfm>.
37. USEPA. *Drinking Water Strategy*. [cited 2012 Aug 2012]; Available from: <http://water.epa.gov/lawsregs/rulesregs/sdwa/dwstrategy/index.cfm>.
38. USEPA. *Integrated Risk Information System: N-Nitrosodimethylamine (CASRN 62-75-9)*. Aug 2012]; Available from: <http://www.epa.gov/iris/subst/0045.htm>.
39. IRAC. *Agents Classified by the IARC Monographs, Volumes 1-105*. Aug 2012]; Available from: <http://monographs.iarc.fr/ENG/Classification/ClassificationsAlphaOrder.pdf>.

40. Bond, T., et al., *Occurrence and control of nitrogenous disinfection by-products in drinking water - A review*. Water Research, 2011. **45**(15): p. 4341-4354.
41. Kolpin, D.W., et al., *Pharmaceuticals, hormones, and other organic wastewater contaminants in U.S. streams, 1999-2000: a national reconnaissance*. Environ Sci Technol, 2002. **36**(6): p. 1202-11.
42. Benotti, M.J., et al., *Pharmaceuticals and Endocrine Disrupting Compounds in US Drinking Water*. Environmental Science & Technology, 2009. **43**(3): p. 597-603.
43. Kummerer, K., *Antibiotics in the aquatic environment - A review - Part II*. Chemosphere, 2009. **75**(4): p. 435-441.
44. Alder Alfredo, C., et al., *Occurrence and Fate of Fluoroquinolone, Macrolide, and Sulfonamide Antibiotics during Wastewater Treatment and in Ambient Waters in Switzerland*, in *Pharmaceuticals and Care Products in the Environment*. 2001, American Chemical Society. p. 56-69.
45. Giger, W., et al., *Occurrence and fate of antibiotics as trace contaminants in wastewaters, sewage sludges, and surface waters*. Chimia, 2003. **57**(9): p. 485-491.
46. Sarmah, A.K., M.T. Meyer, and A.B.A. Boxall, *A global perspective on the use, sales, exposure pathways, occurrence, fate and effects of veterinary antibiotics (VAs) in the environment*. Chemosphere, 2006. **65**(5): p. 725-759.
47. Szczepanowski, R., et al., *Detection of 140 clinically relevant antibiotic-resistance genes in the plasmid metagenome of wastewater treatment plant bacteria showing reduced susceptibility to selected antibiotics*. Microbiology-Sgm, 2009. **155**: p. 2306-2319.
48. Martinez, J.L., *Environmental pollution by antibiotics and by antibiotic resistance determinants*. Environmental Pollution, 2009. **157**(11): p. 2893-2902.
49. Watkinson, A.J., E.J. Murby, and S.D. Costanzo, *Removal of antibiotics in conventional and advanced wastewater treatment: Implications for environmental discharge and wastewater recycling*. Water Research, 2007. **41**(18): p. 4164-4176.
50. Gulkowska, A., et al., *Removal of antibiotics from wastewater by sewage treatment facilities in Hong Kong and Shenzhen, China*. Water research, 2008. **42**(1-2): p. 395-403.
51. Adams, C., et al., *Removal of antibiotics from surface and distilled water in conventional water treatment processes*. Journal of Environmental Engineering-Asce, 2002. **128**(3): p. 253-260.
52. Sarmah, A.K., M.T. Meyer, and A.B.A. Boxall, *A global perspective on the use, sales, exposure pathways, occurrence, fate and effects of veterinary antibiotics (VAs) in the environment*. Chemosphere, 2006. **65**(5): p. 725-729.

53. Boxall, A.B.A., et al., *Are Veterinary Medicines Causing Environmental Risks?* Environmental Science & Technology, 2003. **37**(15): p. 286A-294A.
54. Hirsch, R., et al., *Occurrence of antibiotics in the aquatic environment*. The Science of the Total Environment, 1999. **225**: p. 109-118.
55. Nakada, N., et al., *Removal of selected pharmaceuticals and personal care products (PPCPs) and endocrine-disrupting chemicals (EDCs) during sand filtration and ozonation at a municipal sewage treatment plant*. Water research, 2007. **41**(19): p. 4373-4382.
56. Le-Minh, N., et al., *Fate of antibiotics during municipal water recycling treatment processes*. Water Research, 2010. **44**(15): p. 4295-4323.
57. Kemper, N., *Veterinary antibiotics in the aquatic and terrestrial environment*. Ecological Indicators, 2008. **8**(1): p. 1-13.
58. Zielesny, Y., et al., *Impact of sulfadiazine and chlorotetracycline on soil bacterial community structure and respiratory activity*. Soil Biology and Biochemistry, 2006. **38**(8): p. 2372-2380.
59. Yin, G., et al., *Effects of multiple antibiotics exposure on denitrification process in the Yangtze Estuary sediments*. Chemosphere.
60. DeVries, S.L. and P. Zhang, *Antibiotics and the Terrestrial Nitrogen Cycle: A Review*. Current Pollution Reports, 2016. **2**(1): p. 51-67.
61. DeVries, S.L., et al., *The effect of ultralow-dose antibiotics exposure on soil nitrate and N₂O flux*. Scientific Reports, 2015. **5**: p. 16818.
62. Rivera-Utrilla, J., et al., *Removal of nitroimidazole antibiotics from aqueous solution by adsorption/bioadsorption on activated carbon*. Journal of Hazardous Materials, 2009. **170**(1): p. 298-305.
63. Ding, R., et al., *Removal of antibiotics from water using sewage sludge- and waste oil sludge-derived adsorbents*. Water Research, 2012. **46**(13): p. 4081-4090.
64. Lee, C.L. and L.J. Kuo, *Quantification of the dissolved organic matter effect on the sorption of hydrophobic organic pollutant: application of an overall mechanistic sorption model*. Chemosphere, 1999. **38**(4): p. 807-21.
65. Amiri, F., H. Bornick, and E. Worch, *Sorption of phenols onto sandy aquifer material: the effect of dissolved organic matter (DOM)*. Water research, 2005. **39**(5): p. 933-41.

66. Hu, J., et al., *Anionic exchange for NOM removal and the effects on micropollutant adsorption competition on activated carbon*. Separation and Purification Technology, 2014. **129**(0): p. 25-31.
67. Ding, Y., et al., *Measurement of associations of pharmaceuticals with dissolved humic substances using solid phase extraction*. Chemosphere, 2013. **91**(3): p. 314-319.
68. Gatselou, V.A., D.L. Giokas, and A.G. Vlessidis, *Determination of dissolved organic matter based on UV-light induced reduction of ionic silver to metallic nanoparticles by humic and fulvic acids*. Analytica Chimica Acta, 2014. **812**: p. 121-128.
69. McDonough, K.M., J.L. Fairey, and G.V. Lowry, *Adsorption of polychlorinated biphenyls to activated carbon: Equilibrium isotherms and a preliminary assessment of the effect of dissolved organic matter and biofilm loadings*. Water research, 2008. **42**(3): p. 575-584.
70. Guo, Y., A. Yadav, and T. Karanfil, *Approaches to mitigate the impact of dissolved organic matter on the adsorption of synthetic organic contaminants by porous carbonaceous sorbents*. Environmental science & technology, 2007. **41**(22): p. 7888-94.
71. Hao, C., R. Clement, and P. Yang, *Liquid chromatography–tandem mass spectrometry of bioactive pharmaceutical compounds in the aquatic environment—a decade’s activities*. Analytical and Bioanalytical Chemistry, 2007. **387**(4): p. 1247-1257.
72. Ruiz, S.H., et al., *Complexation of trace organic contaminants with fractionated dissolved organic matter: Implications for mass spectrometric quantification*. Chemosphere, 2013. **91**(3): p. 344-350.
73. Schug, K.A. and W. Lindner, *Noncovalent Binding between Guanidinium and Anionic Groups: Focus on Biological- and Synthetic-Based Arginine/Guanidinium Interactions with Phosph[on]ate and Sulf[on]ate Residues*. Chemical Reviews, 2004. **105**(1): p. 67-114.
74. Yamamoto, H., et al., *Effects of physical-chemical characteristics on the sorption of selected endocrine disruptors by dissolved organic matter surrogates*. Environmental science & technology, 2003. **37**(12): p. 2646-57.
75. Thomsen, M., et al., *Reverse quantitative structure-activity relationship for modelling the sorption of esfenvalerate to dissolved organic matter. A multivariate approach*. Chemosphere, 2002. **49**(10): p. 1317-25.
76. Georgi, A., et al., *Influence of Sorption to Dissolved Humic Substances on Transformation Reactions of Hydrophobic Organic Compounds in Water. I. Chlorination of PAHs*. Environmental science & technology, 2007. **41**(20): p. 7003-7009.

77. Georgi, A., et al., *Influence of sorption to dissolved humic substances on transformation reactions of hydrophobic organic compounds in water. Part II: hydrolysis reactions*. Chemosphere, 2008. **71**(8): p. 1452-60.
78. Rivera, Z.H., et al., *Influence of natural organic matter on the screening of pharmaceuticals in water by using liquid chromatography with full scan mass spectrometry*. Analytica Chimica Acta, 2011. **700**(1-2): p. 114-125.
79. Wickramasekara, S., et al., *Natural dissolved organic matter affects electrospray ionization during analysis of emerging contaminants by mass spectrometry*. Analytica Chimica Acta, 2012. **717**: p. 77-84.
80. Hernandez-Ruiz, S., et al., *Quantifying PPCP interaction with dissolved organic matter in aqueous solution: Combined use of fluorescence quenching and tandem mass spectrometry*. Water Research, 2012. **46**(4): p. 943-954.
81. Liu, J.-L. and M.-H. Wong, *Pharmaceuticals and personal care products (PPCPs): A review on environmental contamination in China*. Environment International, 2013. **59**(0): p. 208-224.
82. Guo, J., et al., *Dissolved organic matter in biologically treated sewage effluent (BTSE): Characteristics and comparison*. Desalination, 2011. **278**(1-3): p. 365-372.
83. Ma, H., H.E. Allen, and Y. Yin, *Characterization of isolated fractions of dissolved organic matter from natural waters and a wastewater effluent*. Water Research, 2001. **35**(4): p. 985-996.
84. Field, A., *Discovering Statistics Using SPSS: Book Plus Code for E Version of Text*. 2009: Sage.
85. Keiluweit, M. and M. Kleber, *Molecular-Level Interactions in Soils and Sediments: The Role of Aromatic π -Systems*. Environmental Science & Technology, 2009. **43**(10): p. 3421-3429.
86. Daniel, J.M., et al., *Quantitative determination of noncovalent binding interactions using soft ionization mass spectrometry*. International Journal of Mass Spectrometry, 2002. **216**(1): p. 1-27.
87. Loo, J.A., *Electrospray ionization mass spectrometry: a technology for studying noncovalent macromolecular complexes*. International Journal of Mass Spectrometry, 2000. **200**(1-3): p. 175-186.
88. Touboul, D., et al., *How to Deal with Weak Interactions in Noncovalent Complexes Analyzed by Electrospray Mass Spectrometry: Cyclopeptidic Inhibitors of the Nuclear Receptor Coactivator 1-STAT6*. Journal of the American Society for Mass Spectrometry, 2009. **20**(2): p. 303-311.

89. He, F., et al., *Differentially heated capillary for thermal dissociation of noncovalently bound complexes produced by electrospray ionization*. International Journal of Mass Spectrometry, 1999. **182–183**(0): p. 261-273.
90. Singh, N.J., et al., *Comprehensive Energy Analysis for Various Types of π -Interaction*. Journal of Chemical Theory and Computation, 2009. **5**(3): p. 515-529.
91. Wendler, K., et al., *Estimating the Hydrogen Bond Energy*. The Journal of Physical Chemistry A, 2010. **114**(35): p. 9529-9536.
92. El-Hawiet, A., E.N. Kitova, and J.S. Klassen, *Quantifying Carbohydrate–Protein Interactions by Electrospray Ionization Mass Spectrometry Analysis*. Biochemistry, 2012. **51**(21): p. 4244-4253.
93. Silveira, J.A., et al., *From Solution to the Gas Phase: Stepwise Dehydration and Kinetic Trapping of Substance P Reveals the Origin of Peptide Conformations*. Journal of the American Chemical Society, 2013. **135**(51): p. 19147-19153.
94. David, W.M. and J.S. Brodbelt, *Threshold dissociation energies of protonated amine/polyether complexes in a quadrupole ion trap*. Journal of the American Society for Mass Spectrometry, 2003. **14**(4): p. 383-392.
95. Garcia, B., et al., *Thermal dissociation of protonated cyclodextrin-amino acid complexes in the gas phase*. International Journal of Mass Spectrometry, 2001. **210–211**(0): p. 215-222.
96. Frański, R. and B. Gierczyk, *ESI-MS Detection of Very Weak π -Stacking Interactions in the Mixed-Ligand Sandwich Complexes Formed by Substituted Benzo-Crown Ethers and Metal Cations*. Journal of the American Society for Mass Spectrometry, 2010. **21**(4): p. 545-549.
97. Fandrich, M., et al., *Observation of the noncovalent assembly and disassembly pathways of the chaperone complex MtGimC by mass spectrometry*. Proc Natl Acad Sci U S A, 2000. **97**(26): p. 14151-5.
98. Rogniaux, H., et al., *Binding of aldose reductase inhibitors: correlation of crystallographic and mass spectrometric studies*. Journal of the American Society for Mass Spectrometry, 1999. **10**(7): p. 635-647.
99. Wickramasekara, S., et al., *Natural dissolved organic matter affects electrospray ionization during analysis of emerging contaminants by mass spectrometry*. Analytica Chimica Acta, 2012. **717**: p. 77-84.
100. Leenheer, J.A., et al., *Molecular resolution and fragmentation of fulvic acid by electrospray ionization/multistage tandem mass spectrometry*. Analytical Chemistry, 2001. **73**(7): p. 1461-1471.

101. Louie, S.M., R.D. Tilton, and G.V. Lowry, *Effects of Molecular Weight Distribution and Chemical Properties of Natural Organic Matter on Gold Nanoparticle Aggregation*. Environmental Science & Technology, 2013. **47**(9): p. 4245-4254.
102. Sutton, R. and G. Sposito, *Molecular Structure in Soil Humic Substances: The New View*. Environmental Science & Technology, 2005. **39**(23): p. 9009-9015.
103. Rostad, C.E. and J.A. Leenheer, *Factors that affect molecular weight distribution of Suwannee river fulvic acid as determined by electrospray ionization/mass spectrometry*. Analytica Chimica Acta, 2004. **523**(2): p. 269-278.
104. Thorn, K.A., D.W. Folan, and P. Maccarthy, *Characterization of the International Humic Substances Society standard and reference fulvic and humic acids by solution state carbon-13 (¹³C) and hydrogen-1 (¹H) nuclear magnetic resonance spectrometry*, in *Water-Resources Investigations Report 89-4196*. 1989, U.S. Geological Survey: Denver, CO. p. 93.
105. USEPA, *Biosolids regeneration, Use, and Disposal in the United States*. 1999, U.S. Environmental Protection Agency: Washington, D.C.
106. Bagreev, A., et al., *Sewage sludge-derived materials as efficient adsorbents for removal of hydrogen sulfide*. Environmental Science and Technology, 2001. **35**(7): p. 1537-1543.
107. Bashkova, S., et al., *Sewage Sludge Derived materials as Adsorbents for H₂S and SO₂*, in *Fundamentals of Adsorption -7*, K. Kaneko, H. Kanoh, and Y. Hanzawa, Editors. 2002, IK International: Chiba, Japan. p. 239-246.
108. Seredych, M. and T.J. Bandosz, *Removal of cationic and ionic dyes on industrial-municipal sludge based composite adsorbents*. Industrial and Engineering Chemistry Research, 2007. **46**(6): p. 1786-1793.
109. Qian, Q., et al., *Removal of copper from aqueous solution using iron-containing adsorbents derived from methane fermentation sludge*. Journal of Hazardous Materials, 2009. **172**(2-3): p. 1137-1144.
110. Zhang, F.-S. and H. Itoh, *Adsorbents made from waste ashes and post-consumer PET and their potential utilization in wastewater treatment*. Journal of Hazardous Materials, 2003. **101**(3): p. 323-337.
111. Ros, A., et al., *Dried sludges and sludge-based chars for H₂S removal at low temperature: Influence of sewage sludge characteristics*. Environmental Science and Technology, 2006. **40**(1): p. 302-309.
112. Wise, R., *Antimicrobial resistance: priorities for action*. Journal of Antimicrobial Chemotherapy, 2002. **49**(4): p. 585-586.

113. Kümmerer, K., *Antibiotics in the aquatic environment - A review - Part I*. Chemosphere, 2009. **75**(4): p. 417-434.
114. Radjenovic, J., et al., *Evidencing generation of persistent ozonation products of antibiotics roxithromycin and trimethoprim*. Environmental Science & Technology, 2009. **43**(17): p. 6808-6815.
115. von Gunten, U., et al., *Removal of PPCP during drinking water treatment*. Human Pharmaceutical, Hormones and Fragrances: The Challenge of Micropollutants in Urban Water Management, ed. T.A. Ternes and A. Joss. 2006, London: IWA Publishing. 293-322.
116. Adams, C., et al., *Removal of antibiotics from surface and distilled water in conventional water treatment processes*. Journal of Environmental Engineering, 2002. **128**(3): p. 253-260.
117. Kim, I., N. Yamashita, and H. Tanaka, *Performance of UV and UV/H₂O₂ processes for the removal of pharmaceuticals detected in secondary effluent of a sewage treatment plant in Japan*. Journal of Hazardous Materials, 2009. **166**(2-3): p. 1134-1140.
118. Simon, A., et al., *Effects of membrane degradation on the removal of pharmaceutically active compounds (PhACs) by NF/RO filtration processes*. Journal of Membrane Science, 2009. **340**(1-2): p. 16-25.
119. Elmolla, E.S. and M. Chaudhuri, *Photocatalytic degradation of amoxicillin, ampicillin and cloxacillin antibiotics in aqueous solution using UV/TiO₂ and UV/H₂O₂/TiO₂ photocatalysis*. Desalination, 2010. **252**(1-3): p. 46-52.
120. Gonzalez, O., C. Sans, and S. Esplugas, *Sulfamethoxazole abatement by photo-Fenton. Toxicity, inhibition and biodegradability assessment of intermediates*. Journal of Hazardous Materials, 2007. **146**(3): p. 459-464.
121. Wang, Z., et al., *Norfloxacin sorption and its thermodynamics on surface-modified carbon nanotubes*. Environmental Science and Technology, 2010. **44**(3): p. 978-984.
122. Avisar, D., et al., *Sorption of sulfonamides and tetracyclines to montmorillonite clay*. Water, Air, and Soil Pollution, 2010. **209**(1-4): p. 439-450.
123. Bajpai, S.K. and M. Bhowmik, *Poly(acrylamide-co-itaconic acid) as a potential ion-exchange sorbent for effective removal of antibiotic drug-ciprofloxacin from aqueous solution*. Journal of Macromolecular Science, Part A: Pure and Applied Chemistry, 2011. **48**(2): p. 108-118.
124. Seredych, M. and T.J. Bandosz, *Removal of copper on composite sewage sludge/industrial sludge-based adsorbents: The role of surface chemistry*. Journal of Colloid and Interface Science, 2006. **302**(2): p. 379-388.

125. Jagiello, J., T.J. Bandosz, and J.A. Schwarz, *Study of carbon microstructure by using inverse gas chromatography*. Carbon, 1994. **32**(4): p. 687-691.
126. Marczewski, A.W., A. Derylomarczewska, and M. Jaroniec, *Correlations of heterogeneity parameters for single-solute and multi-solute adsorption from dilute-solutions*. Journal of the Chemical Society-Faraday Transactions I, 1988. **84**: p. 2951-2957.
127. Everett, D.H. and J.C. Powl, *Adsorption in slit-like and cylindrical micropores in henrys law region - model for microporosity of carbons*. Journal of the Chemical Society-Faraday Transactions I, 1976. **72**: p. 619-636.
128. Seredych, M., M. Khine, and T.J. Bandosz, *Enhancement in dibenzothiophene reactive adsorption from liquid fuel via incorporation of sulfur heteroatoms into the nanoporous carbon matrix*. Chemsuschem, 2011. **4**(1): p. 139-147.
129. Bandosz, T.J. and K. Block, *Effect of pyrolysis temperature and time on catalytic performance of sewage sludge/industrial sludge-based composite adsorbents*. Applied Catalysis B: Environmental, 2006. **67**(1-2): p. 77-85.
130. Rivera-Garza, M., et al., *Silver supported on natural Mexican zeolite as an antibacterial material*. Microporous and Mesoporous Materials, 2000. **39**(3): p. 431-444.
131. USEPA, *Biosolids regeneration, Use, and Disposal in the United States*. United States Environmental Protection Agency, 1999.
132. Islam, M.S., S. Khan, and M. Tanaka, *Waste loading in shrimp and fish processing effluents: potential source of hazards to the coastal and nearshore environments*. Marine Pollution Bulletin, 2004. **49**(1-2): p. 103-110.
133. Xu, G., X. Yang, and L. Spinosa, *Development of sludge-based adsorbents: Preparation, characterization, utilization and its feasibility assessment*. Journal of Environmental Management, 2015. **151**: p. 221-232.
134. Fang, W., Y. Wei, and J. Liu, *Comparative characterization of sewage sludge compost and soil: Heavy metal leaching characteristics*. Journal of Hazardous Materials, 2016. **310**: p. 1-10.
135. Jin, H., et al., *Leaching of heavy metals from fast pyrolysis residues produced from different particle sizes of sewage sludge*. Journal of Analytical and Applied Pyrolysis, 2014. **109**: p. 168-175.
136. Hernandez, A.B., et al., *Mineralogy and leachability of gasified sewage sludge solid residues*. Journal of Hazardous Materials, 2011. **191**(1-3): p. 219-227.
137. Benotti, M.J., et al., *Pharmaceuticals and Endocrine Disrupting Compounds in U.S. Drinking Water*. Environmental Science & Technology, 2009. **43**(3): p. 597-603.

138. Krasner, S.W., et al., *Formation, precursors, control, and occurrence of nitrosamines in drinking water: A review*. Water Research, 2013. **47**(13): p. 4433-4450.
139. USEPA, *Basic Information about the Unregulated Contaminant Monitoring Rule 2 (UCMR 2)*. 2012.
140. USEPA, *EPA Test Method 1311-TCLP, Toxicity Characteristic Leaching Procedure*. 1992.
141. USEPA, *Determination of trace elements in waters and wastes by inductively coupled plasma - mass spectrometry; Method 200.8, Revision 5.4*. 1994.
142. Jeppu, G.P. and T.P. Clement, *A modified Langmuir-Freundlich isotherm model for simulating pH-dependent adsorption effects*. Journal of Contaminant Hydrology, 2012. **129–130**: p. 46-53.
143. USEPA, *National Primary Drinking Water Regulations (NPDWRs)*.
144. USEPA, *National Secondary Drinking Water Regulations (NSDWRs)*.
145. Lee, C.S., J. Robinson, and M.F. Chong, *A review on application of flocculants in wastewater treatment*. Process Safety and Environmental Protection, 2014. **92**(6): p. 489-508.
146. Wagh, A.S., S. Grover, and S.Y. Jeong, *Chemically Bonded Phosphate Ceramics: II, Warm-Temperature Process for Alumina Ceramics*. Journal of the American Ceramic Society, 2003. **86**(11): p. 1845-1849.
147. Ros, A., et al., *High surface area materials prepared from sewage sludge-based precursors*. Chemosphere, 2006. **65**(1): p. 132-140.
148. Tay, J.H., et al., *Optimising the preparation of activated carbon from digested sewage sludge and coconut husk*. Chemosphere, 2001. **44**(1): p. 45-51.
149. Zou, J., et al., *Structure and adsorption properties of sewage sludge-derived carbon with removal of inorganic impurities and high porosity*. Bioresource Technology, 2013. **142**: p. 209-217.
150. Velghe, I., et al., *Characterisation of adsorbents prepared by pyrolysis of sludge and sludge/disposal filter cake mix*. Water Research, 2012. **46**(8): p. 2783-2794.
151. Fitzmorris, K.B., et al., *Anion and Cation Leaching or Desorption from Activated Carbons from Municipal Sludge and Poultry Manure as Affected by pH*. Water Environment Research, 2006. **78**(12): p. 2324-2329.
152. Tönsuaadu, K., et al., *A review on the thermal stability of calcium apatites*. Journal of Thermal Analysis and Calorimetry, 2012. **110**(2): p. 647-659.

153. Devi, P. and A.K. Saroha, *Effect of pyrolysis temperature on polycyclic aromatic hydrocarbons toxicity and sorption behaviour of biochars prepared by pyrolysis of paper mill effluent treatment plant sludge*. Bioresource Technology, 2015. **192**: p. 312-320.
154. Daud, W.M.A.W., W.S.W. Ali, and M.Z. Sulaiman, *The effects of carbonization temperature on pore development in palm-shell-based activated carbon*. Carbon, 2000. **38**(14): p. 1925-1932.
155. Chiang, H.-L., et al., *RESIDUE CHARACTERISTICS AND PORE DEVELOPMENT OF PETROCHEMICAL INDUSTRY SLUDGE PYROLYSIS*. Water Research, 2001. **35**(18): p. 4331-4338.
156. de Ridder, D.J., et al., *Zeolites for nitrosamine and pharmaceutical removal from demineralised and surface water: Mechanisms and efficacy*. Separation and Purification Technology, 2012. **89**: p. 71-77.
157. Rakić, V., et al., *The adsorption of salicylic acid, acetylsalicylic acid and atenolol from aqueous solutions onto natural zeolites and clays: Clinoptilolite, bentonite and kaolin*. Microporous and Mesoporous Materials, 2013. **166**: p. 185-194.
158. Rakić, V., et al., *The adsorption of pharmaceutically active compounds from aqueous solutions onto activated carbons*. Journal of Hazardous Materials, 2015. **282**: p. 141-149.
159. Cabrera-Lafaurie, W.A., F.R. Román, and A.J. Hernández-Maldonado, *Removal of salicylic acid and carbamazepine from aqueous solution with Y-zeolites modified with extraframework transition metal and surfactant cations: Equilibrium and fixed-bed adsorption*. Journal of Environmental Chemical Engineering, 2014. **2**(2): p. 899-906.
160. Cai, N. and P. Larese-Casanova, *Sorption of carbamazepine by commercial graphene oxides: A comparative study with granular activated carbon and multiwalled carbon nanotubes*. Journal of Colloid and Interface Science, 2014. **426**: p. 152-161.
161. Ho, L., et al., *Assessing granular media filtration for the removal of chemical contaminants from wastewater*. Water Research, 2011. **45**(11): p. 3461-3472.
162. Dai, X., et al., *Adsorption characteristics of N-nitrosodimethylamine from aqueous solution on surface-modified activated carbons*. Journal of Hazardous Materials, 2009. **168**(1): p. 51-56.
163. Wang, H., et al., *Infrared Signature of the Cation- π Interaction between Calcite and Aromatic Hydrocarbons*. Langmuir, 2015. **31**(21): p. 5820-5826.
164. IMS, *IMS Health: Market Prognosis*. 2011.

165. Wise, R., *Antimicrobial resistance: priorities for action*. J Antimicrob Chemother, 2002. **49**(4): p. 585-6.
166. Ekpeghere, K.I., et al., *Determination and characterization of pharmaceuticals in sludge from municipal and livestock wastewater treatment plants*. Chemosphere, 2017. **168**: p. 1211-1221.
167. Montforts, M.H.M.M., et al., *The exposure assessment for veterinary medicinal products*. Science of The Total Environment, 1999. **225**(1-2): p. 119-133.
168. Khan, S.J. and J.E. Ongerth, *Modelling of pharmaceutical residues in Australian sewage by quantities of use and fugacity calculations*. Chemosphere, 2004. **54**(3): p. 355-367.
169. Carballa, M., F. Omil, and J.M. Lema, *Comparison of predicted and measured concentrations of selected pharmaceuticals, fragrances and hormones in Spanish sewage*. Chemosphere, 2008. **72**(8): p. 1118-1123.
170. Radke, M., et al., *Fate of the Antibiotic Sulfamethoxazole and Its Two Major Human Metabolites in a Water Sediment Test*. Environmental Science & Technology, 2009. **43**(9): p. 3135-3141.
171. Daughton, C.G. and T.A. Ternes, *Pharmaceuticals and personal care products in the environment: agents of subtle change?* Environmental Health Perspectives, 1999. **107**(Suppl 6): p. 907-938.
172. Le-Minh, N., et al., *Fate of antibiotics during municipal water recycling treatment processes*. Water Res, 2010. **44**(15): p. 4295-323.
173. Mohapatra, S., et al., *Occurrence and fate of pharmaceuticals in WWTPs in India and comparison with a similar study in the United States*. Chemosphere, 2016. **159**: p. 526-535.
174. Alder, A.C., et al., *Occurrence and Fate of Fluoroquinolone, Macrolide, and Sulfonamide Antibiotics during Wastewater Treatment and in Ambient Waters in Switzerland, in Pharmaceuticals and Care Products in the Environment*. 2001, American Chemical Society. p. 56-69.
175. Giger, W., et al., *Occurrence and Fate of Antibiotics as Trace Contaminants in Wastewaters, Sewage Sludges, and Surface Waters*. CHIMIA International Journal for Chemistry, 2003. **57**(9): p. 485-491.
176. Gurke, R., et al., *Occurrence and removal of frequently prescribed pharmaceuticals and corresponding metabolites in wastewater of a sewage treatment plant*. Science of The Total Environment, 2015. **532**: p. 762-770.

177. Göbel, A., et al., *Fate of sulfonamides, macrolides, and trimethoprim in different wastewater treatment technologies*. Science of The Total Environment, 2007. **372**(2–3): p. 361-371.
178. Kolpin, D.W., et al., *Pharmaceuticals, Hormones, and Other Organic Wastewater Contaminants in U.S. Streams, 1999–2000: A National Reconnaissance*. Environmental Science & Technology, 2002. **36**(6): p. 1202-1211.
179. Ando, T., et al., *A novel method using cyanobacteria for ecotoxicity test of veterinary antimicrobial agents*. Environmental Toxicology and Chemistry, 2007. **26**(4): p. 601-606.
180. Kümmerer, K., *Effects of Antibiotics and Virustatics in the Environment*, in *Pharmaceuticals in the Environment: Sources, Fate, Effects and Risks*, K. Kümmerer, Editor. 2008, Springer Berlin Heidelberg: Berlin, Heidelberg. p. 223-244.
181. Zhang, Y., et al., *Wastewater treatment contributes to selective increase of antibiotic resistance among Acinetobacter spp.* Science of The Total Environment, 2009. **407**(12): p. 3702-3706.
182. Aydin, S., B. Ince, and O. Ince, *Development of antibiotic resistance genes in microbial communities during long-term operation of anaerobic reactors in the treatment of pharmaceutical wastewater*. Water Research, 2015. **83**: p. 337-344.
183. Munir, M., K. Wong, and I. Xagorarakis, *Release of antibiotic resistant bacteria and genes in the effluent and biosolids of five wastewater utilities in Michigan*. Water Research, 2011. **45**(2): p. 681-693.
184. Bouki, C., D. Venieri, and E. Diamadopoulos, *Detection and fate of antibiotic resistant bacteria in wastewater treatment plants: A review*. Ecotoxicology and Environmental Safety, 2013. **91**: p. 1-9.
185. Chen, Q., et al., *Long-term field application of sewage sludge increases the abundance of antibiotic resistance genes in soil*. Environment International, 2016. **92–93**: p. 1-10.
186. Zhang, F.-S., J.O. Nriagu, and H. Itoh, *Mercury removal from water using activated carbons derived from organic sewage sludge*. Water Research, 2005. **39**(2–3): p. 389-395.
187. Jindarom, C., et al., *Surface characterization and dye adsorptive capacities of char obtained from pyrolysis/gasification of sewage sludge*. Chemical Engineering Journal, 2007. **133**(1–3): p. 239-246.
188. Yu, L. and Q. Zhong, *Preparation of adsorbents made from sewage sludges for adsorption of organic materials from wastewater*. Journal of Hazardous Materials, 2006. **137**(1): p. 359-366.

189. Kizilkaya, B., A.A. Tekinay, and Y. Dilgin, *Adsorption and removal of Cu (II) ions from aqueous solution using pretreated fish bones*. *Desalination*, 2010. **264**(1–2): p. 37-47.
190. Ribeiro, C., et al., *Characterization of Oreochromis niloticus fish scales and assessment of their potential on the adsorption of reactive blue 5G dye*. *Colloids and Surfaces A: Physicochemical and Engineering Aspects*, 2015. **482**: p. 693-701.
191. Zhang, P., et al., *A Sewage Sludge Derived Composite Material for Adsorption of Antibiotics – Kinetics*. *Advances in Materials Physics and Chemistry*, 2012. **2**: p. 35-37.
192. Marczewski, A.W., A. Derylo-Marczewska, and M. Jaroniec, *Correlations of heterogeneity parameters for single-solute and multi-solute adsorption from dilute solutions*. *Journal of the Chemical Society, Faraday Transactions 1: Physical Chemistry in Condensed Phases*, 1988. **84**(9): p. 2951-2957.
193. Bagreev, A., F. Adib, and T.J. Bandosz, *pH of activated carbon surface as an indication of its suitability for H₂S removal from moist air streams*. *Carbon*, 2001. **39**(12): p. 1897-1905.
194. USEPA, *Second Unregulated Contaminant Monitoring Rule*. 2007.
195. Wang, W., et al., *Occurrence of nine nitrosamines and secondary amines in source water and drinking water: Potential of secondary amines as nitrosamine precursors*. *Water Research*, 2011. **45**(16): p. 4930-4938.
196. Asami, M., M. Oya, and K. Kosaka, *A nationwide survey of NDMA in raw and drinking water in Japan*. *Science of The Total Environment*, 2009. **407**(11): p. 3540-3545.
197. Zhao, Y.-Y., et al., *Characterization of New Nitrosamines in Drinking Water Using Liquid Chromatography Tandem Mass Spectrometry*. *Environmental Science & Technology*, 2006. **40**(24): p. 7636-7641.
198. Bond, T., et al., *Occurrence and control of nitrogenous disinfection by-products in drinking water – A review*. *Water Research*, 2011. **45**(15): p. 4341-4354.
199. Lee, J.-H. and J.-E. Oh, *A comprehensive survey on the occurrence and fate of nitrosamines in sewage treatment plants and water environment*. *Science of The Total Environment*, 2016. **556**: p. 330-337.
200. Afzal, A., et al., *Degradation and fate of N-nitrosamines in water by UV photolysis*. *International Journal of Greenhouse Gas Control*, 2016. **52**: p. 44-51.
201. Lee, C., W. Choi, and J. Yoon, *UV Photolytic Mechanism of N-Nitrosodimethylamine in Water: Roles of Dissolved Oxygen and Solution pH*. *Environmental Science & Technology*, 2005. **39**(24): p. 9702-9709.

202. Sørensen, L., et al., *Photodegradation in natural waters of nitrosamines and nitramines derived from CO₂ capture plant operation*. International Journal of Greenhouse Gas Control, 2015. **32**: p. 106-114.
203. Xu, B., et al., *Comparison of N-nitrosodiethylamine degradation in water by UV irradiation and UV/O₃: Efficiency, product and mechanism*. Journal of Hazardous Materials, 2010. **179**(1–3): p. 976-982.
204. Yang, J., et al., *Selective adsorption of zeolite towards nitrosamine in organic solution*. Microporous and Mesoporous Materials, 2009. **120**(3): p. 381-388.
205. Lin, W.G., et al., *Adsorption of nitrosamines by mesoporous zeolite*. Journal of Colloid and Interface Science, 2010. **348**(2): p. 621-627.
206. Sun, X.D., et al., *Liquid adsorption of tobacco specific N-nitrosamines by zeolite and activated carbon*. Microporous and Mesoporous Materials, 2014. **200**: p. 260-268.
207. Sun, X.D., et al., *Capturing tobacco specific N-nitrosamines (TSNA) in industrial tobacco extract solution by ZnO modified activated carbon*. Microporous and Mesoporous Materials, 2016. **222**: p. 160-168.
208. Yang, J.Y., et al., *Effective nitrosamines trap derived from the in situ carbonized mesoporous silica MCM-41*. Journal of Hazardous Materials, 2010. **176**(1–3): p. 602-608.
209. Gu, F.N., et al., *Effect of copper cation on the adsorption of nitrosamines in zeolite*. Solid State Sciences, 2008. **10**(11): p. 1658-1665.
210. Chiu, P.C., *Applications of Zero-Valent Iron (ZVI) and Nanoscale ZVI to Municipal and Decentralized Drinking Water Systems—A Review*, in *Novel Solutions to Water Pollution*. 2013, American Chemical Society. p. 237-249.
211. Liu, S., M. Lim, and R. Amal, *TiO₂-coated natural zeolite: Rapid humic acid adsorption and effective photocatalytic regeneration*. Chemical Engineering Science, 2014. **105**: p. 46-52.
212. Cheng, Z.-L. and S. Han, *Preparation of a novel composite electrode based on N-doped TiO₂-coated NaY zeolite membrane and its photoelectrocatalytic performance*. Chinese Chemical Letters, 2016. **27**(3): p. 467-470.
213. Nguyen, T.C., et al., *Simultaneous adsorption of Cd, Cr, Cu, Pb, and Zn by an iron-coated Australian zeolite in batch and fixed-bed column studies*. Chemical Engineering Journal, 2015. **270**: p. 393-404.
214. Wan, J.F., et al., *Biological As^{III} oxidation and arsenic sequestration onto ZVI-coated sand in an up-flow fixed-bed reactor*. Water Science and Technology: Water Supply, 2012. **12**(1): p. 82-89.

215. Dai, Q., et al., *Formation of PAHs during the pyrolysis of dry sewage sludge*. Fuel, 2014. **130**: p. 92-99.
216. Fan, H., K. He, and J. Wang, *Study of sewage sludge pyrolysis liquids using comprehensive two-dimensional gas chromatography/time-of-flight mass spectrometry*. Fuel, 2016. **185**: p. 281-288.
217. Luo, S. and Y. Feng, *The production of hydrogen-rich gas by wet sludge pyrolysis using waste heat from blast-furnace slag*. Energy, 2016. **113**: p. 845-851.
218. Bhandari, A., Environmental Council of the States (U.S.), Emerging Contaminants of Concern Task Committee., and Environmental and Water Resources Institute (U.S.), *Contaminants of emerging environmental concern*. 2009, Reston, Va.: American Society of Civil Engineers. 490.
219. Urraca, J.L., et al., *Direct Extraction of Penicillin G and Derivatives from Aqueous Samples Using a Stoichiometrically Imprinted Polymer*. Analytical Chemistry, 2006. **79**(2): p. 695-701.
220. Qiang, Z. and C. Adams, *Potentiometric determination of acid dissociation constants (pKa) for human and veterinary antibiotics*. Water Research, 2004. **38**(12): p. 2874-2890.
221. Seedher, N. and P. Agarwal, *Various solvent systems for solubility enhancement of enrofloxacin*. Indian Journal of Pharmaceutical Sciences, 2009. **71**(1): p. 82-87.
222. Tolls, J., *Sorption of veterinary pharmaceuticals in soils: a review*. Environmental science & technology, 2001. **35**(17): p. 3397-406.
223. Drakopoulos, A.I. and P.C. Ioannou, *Spectrofluorimetric study of the acid-base equilibria and complexation behavior of the fluoroquinolone antibiotics ofloxacin, norfloxacin, ciprofloxacin and pefloxacin in aqueous solution*. Analytica Chimica Acta, 1997. **354**(1-3): p. 197-204.
224. Sukul, P., et al., *Sorption and desorption of sulfadiazine in soil and soil-manure systems*. Chemosphere, 2008. **73**(8): p. 1344-1350.
225. Zhang, C.-L., F.-A. Wang, and Y. Wang, *Solubilities of sulfadiazine, sulfamethazine, sulfadimethoxine, sulfamethoxydiazine, sulfamonomethoxine, sulfamethoxazole, and sulfachloropyrazine in water from (298.15 to 333.15) K*. Journal of Chemical & Engineering Data, 2007. **52**(5): p. 1563-1566.
226. Jacobsen, A.M., et al., *Simultaneous extraction of tetracycline, macrolide and sulfonamide antibiotics from agricultural soils using pressurised liquid extraction, followed by solid-phase extraction and liquid chromatography-tandem mass spectrometry*. Journal of Chromatography A, 2004. **1038**(1-2): p. 157-170.
227. Lewis, F.M., *Method of pyrolyzing sewage sludge to produce activated carbon*. 1978: US.

228. Herbert, B.J. and J.G. Dorsey, *n-Octanol-water partition coefficient estimation by micellar electrokinetic capillary chromatography*. Analytical Chemistry, 1995. **67**(4): p. 744-749.
229. Vargas Mamani, M.C., F.G. Reyes Reyes, and S. Rath, *Multiresidue determination of tetracyclines, sulphonamides and chloramphenicol in bovine milk using HPLC-DAD*. Food Chemistry, 2009. **117**(3): p. 545-552.
230. Jones, O.A.H., N. Voulvoulis, and J.N. Lester, *Aquatic environmental assessment of the top 25 English prescription pharmaceuticals*. Water Research, 2002. **36**(20): p. 5013-5022.
231. Scheytt, T., et al., *1-Octanol/Water Partition Coefficients of 5 Pharmaceuticals from Human Medical Care: Carbamazepine, Clofibric Acid, Diclofenac, Ibuprofen, and Propyphenazone*. Water, Air, & Soil Pollution, 2005. **165**(1): p. 3-11.
232. Xu, P., et al., *Rejection of emerging organic micropollutants in nanofiltration-reverse osmosis membrane applications*. Water Environment Research, 2005. **77**(1): p. 40-48.
233. Jouyban, A., S. Sajed-Amin, and V. Panahi-Azar, *Solubility of atenolol, amiodarone HCl and lamotrigine in polyethylene glycol 200 + water mixtures in the presence of β -cyclodextrin*. Journal of Drug Delivery Science and Technology, 2014. **24**(5): p. 543-547.
234. Barbieri, M., et al., *Fate of β -blockers in aquifer material under nitrate reducing conditions: Batch experiments*. Chemosphere, 2012. **89**(11): p. 1272-1277.
235. Schönherr, D., et al., *Characterisation of selected active agents regarding pKa values, solubility concentrations and pH profiles by SiriusT3*. European Journal of Pharmaceutics and Biopharmaceutics, 2015. **92**: p. 155-170.
236. Gao, M.-l., et al., *Impact of atrazine and nitrogen fertilizers on the sorption of chlorotoluron in soil and model sorbents*. Journal of Environmental Sciences, 2007. **19**(3): p. 327-331.
237. Plust, S.J., et al., *Kinetics and mechanism of hydrolysis of chloro-1,3,5-triazines. Atrazine*. The Journal of Organic Chemistry, 1981. **46**(18): p. 3661-3665.
238. Kumar, A. and I. Xagorarakis, *Human health risk assessment of pharmaceuticals in water: An uncertainty analysis for meprobamate, carbamazepine, and phenytoin*. Regulatory Toxicology and Pharmacology, 2010. **57**(2-3): p. 146-156.
239. Naghdi, M., et al., *Pine-Wood derived Nanobiochar for Removal of Carbamazepine from Aqueous Media: Adsorption Behavior and Influential Parameters*. Arabian Journal of Chemistry.
240. Westerhoff, P., et al., *Fate of Endocrine-Disruptor, Pharmaceutical, and Personal Care Product Chemicals during Simulated Drinking Water Treatment Processes*. Environmental Science & Technology, 2005. **39**(17): p. 6649-6663.

241. Stevens-Garmon, J., et al., *Sorption of emerging trace organic compounds onto wastewater sludge solids*. Water Research, 2011. **45**(11): p. 3417-3426.
242. Tian, Q., et al., *Preparation of high solubilizable microemulsion of naproxen and its solubilization mechanism*. International Journal of Pharmaceutics, 2012. **426**(1–2): p. 202-210.
243. Latrofa, A., et al., *Complexation of phenytoin with some hydrophilic cyclodextrins: effect on aqueous solubility, dissolution rate, and anticonvulsant activity in mice*. European Journal of Pharmaceutics and Biopharmaceutics, 2001. **52**(1): p. 65-73.
244. Jansod, S., et al., *Phenytoin speciation with potentiometric and chronopotentiometric ion-selective membrane electrodes*. Biosensors and Bioelectronics, 2016. **79**: p. 114-120.
245. Rodríguez-Escales, P. and X. Sanchez-Vila, *Fate of sulfamethoxazole in groundwater: Conceptualizing and modeling metabolite formation under different redox conditions*. Water Research, 2016. **105**: p. 540-550.
246. Li, N., et al., *Inclusion complex of trimethoprim with β -cyclodextrin*. Journal of Pharmaceutical and Biomedical Analysis, 2005. **39**(3–4): p. 824-829.
247. Fujioka, T., et al., *Effects of feed solution characteristics on the rejection of N-nitrosamines by reverse osmosis membranes*. Journal of Membrane Science, 2012. **409–410**: p. 66-74.